POLITECNICO DI MILANO

Scuola di Ingegneria Industriale e dell'Informazione
Dipartimento di Science e Tecnologie Aerospaziali
Laurea Magistrale in Ingegneria Aeronautica

PARAMETRIC FLUTTER ANALYSIS OF A WIND TUNNEL CONVENTIONAL AIRCRAFT MODEL

Relatore: Prof. Sergio Ricci

Tesi di Laurea Magistrale di:

Mario Andrades Márquez

Matricola: 877637

Anno accademico 2017/2018

ACKNOWLEDGMENTS

First of all, I would like to thank Prof. Sergio Ricci the opportunity given to me to do my Master Thesis taking part of this amazing project. I would like to thank Federico Fonte for his kind help and consideration.

Secondly, I would also thank Universidad Politecnica de Madrid for giving me the possibility to live this experience in Italy.

A sincerely thanks is dedicated to all my friends Chacón, Toni, Álex, Luismi, Diego, Jose, Manolo, David, Isa, Manu, Argu, Álex, Dani, Cule, Víctor, Mariano, Jesús, Paula, Enrique, Raúl and a large etcetera. Moreover, grazie mille a tutta la mia famiglia Erasmus per fare questi due anni una sperienza indimenticabile, specialmente a Luis, Trini, Kulti, Zeca, Mikail, Kristian, Gloria, Andrea, Oma e Camille.

At last and the most important, my family. Muchas gracias a mis padres, abuelos y tatos por apoyarme siempre y ayudarme a superar los momentos difíciles. Por supuesto gracias a Simona por entenderme y ayudarme siempre. Os quiero mucho a todos.

A new life is to start and I really want to share it with all of you!

ABSTRACT

L'aeroelasticità assume una parte importante del processo di certificazione perchè implica fenomeni di instabilità che possono avere conseguenze disastrose, come il flutter. Questo processo è rigoroso e complicato, con molti requisiti che devono essere soddisfatti contemporaneamente. Per ciò che concerne il flutter, esistono esempi di sistemi di controllo attivo per la sua soppressione che possono essere utilizzati ma non è ancora possibile certificarli, rimanendo quale requisito di certificazione l'assenza di flutter nell'inviluppo di volo. Recentemente, è stato avviato un progetto di ricerca, finanziato dall'ente di certificazione statunitense FAA con lo scopo di appofondire l'uso di sistemi di controllo attivo del flutter e l'impatto sulle loro prestazioni delle inevitabili incertezze, al fine di, un domani, poterli certificare. Il Politecnico di Milano partecipa a questo progetto, questa tesi ha l'obiettivo di sviluppare un modello computazionale del modello di velivolo che sarà costruito per realizzare i diversi test di flutter in galleria del vento. In particolare, è stata svolta anche una analisi parametrica sulle caratteristiche di massa del modello stesso in modo da generare diverse tipologie di flutter con caratteristiche differenti.

ABSTRACT (ENGLISH)

Aeroelasticity takes an important part of the certification process because it involves instability phenomena that can have severe consequences such as flutter. The certification process is strict and complicated; many requirements must be fulfilled at the same time. Concerning the flutter, there exist examples of active control systems for flutter suppression that can be used but it is not possible to certify them yet, remaining the first certification requirements. Recently, a research project has been launched, funded by the US certification authority FAA, with the aim of deepening the use of systems for active flutter control and the impact on their performance of the inevitable uncertainties in order to, in the near future, certify them. Politecnico di Milano takes part of this project, this thesis has the objective of developing a computational model of the wind tunnel aircraft model in order to choose the correct configuration for the flutter tests. In particular, a computational parametric analysis of flutter depending on the model mass characteristics has been performed.

TABLE OF CONTENTS

LIST OF FIGURES

LIST OF TABLES

1. INTRODUCTION

An aircraft must be certified to be able to fly. Aeroelasticity takes an important part of the certification process because it involves phenomena that may be unstable such as divergence or flutter, what are synonyms of danger. The certification process is strict and complicated; many requirements must be fulfilled at the same time: among them, the strict limitation about flutter velocity that cannot be present inside the flight envelope.

Nowadays there exist many studies related to active control systems for flutter suppression that can be used to avoid flutter when it should theoretically appear, by moving correctly the aerodynamic surfaces (ailerons, elevators, rudder…). Nonetheless, and even if these systems seem to work properly, it is not possible to certify them yet, what means that the maximum flight velocity must be lower than the flutter one (scaled with a safety factor).

To certificate this technology and achieve to certificate higher flight velocities, it is necessary to define appropriate tests and requirements that the system must fulfill to be certified. Prof. Eli Livne, from University of Washington, has looked into the situation and written a document [1] full of information and bibliography in order to organize the work done until now, the research lines to be opened and the problems about active flutter suppression system certification.

In collaboration with prof. Eli Livne, prof. Sergio Ricci from Politecnico di Milano is developing a conventional aircraft model to be tested in the Politecnico di Milano wind tunnel. Inside this project, this thesis appears with the objective to develop a computational model of the wind tunnel model in order to choose the correct configuration to for the flutter tests. In addition, for the purpose of collaborating with the big project to store up enough knowledge and experience, a computational parametric analysis of flutter velocity, modes and frequencies is performed by small variation of the model masses.

This thesis is structured in six chapters. The first one is this introduction, followed by an overview of the certification process starting from the different types of certifications that exist, followed by some ground and flight test highlights and finishing with the main problems of active flutter suppression system certification. The third chapter is formed by the steps from the initial model that was used for other flutter test to the present one, explaining the requirements and its evolution until decide the final configuration. Chapter four contains the computational model details and how it has been transformed from Nastran to NeoCASS, that is a tool developed at Politecnico di Milano. How fuselage, wing and tail are modeled is explained, and joints defined. After this, in chapter 5, computational parametric flutter analysis has been carried out, using as parameters an added lumped mass and its position spanwise and chordwise. Conclusions and future research lines close this thesis as chapter 6.

2. AIRCRAFT CERTIFICATION

2.1. FLUTTER EQUATION

Aeroelasticity is the science that studies the interaction between aerodynamic, elastic and inertia forces. This is the reason why it is complex and requires a big knowledge in different sciences. This section intends to be an introduction to flutter, an aeroelastic instability, in order to place the reader in the thesis context.

The flutter equation for an aircraft has a matrix form as follows:

$$[M_{aa}]\{\ddot{u}_a\} + [B_{aa}]\{\dot{u}_a\} + [K_{aa}]\{u_a\} = \{Q_a^A(\ddot{u}_a, \dot{u}_a, u_a)\} + \{Q_a^E(t)\}$$

Where:

- $[M_{aa}]$: Mass Matrix (lumped masses)
- $[B_{aa}]$: Damping Matrix
- $[K_{aa}]$: Stiffness Matrix
- $\{Q_a^A(\ddot{u}_a, \dot{u}_a, u_a)\}$: generalized aerodynamic forces
- $\{Q_a^E(t)\}$: generalized non-steady forces
- $\{u_a\}$: vibration modes

As it can be seen, it is a difficult equation to deal with mainly due to the presence and form of the generalized unsteady aerodynamic forces. That is why several methods have been developed to resolve it in an efficient way. One of the most famous and useful methods is the continuation method [22]. This is the method chosen to perform the flutter analysis in this thesis.

In advance, the aeroelasticity certification consists on obtaining the limit velocity at which the aircraft can fly without encountering the flutter conditions. Figure 1 shows how the three main aeroelastic phenomena depends on the aircraft configuration, in this case the wing swept angle.

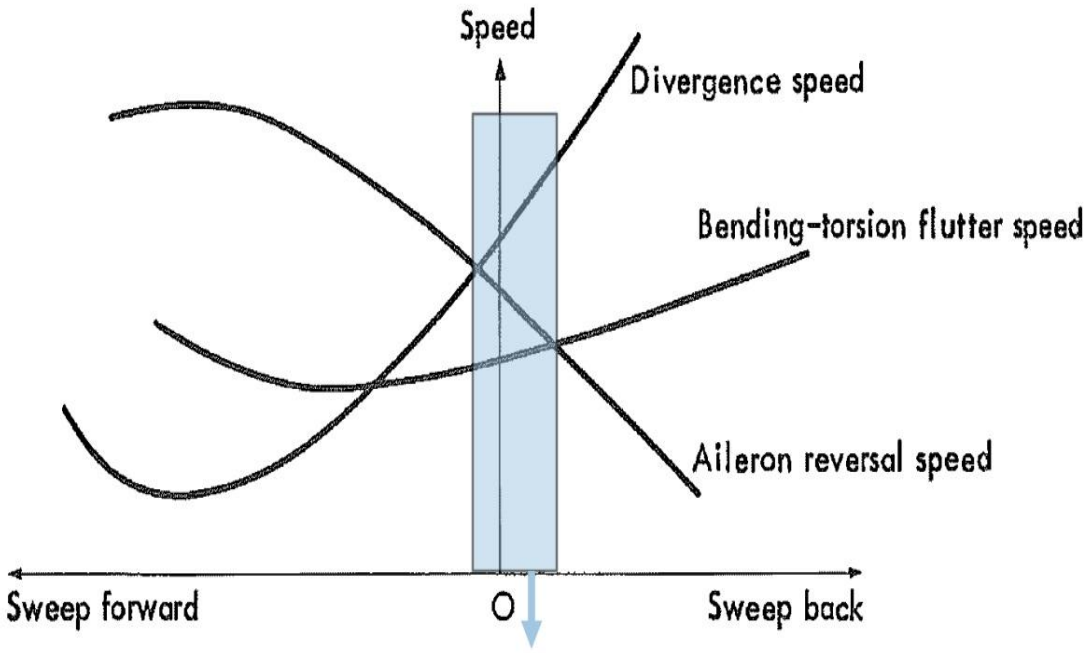

Figure 1. Critical velocity depending on the wing sweep [2].

2.2. THE CERTIFICATION PROCESS

To certificate an aircraft means to fulfill all the requirements imposed by the certification authorities (EASA in Europe and FAA in USA) in order to guarantee the safety aircraft flight during a mission. The problem is not simple because during the design process many uncertainties exist. To introduce the certification process an overview of the most important aeronautical certificates is done: Type certificate, Airworthiness certificate and Supplemental type.

The idea is to frame the aeroelasticity, and in special the flutter, into the certification process. Its main part can be found during the ground and flight tests.

2.2.1. TYPE CERTIFICATE

Obtaining this certificate is a long and difficult process that starts from the conceptual design and ends by making some prototypes and testing them. Once the type certificate is acquired it is possible to apply for an Airworthiness certificate.

Starting from the conceptual design, the Type certificate must be applied at the same time given the following data:

- The three primary views
- Dimensions
- Materials
- Passengers
- Engines technical specifications
- Approximated performances
- Others

After this, the work will be done in parallel with the certification process in order to ensure that the aircraft built will satisfy the requirements. Various meetings will take place until arriving to the Type Design whose construction plans and specifications show that the imposed rules are followed. The situation ends in a loop because this detailed information needs to be controlled and many changes are done with the target of solving the potential problems. This done, the process arrives to the Frozen Design, with all the conceptual design information detailed and also other information added as:

- Detailed information of manufacturing processes
- Performances
- Ground and flight tests

At this point, the manufacturing process of the components starts but it has also an important feedback from the certification authority. To ensure the necessary quality the Production Certificate is needed. Two or three prototypes are built and they will be used during the certificate process by testing them. Fulfilling all the requirements the Type Certificate is obtained.

Aeroelasticity takes part of the ground and flight tests starting from the computational models (simplified and then complex), wind tunnel models, and prototypes ground and flight tests. This means that almost during the whole process aeroelasticity must be present. In next sections this thesis focuses on these tests.

2.2.2. AIRWORTHINESS CERTIFICATE

This document states that an aircraft (a document for each one) is legally and technically in good conditions to operate. To obtain the airworthiness it is necessary to prove that the maintenance is

being carried out following the Type Certificate and the EASA or FAA rules. There exist two different maintenances that must be made:

- **Scheduled maintenance:** depending on the Type Certificate and the maintenance program accepted by the aeronautical certification authority.
- **Non Scheduled maintenance:** specific depending on the conditions (for example, if a failure occurs this maintenance must be carried out).

The Airworthiness certificate has not an expiration date, it will be available while both maintenances are implemented.

2.2.3. SUPPLEMENTAL TYPE

This document is used when one desires to do a major modification in an aircraft with the Type Certificate (maybe it is necessary a new Type Certification, it depends on how important the modification is). There are two types of Supplemental types: one applied to a specific aircraft (only one) and another applied to series of aircraft.

2.3. FLUTTER CERTIFICATION

After explaining the usual certification process, it is time to focus on the aeroelasticity certification, and mainly on flutter. To do this, some Advisory Circulars (AC) from Federal Aviation Administration (FAA) have been analyzed in order to include on this thesis the most relevant information about aeroelasticity certification. This AC provides a guide for acceptable means of demonstrating compliance with the specifications asked by the FAA (it does not mean that this is the only way to prove them).

Aeroelastic instabilities have been a very significant part of the aircraft development and so they have become an essential part of the airworthiness criteria for civil airplanes. From the beginning, the initial requirements for flutter in the 1931 were tiny, only saying 'no surface shall show any signs of flutter or appreciable vibration in any attitude or condition of flight' [3]. Later in 1934 this was revised adding flutter prevention measures and creating the first ground vibration tests. Years later and most significantly, a speed and attitude limit to ensure safety with respect to aeroelastic instabilities is defined. Even if some active control systems for flutter suppression exist, it is not possible to ensure its operation (for now) to certificate that flying with a higher velocity than the flutter limit is also safety if this control is used.

In terms of how important aeroelasticity is in the certification process, a list of the 14 CFR Regulations in which some aeroelastic points are included can be found at [4].The outstanding sections are:

- Section 25.251, Vibration and buffeting.
- Section 25.335, Design airspeeds.
- Section 25.629, Aeroelastic stability requirements.

This section starts with the AC No: 25.629-1B [4] that talks about the design requirements for the aeroelastic instabilities. This done, the AC No: 23.629-1B [5], which it is specific about flutter, is examined.

2.3.1. AEROELASTIC STABILITY

This AC No: 25.629-1B is helpful to 'provide guidance material for acceptable means, but not the only means, of demonstrating compliance with the provisions of Title 14, Code of Federal Regulations part 25 associated with the design requirements for transport category airplanes to preclude the aeroelastic instabilities of flutter, divergence, and control reversal'. This is why analyzing this AC it is important to understand what it is necessary to demonstrate to finally obtain the aircraft certification in aeroelastic terms. Firstly, the discussion of requirements is done and then it shows a way to demonstrate the compliance. Because of this project is dedicated to the analytical analysis of the wind tunnel model, the conditions without failures will be underscored. For more information the reference [4] can be consulted.

The requirements start with the Aeroelastic Stability Envelope to conclude containing many failure possibilities. It shows, enclosed in the diagram, all the combinations of airspeed and altitude encapsulated by the design dive speed (V_D) and the design dive Mach number (M_D) that the aircraft can perform in safety conditions. On Figure 2 can be seen a typical Aeroelastic Stability Envelope. The dive speed is defined as the absolute maximum speed above which the aircraft must not fly because it can damage the aircraft structural integrity due to extreme vibrations.

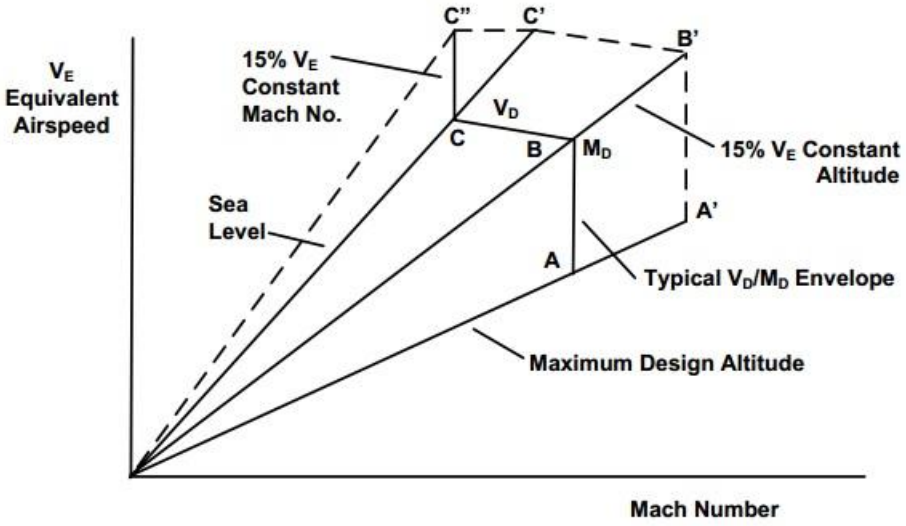

Figure 2. Minimum Required Aeroelastic Stability Margin [4]

Three main limits can be found on Figure 2:

- Flight altitude: from sea level (even lower in some cases) to maximum design altitude.
- The dive speed V_D : this velocity will be determined by the aeronautics codes depending on load requirements with a safety factor (including gust loads, maneuvering loads, and etcetera)
- The V_D/M_D: determined by 14 CFD Regulations, Section 25.335, Design airspeeds.

In poor words, the goal of the certification process is to clarify this diagram, together with failure and others, in order to obtain the safety aeroelastic flying envelope. To complete this diagram and as an example, specific values of the Airbus A320 can be found at Appendix D [6].

Some failure certification criteria are:

- Wings and stabilizers: after designing them to fulfill the aeroelastic stability criteria for nominal condition, the fail-safe criteria should be also satisfied.
- Control surfaces and tabs: must be studied for failure modes, including structural failures.

Also the interaction with the control systems such as fly by ware must be considered. This will be discussed in the section 2.3.

Once the main requirements for certification have been explained, the airplane must demonstrate its compliance by analysis and tests. Analyses are used to determine the aeroelastic stability margins for normal operations (including some failure modes). Ground tests to know the stiffness of the aircraft and its components. Flying tests to finally demonstrate compliance.

2.3.2. ANALYTICAL MODELING

In this part of the AC it is explained the level of accuracy that must be used in order to obtain valid results from the certification point of view. This paragraph is important for this thesis because it is directly related to the objective: to create an analytical model of the future wing tunnel model of a conventional aircraft to make a flutter analysis.

Beginning with the structural modeling, both lumped mass beam and finite elements can be used, if and only if the critical modes of deformations are good enough reflected. Analysis results must be compared to ground tests data, which means to check stiffness, damping and some vibration modes.

On the other hand, there is the aerodynamic modeling. In this case, and depending on the complexity of the problem, it is accepted a 2D or 3D panel theory. Another point to analyze is the use of compressible or incompressible flow. To check these tests, it is recommended to look into other experiences with similar configurations. It is common to introduce aerodynamic factors to consider some effects (mainly during the design process), check it with wing tunnel experiments.

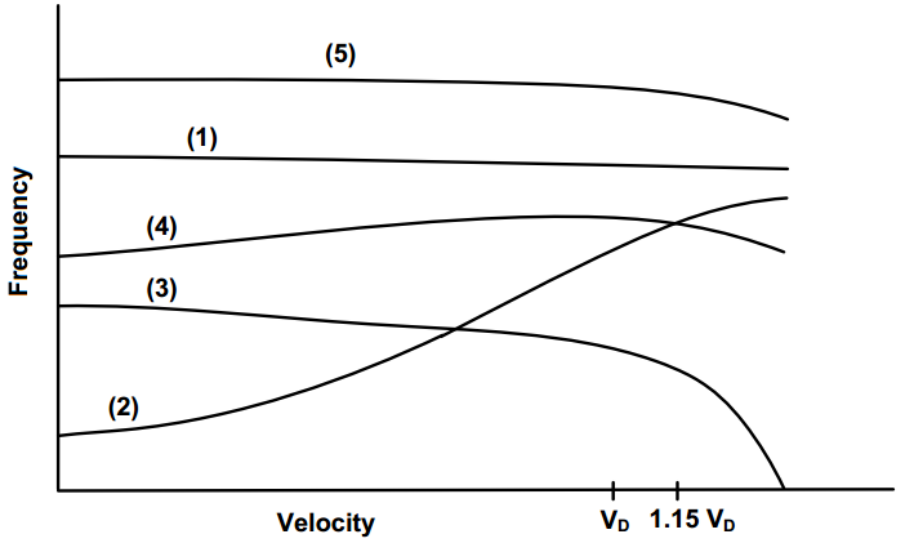

Figure 3. Flutter frequency-velocity curves (original from [4], modified to be included in this thesis)

2.3.3. ANALYTICAL ANALYSES

The first analyses to be performed are non-oscillatory (divergence and control reversal). This done, it is time to check flutter, it must involve the modal analysis with unsteady aerodynamic forced. Finally, it is obtained a damping margin that fulfills the requirements. There are some important diagrams that are used to represent the flutter analyses. Figure 3 shows the mode frequency evolution with the

velocity. Not all the modes have the same importance. Low frequency modes are, in general, not dangerous.

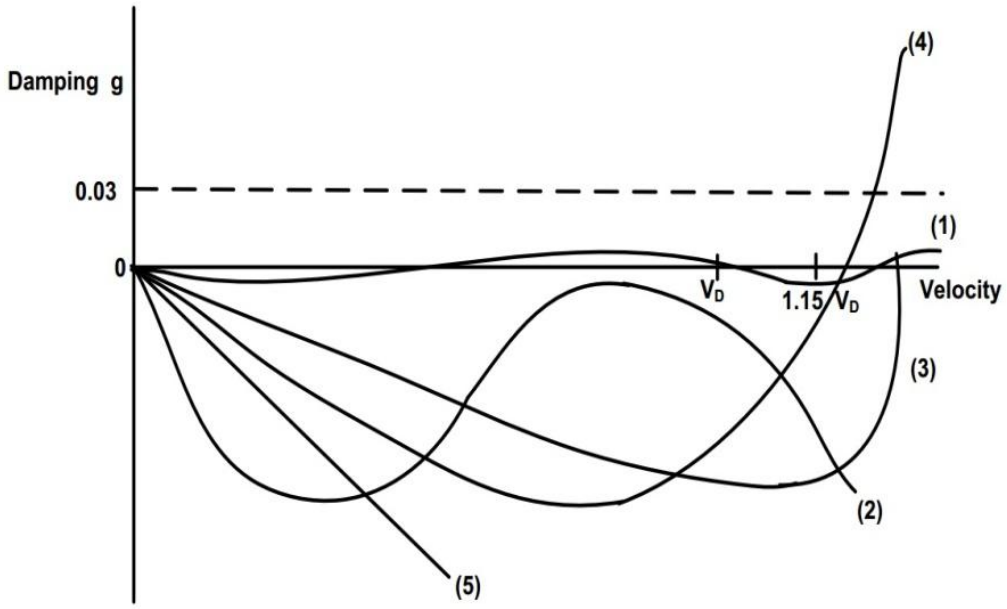

Figure 4. Flutter damping-velocity diagram [4].

To show a proper margin of damping diagrams as the one shown on Figure 4 are used. For example, assuming that the structural damping is g = 0.03, and that it is the same for all the modes. There are two requisites to fulfill:

- Not to intersect the g = 0 line for velocities under v_D
- Not to intersect the g = 0.03 line for velocities under $1.15\ v_D$

In the example of Figure 4, five flutter modes are represented:

- Mode 1 is unstable but, it is not a problem because these criteria are only applicable to flutter critical modes, and number 1 is not supposed to be.
- Modes 2 and 5 are always under g = 0 line, so they will not be a problem.
- Modes 3 and 4 intersect the g = 0 line after $1.15\ v_D$.

This means that considering only these five modes, the flutter damping is acceptable.

2.3.4. TESTING

Every aircraft design is supported by numerous ground and flight tests that validate the theoretical models and check the functionality of on-board systems. Two mainly groups of testing are necessary:

- Ground Vibration Test (GVT): to determine the eigenmodes of the aircraft and whose results are used to validate the structural finite element model.
- Flight Vibration Tests (FVT): to verify the modal answer on flight and whose results are used to validate the aeroelastic model.

Both GVT and FVT must be performed in an advanced stage of the design and manufacturing of the aircraft. The GVT require the aircraft in 'ready for flight' condition, which means that every system should be installed and the internal configuration (seats and others) must be representative of the final airplane. The FVT are carried out using a prototype that must also be representative of the final aircraft. Figure 5 shows the common process until certification.

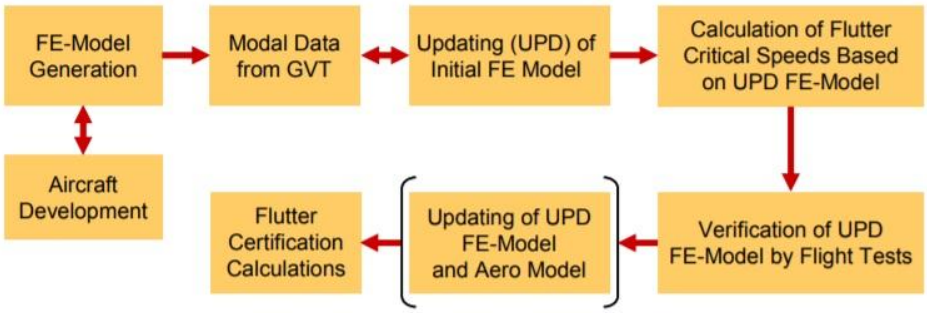

Figure 5. Actual Verification and Validation Process of Aeroelastic Aircraft Models [7]

2.3.5. GROUND VIBRATION TEST (GVT)

Its objective is to obtain experimentally the main dynamic structure characteristics: frequency and modal responses, modal damping and detect non-linearities. Certification rules do not define GVT as necessary but it is mandatory to validate the structural model. Nowadays, all aircraft manufacturers do a GVT in every new aircraft design. In a GVT the structure is held to get a free-free condition in order to obtain a solid rigid mode frequency next to 0 and the eigenmodes are exited with exciters. To catch the answer a lot of accelerometers are used.

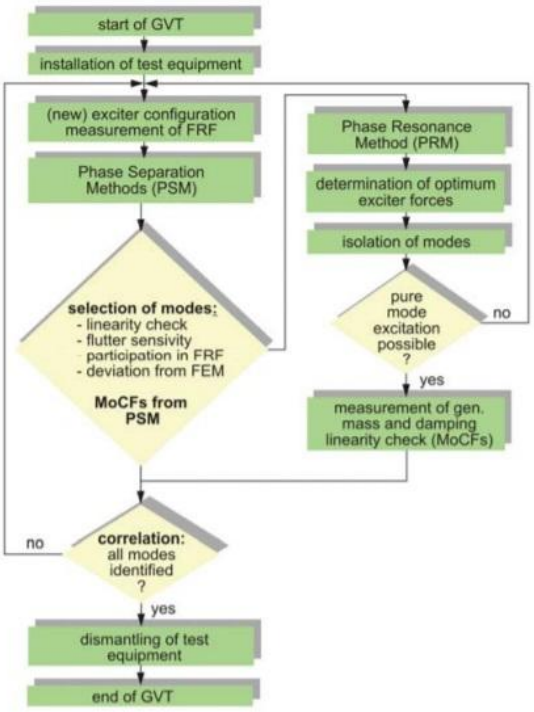

Figure 6. Actual Aircraft Ground Vibration Testing Strategy [7].

The aircraft must be suspended by a system that allows a free-free condition simulation. There are several ways to obtain these conditions, in example:

- Pneumatic system applied at landing gear legs or at jacking points (see Figure 7)
- Elastic bands
- Over its own deflated tires.

Figure 7. Example of hydraulic lifting mechanism supplied by CFM Schiller [8]

The accelerometers are distributed at jacking points of the structure and the number depends on the size of the airplane and on the test. Some standard values are the sampling frequency from 0.02 to 3 [kHz] and the added mass from 5 to 50 [g]. There exist also different kinds of exciters: mechanics, electrodynamics and electro-hydraulics. An example of the position of these elements can be found at Figure 8.

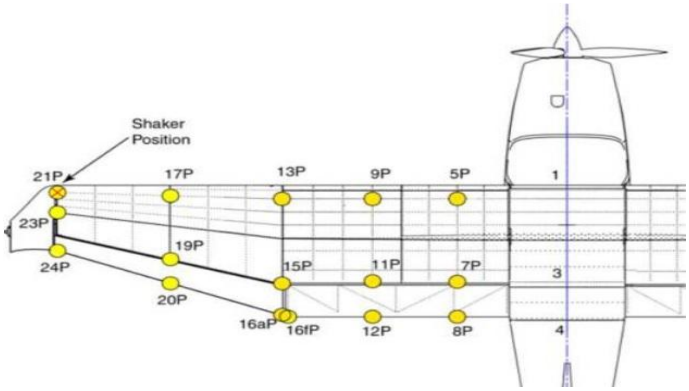

Figure 8. Example of accelerometer positions for a light aircraft GVT [9].

Normally, the GVT include:

- **Ground Vibration Testing:** obtain the vibration mode frequencies, shapes and damping.
- **Control surfaces and tab mass properties determination**: these mass are very important to understand flutter modes and so it is necessary to verify them.
- **Stiffness Tests of wings, stabilizers and etcetera**: obtain and check the stiffness of the different parts.
- **Rotational frequency for all control surfaces and tabs:** check this frequency because it will excite the aircraft during the flight.
- Free play measurements of all control surfaces and tabs.
- Rotational stiffness for control system and tab system.

2.3.6. FLIGHT VIBRATION TEST (FVT)

This test is required for airworthiness. Its purpose is to prove that the aircraft has not aeroelastic instabilities and also to check the aeroelastic model. The test must cover all the flight envelope, including V_D/M_D. The firsts are flutter tests (high risk) because they expand the flight envelope and it will be used during the other tests.

During these tests it is important to choose the correct aircraft configuration. In general, the crew is minimal due to the risk. Depending on the aircraft it is necessary to include the payload simulated by ballast barrels (Figure 9). The fuel is very important owing to it is allocated, in general, inside the wing, meaning that it has stiffness and damping effects.

As a general rule, it is recommended a minimum payload and maximum fuel weight for the first tests.

Figure 9. Ballast barrels in Airbus A380 at Paris Air Show [10]

The instrumentation needed to control the vibration characteristics depends on the modes to be investigated. In any event, accelerometers correctly located are used as during the GVT. However, during FVT it is also important to monitor the velocity, the atmosphere conditions and the altitude in order to draw the diagrams. Telemetry systems exist to register and transmit data to the ground (normally engineers stay on ground and the crew is the minimum possible).

The modes and frequencies can be excited by a lot of techniques. It is necessary to study which excitation method and which frequencies use to analyze flutter correctly. The main techniques are:

- **Pilot induced control surface impulses:** pulsing the control surfaces to excite modes, generally below 8 Hz. It is an easy way to excite modes but depends on the ability of the pilot.
- **Sinusoidal excitation using rotation masses:** from 10 to 50 Hz. It consists on rotating shakers located in the wing tips and the tail section.
- **Excitation using autopilot:** also effective to introduce sinusoidal excitation but limited by the fact that it is not possible to transmit energy to the control surfaces at higher frequencies.

2.4. ACTIVE CONTROL SYSTEM FOR FLUTTER SUPPRESSION

The main considerations to certificate an Active Flutter Suppression (AFS) system are explained. The section is based on the AC 25.672-1 [11] drawing the first ideas of what a control system must be to arrive to its certification problems and the issues in order to demonstrate it.

The idea is based on aero-servo-elasticity that studies the integration of the coupled structure, aerodynamic and control system problem (see Figure 10). The main objectives are reducing cost and weight, and improve performances, or a combination of those.

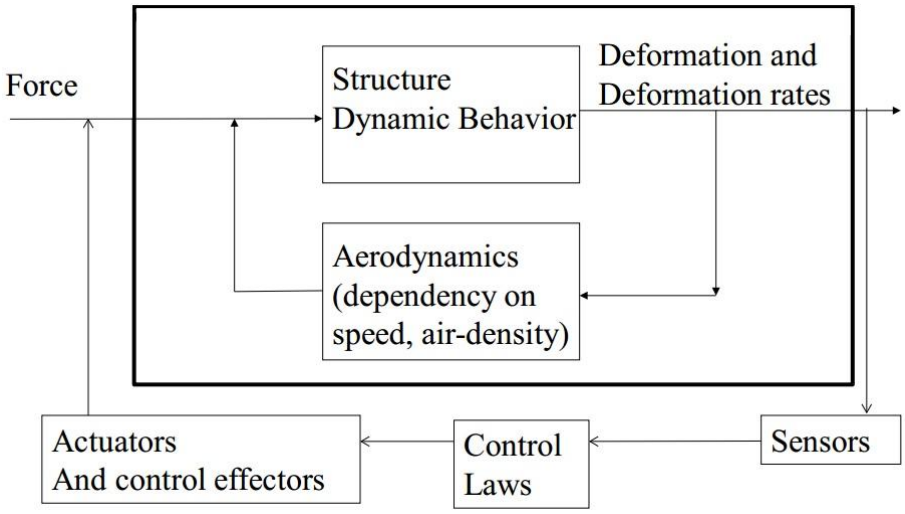

Figure 10. Aero-servo-elasticity scheme [13].

The design criteria for flutter (and loads in general) depends on how reliable the system is. This is why the system failure rates are necessary to be used in probability calculations. It can be based on tests or on experience, taking into consideration that all scenarios and factors must be included. If it is not possible to prove the reliability in service conditions to satisfy certification requirements, the original load level and operating limits will be required. Let's highlight some specific criteria for AFS system collected from the AC 25.672-1 [11]. Even if it is obsolete from Jul 12 2017 [12], it is acceptable to use it as the starting point:

- *'When the FSS is operative, all applicable Part 25 (Federal Aviation Regulations, FAR) shall be met, including design for flutter-free and divergence-free flight up to a speed of* $1.2\ v_D/M_D$.'
- *'The airplane shall be shown by analyses or tests to be free from flutter and divergence at any speed up to* v_D/M_D'.
- *'An aircraft may be certified for alternate configurations, including those with the AFS selected totally inoperative…'*

It provides the possibility to expand the flight possibilities (velocity, flight envelope) while AFS system is active if and only if a correctly implemented and certified AFS fulfills the same requirements. However, it is mandatory to certify the aircraft taking into consideration the AFS system failure. These remarks show that it is not easy to certify an AFS system because of its complex and multidisciplinary condition. It must be stable over all flight conditions, configurations, loads and flutter mechanisms. Furthermore, it has to work with the other active control systems of the aircraft: Stability Augmentation System (SAS), Gust Alleviation System and etcetera.

Control systems needs complete and complex mathematical model that must be checked by testing. These tests are necessary to demonstrate that the system works. As explained at section 2.3 various tests are performed:

- GVTs: static loads, modals, actuators, sensors…
- Control: hardware elements, sensor connections…
- Wing tunnel and flight tests for aerodynamics.

2.4.1. UNCERTAINTY

As it is stated at [1] by Eli Livne: *'All tests of an aeroservoelastic system and its components are subject to test uncertainties due to the limitation of experimental techniques and the uncertainty in the test article, the environment in which it is tested, and even the makeup of the testing team itself'*.

Uncertainty is the main challenge to deal with. At this point, several AFS wind tunnel tests have been carried out since they are cheaper than flight tests, it is feasible to control the test environment and safety. Robustness and uncertainties of the control system can be studied and evaluated correctly even though it is not absolutely accurate with respect to the real aircraft.

The crucial points to be considered are the uncertainty provided by:

- Mathematical models of all the elements and disciplines.
- Tests because of its limitations (limited sample, data analysis…)
- Variability of aircraft as they come off the production line and as they age.
- Damage and hardware failure.

This means that it is necessary to create a robust, adaptable and versatile controller for all the possible uncertainties and configurations during the life cycle of the airplanes.

2.4.2. FAA LIMITS TO CERTIFICATE AFS SYSTEM

The target of this section is to explain present limits in AFS system certification process and relate it to the thesis objectives.

As it has been showed before, the main issues are uncertainties and robustness, both absolutely necessary to certify the Active Flutter Suppression system. The problem is that there is not enough information to certificate AFS systems by FAA conditions. This is the reason why many investigation lines have been opened:

- Creation of reference benchmark test cases.
- Development of accepted formulations of the aeroservoelastic equations of motion.
- Aeroelastic/aeroservoelastic reliability/uncertainty analysis capabilities.
- New control law design.
- Certification.

Robustness is an issue more typically associated to control systems but in this case it become more difficult, covering from the control until the tabs, control surfaces, hydraulic system to move them... in the end, everything that it is necessary to ensure the correct operation of the AFS system. More information about this can be found at [1] and its bibliography.

2.5. THESIS ISSUES

In this thesis a small part of the vast problem is studied: the uncertainties, and concretely, how variability of aircraft as they come off the production line and as they age affects to flutter frequencies, with the objective to help in the development of the AFS system certification method. To do this, a computational parametric flutter analysis is performed.

As seen before, certification is a complex procedure that judges in parallel to the design and manufacturing process if it fulfills the necessary requirements to obtain the different certificates, with the last objective to certify the airworthiness. In this process technical analysis and tests are included. Nowadays, the problem is that not enough information about uncertainties is available and so it is interesting to develop several lines to investigate it for, in a near future, store up enough knowledge and experience to permit AFS systems to be certified by FAA.

This thesis starts from a project developed at Politecnico di Milano [14], [15], [16] and [17] called X-DIA. It consists on active modal control tests on the wing tunnel model with the objective to study an

innovative canard/wing/T-tail configuration. This model is the starting point to generate a new one in order to study the flutter in details, to be able to change its frequencies by means of small property perturbations (extra lumped masses and its position) in order to reliable test platform to be used to test the active flutter suppression systems. The study is carried out evolving the initial model until convert it in a more suitable and traditional configuration.

The whole project is large and ambitious, including wing tunnel tests. This thesis develops the first steps of the project, working on the analytical model of the final physic wing tunnel prototype. This study gives the first information about what to expect and check during the wing tunnel tests.

3. AIRCRAFT WING TUNNEL MODEL

This section explains the requirements to obtain an appropriate wing tunnel model to carry out the desired flutter analysis and tests. Starting from the initial configuration, given by the Politecnico di Milano project called X-DIA, several modifications have been done until obtaining a frozen configuration that satisfies the new project requirements. After that, the new Nastran model has been created and it has been used as starting point to develop the NeoCASS model that is the object of study of this thesis.

3.1. INITIAL MODEL: X-DIA v0

The thesis starts from X-DIA Nastran model v0.0.1, that is the finite element model of the wing tunnel model used before for some active modal control tests. It consists on an unconventional configuration that includes Canard, forward swept-wing and T-tail.

It has 13 control surfaces: 8 LE and TE control surfaces, 2 movable canards, 2 elevators and the rudder. Figures 11 and 12 show the aircraft Nastran model.

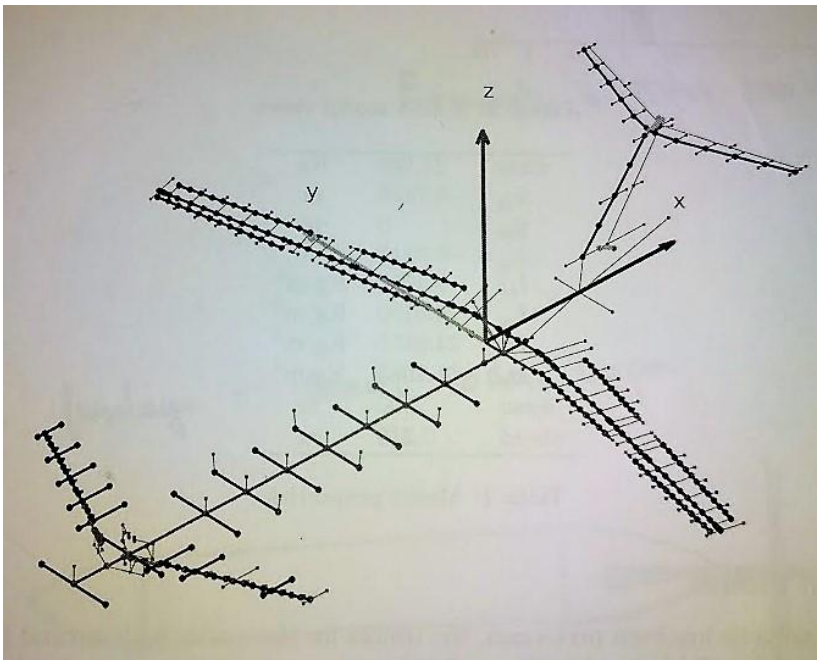

Figure 11. X-DIA structural model [18].

Other interesting characteristics are:

- Full model mass: 27.599 kg
- Span: 3.00 m
- Chord: 0.218 m

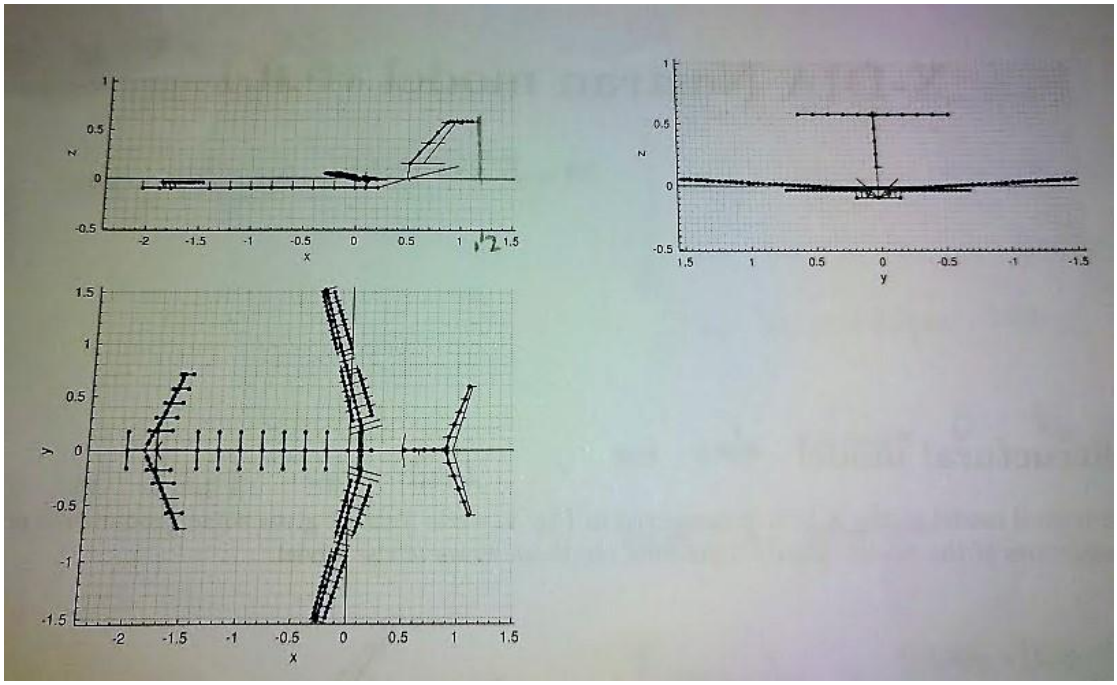

Figure 12. X-DIA model views [18].

3.2. REQUIREMENTS

With the objective to study a wind tunnel model that will be able to reproduce a conventional aircraft configuration and test several conditions to produce flutter and try active control system for flutter suppression tests in wind tunnel, the preliminary analyses show that the aircraft must be simple and flutter modes and flutter control easy to understand to obtain conclusions. In this view, the project leaders agreed to create a new model simpler than the initial one. The new configuration consists on an aircraft without canard, backward swept-wing and still T-tail, in order to reproduce correctly the majority of conventional aircraft configuration. To make the model easier to understand and remove unnecessary effects for the project, multi-control surfaces are removed just remaining common surfaces as two ailerons, two elevators and the rudder.

Even if it is necessary to modify the 'X-DIA v0.0.1' model, it is possible to reuse some parts of the model to build the new one, and so it makes sense to start from this one to develop the new model:

- The fuselage is the same but a little shorter.
- The wing will be reused but changing the forward swept-wing by a more usual backward swept wing, making the correct modification to the spars.
- The new tail is under construction, but after including some modifications, the analytical model does not change mainly.
- The canard is removed, meaning that the new model mass will be smaller.
- All control surfaces are removed, just remaining two ailerons, two elevators and the rudder.

3.3. FROZEN CONFIGURATION

After these decisions, it was necessary to arrive to a frozen configuration to continue developing the project using 'NeoCASS' (a structural, aerodynamic and aeroelastic analysis software tool developed by Politecnico di Milano), in detail 'acbuilder' that is a CAD tool with a powerful user interface that allows to easily create the CAD of an aircraft in a correct format to be read by 'NeoCASS'.

The 'X-DIA v0.0.1' was modified to create the 'X-DIA Conventional Model' (see Figure 13). It had some degrees of freedom to fix to ensure the aircraft stability.

- Wing-fuselage position.
- Tail-fuselage position.

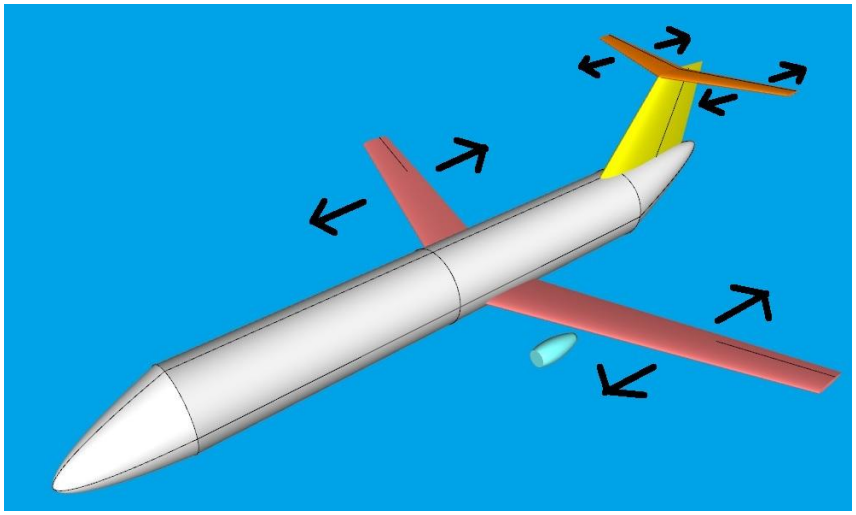

Figure 13. X-DIA Conventional Model degrees of freedom.

The first study has been done by Federico Fonte (Politecnico di Milano), calculating the correct parameters to fix the degrees of freedom and finally close the frozen configuration. This was developed creating the Nastran model called 'X-DIA v1' (finally evolved to version v122, figure 14) and

including several changes in order to fulfill the requirements and to be coherent with the physical model possibilities available in the laboratory.

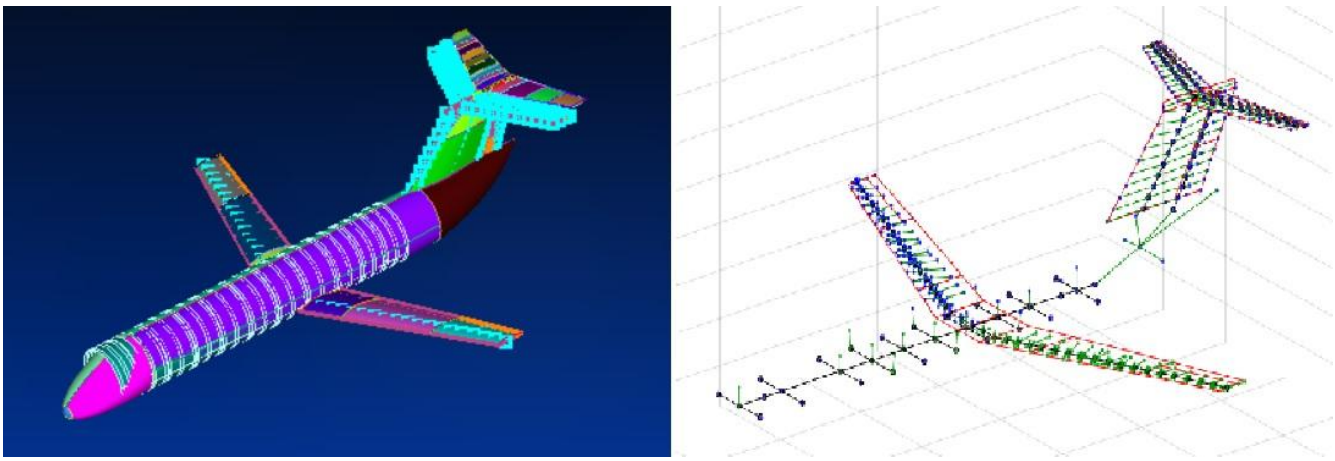

Figure 14. On the left, Femap model of X-DIA v122. On the right, Nastran model of the same model.

4. NEOCASS MODEL

The work consists on using the Politecnico di Milano software: Acbuilder (CAD tool), NeoCASS (analysis tool) and Matlab (base of the others) in order to build the model developed by using a commercial software: Femap (CAD tool) and Nastran (analysis tool). A new model has been generated but it has some small variations with respect to the Nastran one because of:

- Using the model generated by Acbuiler as much as possible.
- Current limits of NeoCASS.

The decision of generation a model in NeoCASS format is related to its versatility in the aeroservoelasticity analysis and synthesis of controllers.

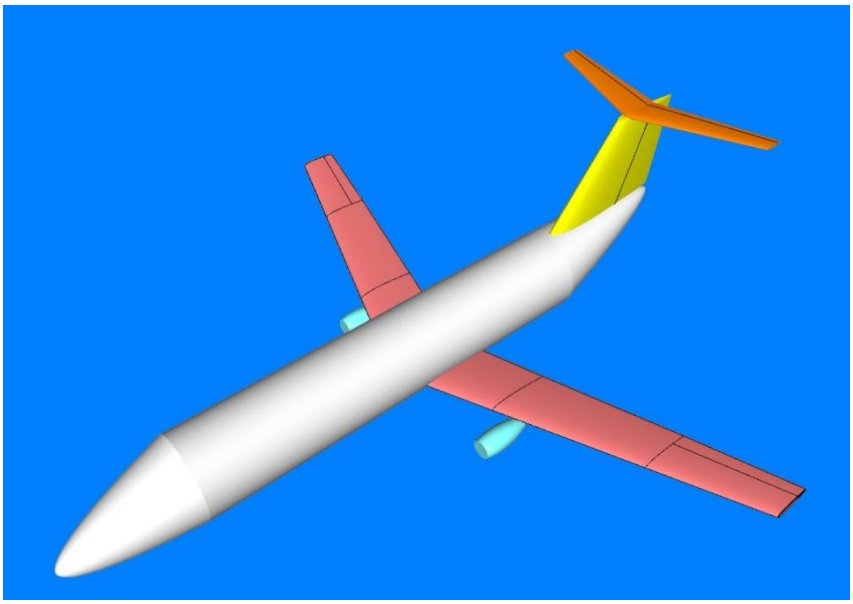

Figure 15. Frozen configuration. First 'Acbuilder' model.

The new model starting point has been created with Acbuilder (see Figure 15) according to the requirements of the frozen configuration with the aim of obtaining a first NeoCASS model to work with. These requirements are a conventional aircraft with a backward-swept wing, two ailerons and T-tail. The main dimensions of the chosen model are:

Fuselage total length (cone + body + tail cone)	**3.03 m**
Wing span	**3 m**
Wing position	**0.485 % of the fuselage length**

Table 1. Main dimensions of the aircraft model.

In this section it is explained how from an initial model created with Acbuilder the model has been modified until arriving to a new model almost similar to the Nastran one by changing:

- Acbuider model to make it as similar as possible to the Femap one in both structural and aerodynamic issues.
- Nodes position.
- Materials.
- Beams and Bar properties.
- Changing and redefining masses.
- Redefining some commands that are not the same or do not exist at NeoCASS.
- Redefining the joins between elements.

4.1. FUSELAGE

The idea has been to use as much as possible of the Acbuilder model. The problem for the fuselage is that, even if dividing the body in the same parts, the nodes are not allocated at the correct position (the Nastran model one).

Eleven nodes have been redefined with the objective of rearranging them in the correct position (see Figure 16).

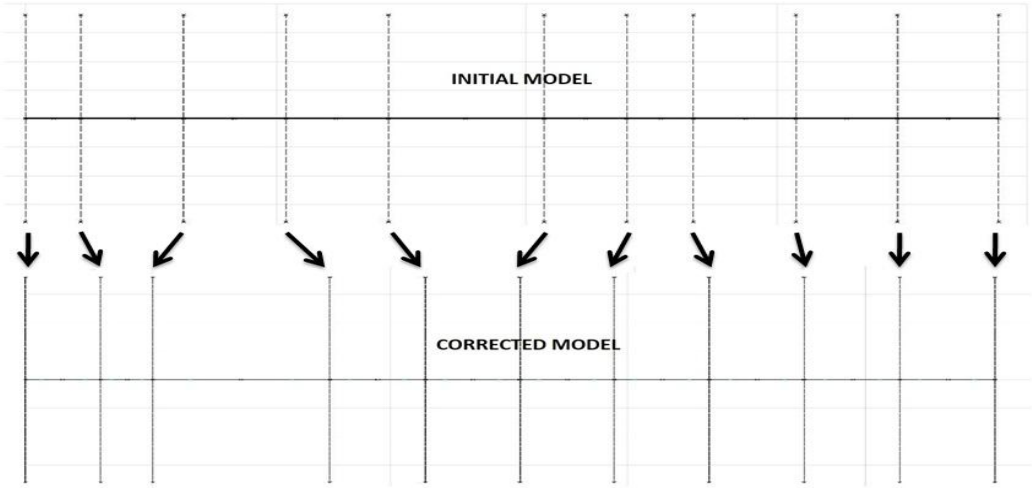

Figure 16. Evolution of the fuselage model.

In the Nastran model these nodes are joined by beam elements (**CBEAM**) and to the aerodynamic nodes with bar elements (**CBAR**) without density. In the new model this has been changed due to the fact that **CBEAM** element is not defined in NeoCASS. The solution adopted has been:

- Replace **CBEAM** by **CBAR**: it means only a definition change (recoding), but not a structural importance.
- Replace the bars that join the main structure with the aerodynamic nodes by rigid bars (RBE0): this change has been adopted to simplify the definition. The reason is that these nodes are not structural and no mass is included on them so it is an easier solution to include rigid bars to simplify the problem.

The material (**MAT1**) and the bar properties (**PBAR**) have been changed respect to the defect ones added by Acbuilder to include the Nastran ones. Table 2 shows the specifications:

MATERIAL	**E (Pa)**	**G (Pa)**	**ν**	**ρ (kg/m3)**
Aluminium	6,89E+10	2,59E+10	0,33	2810
BAR PROPERTIES	**Area (m2)**	**I1 (m4)**	**I2 (m4)**	**J (m4)**
Fuselage bars	5,00E-05	1,00E-04	1,00E-04	1,00E-04

Table 2. Fuselage material and bar properties.

With respect to the masses, lumped masses by using **CONM2** command have been assigned to each main node. To simulate the cone an extra mass has been added to the cone center of gravity. For the fuselage a constant distribution has been used.

About aerodynamic it must be said that at the beginning the fuselage aerodynamic model was considered but due to it is a small model it was problematic and so it has been finally removed.

A three dimensional image of the fuselage model can be found at Figure 17.

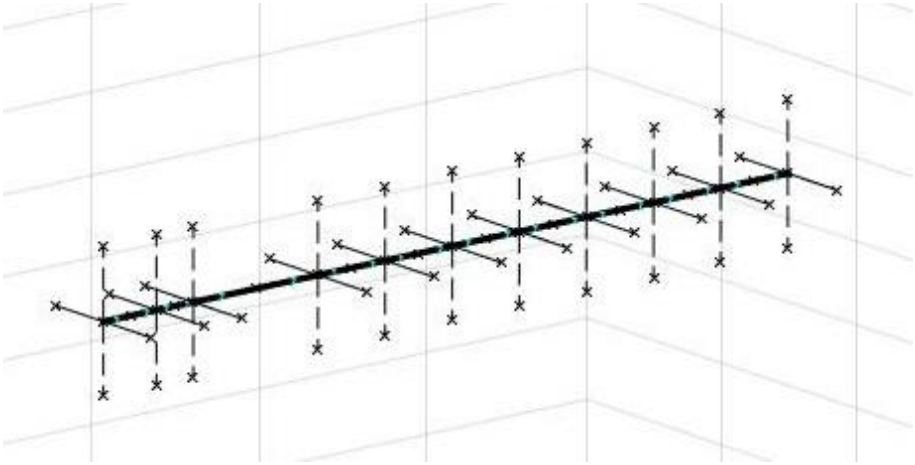

Figure 17. Fuselage structure.

4.2. WING

The first step to create the wing has been to check the structure and the aerodynamic in the Nastran model in order to simulate it in the NeoCASS one starting from Acbuilder. The objective is to simplify the material, bar properties and masses importation from NeoCASS.

After the analysis, one gets the following requirements to fulfill:

- Wing divided in three patches (central, middle and tip).
- Central patch of each semi-wing is divided into 6x5 aerodynamic panels and 6 structural bars.
- Middle patch of each semi-wing is divided into 6x5 aerodynamic panels and 6 structural bars.
- Tip patch is the one that contains the aileron. The tip is divided into 5x4 aerodynamic panels while the aileron has 5x3 panels. The structure has 5 bars.

The acbuilder model ends as shown on Figure 18.

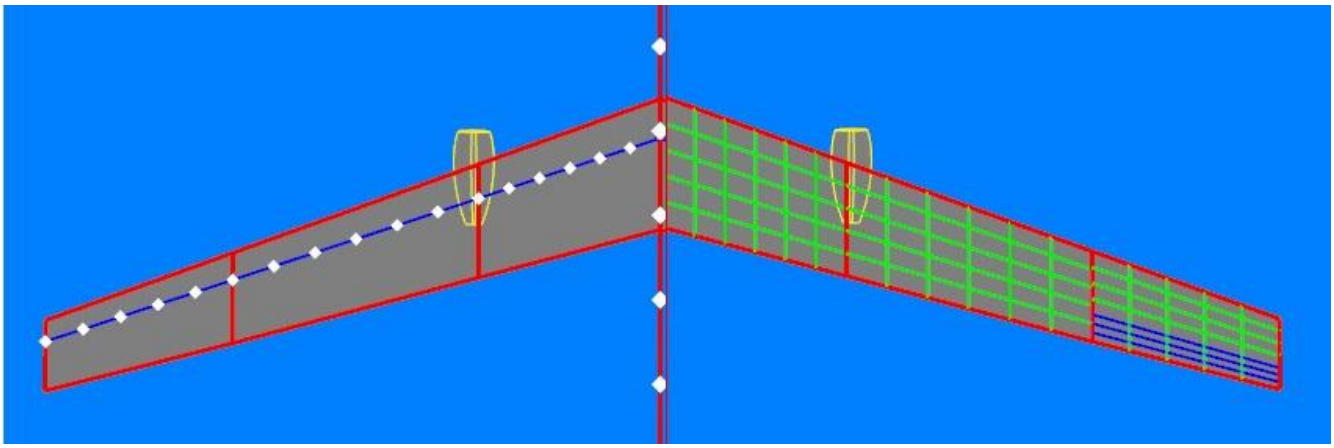

Figure 18. Model obtained by using Acbuilder. Structural model (left) and aerodynamic model (right).

In this case the nodes are not exactly the same as the Nastran ones but they are close enough that it is possible to work directly using the Acbuilder model. To spar model uses a different aluminium from the fuselage structure (see Table 3).

MATERIAL	E (Pa)	G (Pa)	ν	ρ (kg/m3)
Aluminium	9.31E+10	3.50E+10	0.33	2795.72

Table 3. Wing spar material properties

The spar properties have been obtained from the Nastran model (and to be used here where obtained by testing in the laboratory the real one, that it is an Omega spar) and included into the NeoCASS one. The properties are shown on the Figure 19, and it can be seen that there are more structural area and stiffness next to the fuselage (to simulate the wing-box) and it is reduced while arriving to the tip, where less structural properties are needed.

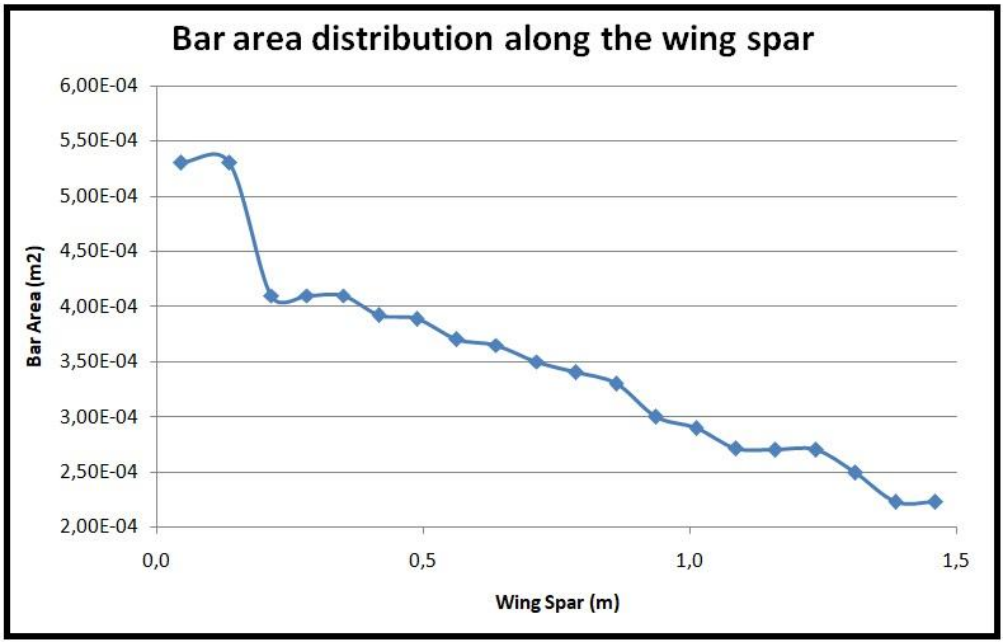

Figure 19. Bar area distribution along the wing spar.

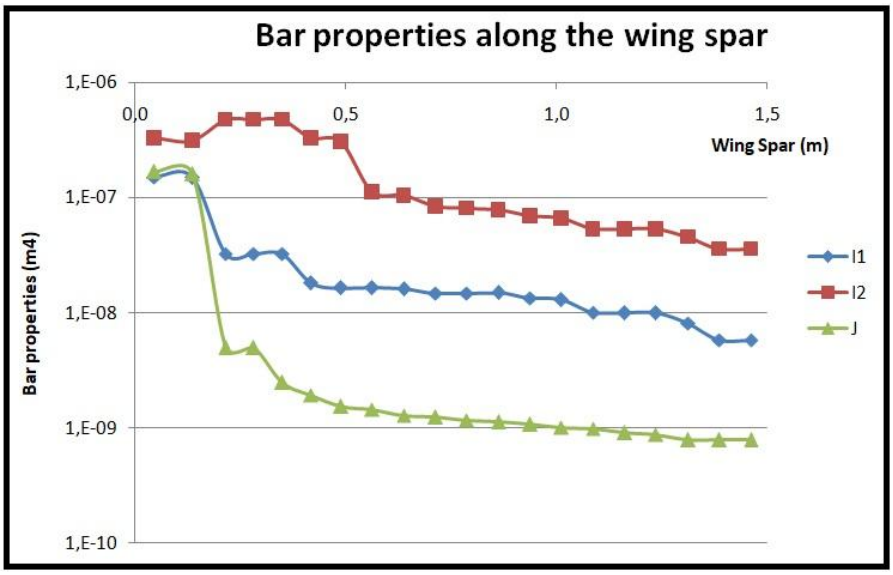

Figure 20. Bar properties along the wing spar.

To continue with the structural model, there are several masses that have been added to the model to complete the simulation of the structure of the wing, in order to include the weight of the wing surfaces, aerodynamic mobile surfaces, joints and others. To do this, it has been necessary to include extra nodes with the objective to situate in the correct position the inertia elements

The elements taken into consideration to add extra mass are:

- Mechanical side: mobile surfaces of the wing (to simulate the ailerons, flaps…)
- Wing aerodynamic surfaces.
- Joints: wing-aileron and other aerodynamic mobile surfaces joints.
- Wing-engines joint.
- Ribs inertia.

These masses have been added in two different ways in the Nastran code: **CONM2** and **CMASS1**. In NeoCASS it is only possible to use **CONM2** and so they have been redefined as lumped masses. [19], [20].

- **CONM2**: lumped mass that are used to introduce inertial loads because of the non-structural masses. With one card it is possible to completely define the inertia tensor.
- **CMASS2**: defines a scalar mass entry and so it is necessary to include more than one card to define the whole inertia tensor.

The mechanical side is done with **CONM2** even in Nastran. It is used to include the inertia of the mobile surfaces of the wing (to simulate the aileron, flaps…). On the other hand, the joints, the ribs inertia and the wing aerodynamic surfaces were defined by using a **CMASS1** command and

consequently the transformation has been done. The final wing structural model is shown on Figure 21.

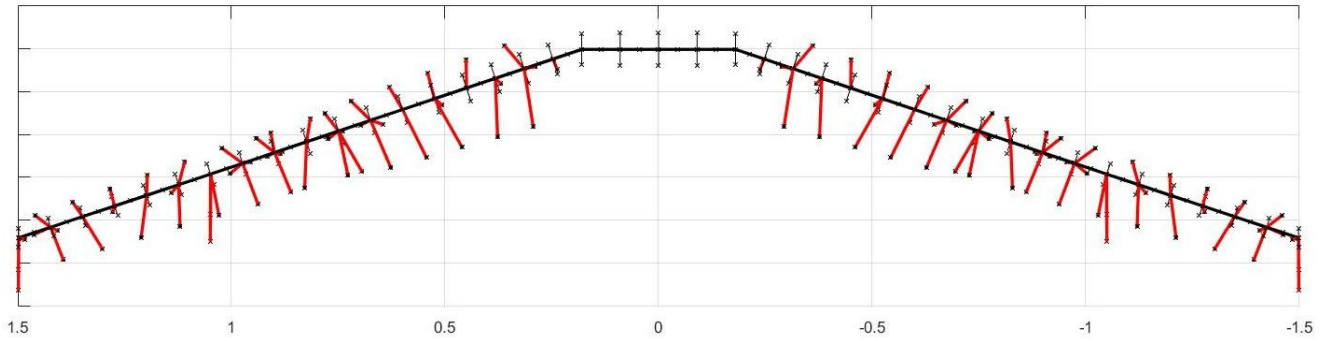

Figure 21. Wing structure with lumped masses.

To define the aerodynamic panels the following parameters are used:

Mean chord, c (m)	**0.25**
Spar (m)	**3**
Wing surface (m2)	**0.746**
Wing airfoils	**NACA 0012**

Table 4. Wing reference values.

Using these references and taking into consideration the model requirements explained on Figure 18, the following cards are used to define the aerodynamic of the wing:

- **CAERO1:** 'used to define all the geometric and mesh parameters for each box of the aerodynamic model which are required by the meshing tool coming from TORNADO Vortex Lattice code.' [21]
- **SET1:** 'used to define an interpolation set of nodes which is used by one of the available spatial coupling method to transfer data between structural and aerodynamic mesh' [20].
- **SPLINE1:** 'it defines a beam spline for interpolating motion and/or forces for aeroelastic problems on aerodynamic geometries defined by regular arrays of aerodynamic points.' [19].

To complete this work was necessary to redefine several parts of the code due to the different definition between Nastran and NeoCASS.

For the wing, the definition was not necessary to be touched due to the fact that the initial Acbuilder model was accurate enough to create a similar aerodynamic mesh, and so it could be exploited.

During the explication of the tail, the differences between both tools are taken into consideration. The wing with both the structural and aerodynamic models is shown on Figure 22.

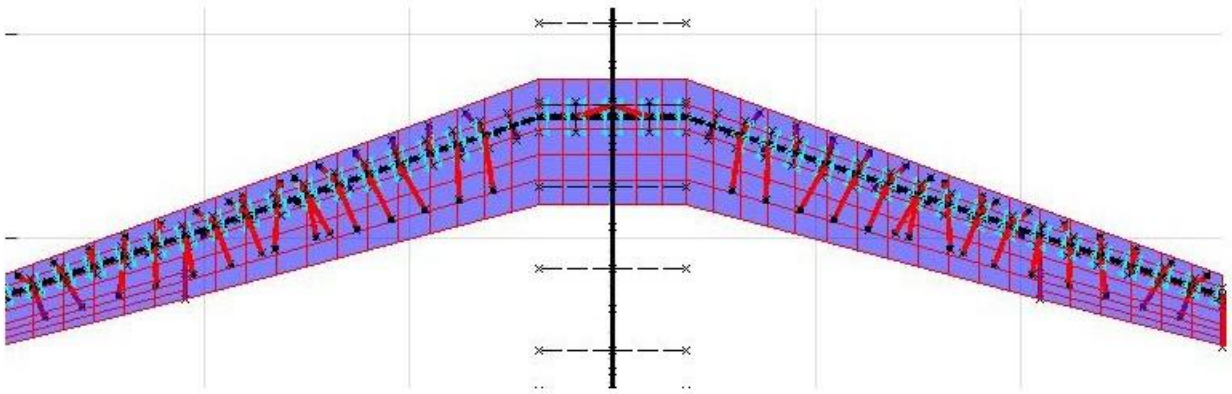

Figure 22. Wing aerodynamic and structural model.

4.3. TAIL

The tail is structured in three separated parts: the cone, that has been created by using the Acbuiler; and the vertical and horizontal tail, that have been taken directly from the Nastran model because of the big difference that existed between both models even after remodeling it by using Acbuilder.

The cone is a prolongation of the fuselage in Acbuilder. From this starting point, the nodes position has been altered to make them coincident with the Nastran model. However, the joint is done in a different way: Acbuilder uses an extra node, and so the new model has 4 nodes instead of 3 that has the original one (see Figure 23). This creates a small difference between models but it is not so important for the flutter analysis.

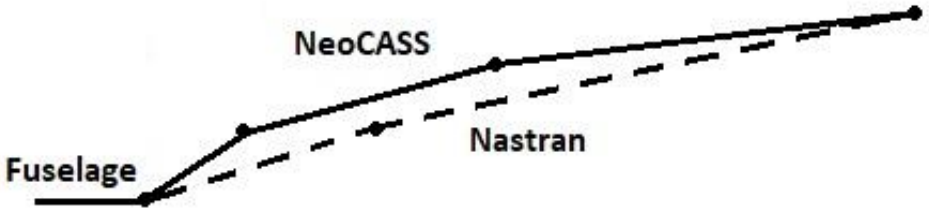

Figure 23. NeoCASS and Nastran tail cone model comparison.

The material has been changed in order to obtain the correct structural properties. In this case, the bar properties where defined by using the card **PBARL**, that it is not available in NeoCASS. To translate it, it was necessary to study the bar properties and introduce them directly in a **PBAR** card. On

Appendix B can be found how it has been done. The material and bar main properties can be found at Table 5.

MATERIAL	E (Pa)	G (Pa)	ν	ρ (kg/m3)
Aluminium	7.31E+10	2,75E+10	0,33	2700
BAR PROPERTIES	**Area (m2)**	**I1 (m4)**	**I2 (m4)**	**J (m4)**
Tail cone bars	9,24E-04	9.15E-07	9.15E-07	1,37E-06

Table 5. Tail cone material and bar structural properties.

Some lumped mass has been added to the tail cone mode to estimate the recover skin mass. In total around 1.6 kg.

The vertical tail includes a bar structure that is connected with rigid bars to the aerodynamic one, similar to the wing structure but in vertical position. Then the vertical stabilizer is joined again by using rigid bars at the bottom and the top of the vertical tail (See Figure 24). This implies some limitations due to the rigid bar possibilities that NeoCASS offers. They are commented in the section 'Joints'.

Again, material and bar properties have been defined to create a structure as similar as possible to the model one. As happened in the wing, the bar properties change along the vertical spar. These properties are shown on Table 6.

MATERIAL	E (Pa)	G (Pa)	ν	ρ (kg/m3)
Aluminium	7.24E+10	2,7E+10	0,33	0
BAR PROPERTIES	**Area (m2)**	**I1 (m4)**	**I2 (m4)**	**J (m4)**
Tip	1.01E-03	1.78E-08	5.27E-08	7.56E-08
Center	3.89E-04	3.19E-08	1.04E-08	7.16E-09

Table 6. Vertical tail spar properties.

The fact that the material density is considered 0 is because the tail was weighted in pieces with the structure done, and so all the structural mass has been included as lumped masses in the right position.

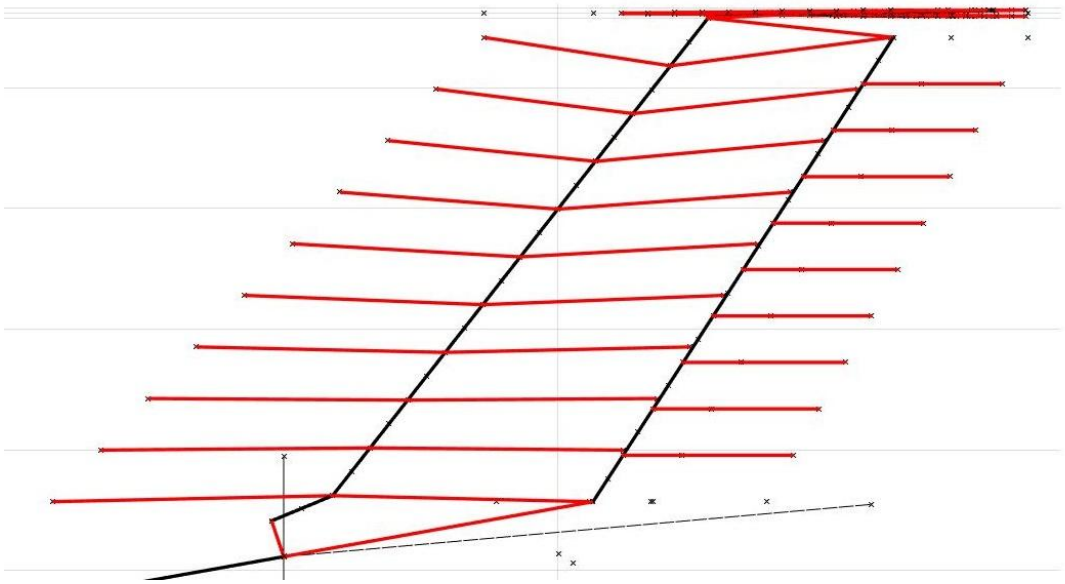

Figure 24. Vertical tail structure.

The aerodynamic has been created following the panels of the Nastran model (Figure 25):

- Vertical tail divided into two parts: vertical tail and vertical stabilizer sectors
- Vertical tail sector is divided into 20x10 aerodynamic panels (framed by red).
- Stabilizer sector is divided into 8x10 panels (framed by green).

These aerodynamic panels have been created in the same way as the wing ones: by using **CAERO** cards (in this case **CAERO0**), and then by defining the **SET1** and **SPLINE1** cards, the aerodynamic forces are linked to the structure.

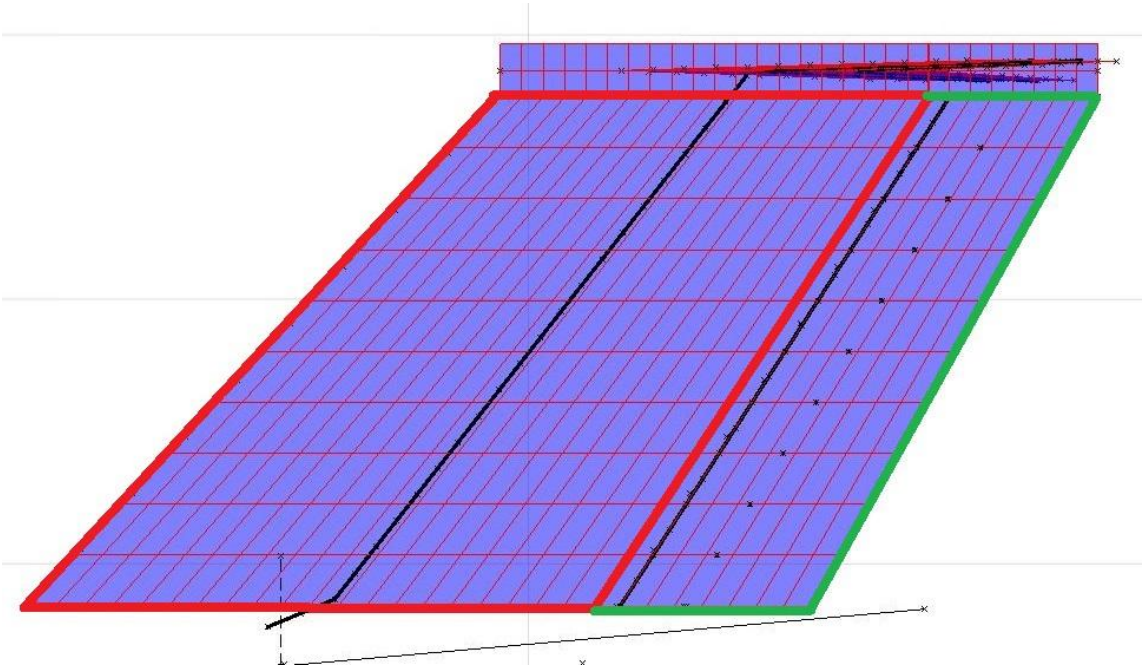

Figure 25. Vertical tail aerodynamic panels.

The horizontal tail is built in a similar way as the wing. The material and bar properties chosen to create the spar are:

MATERIAL	E (Pa)	G (Pa)	ν	ρ (kg/m3)
Aluminium	7.24E+10	2,7E+10	0,33	0
BAR PROPERTIES	**Area (m2)**	**I1 (m4)**	**I2 (m4)**	**J (m4)**
Root	1.73E-04	6.57-09	1.08E-09	7.30E-09
Center	1.20E-04	3.17E-09	5.20E-10	3.52E-09
Tip	9.60E-05	2.88E-09	2.24E-10	2.37E-09

Table 7. Horizontal tail spar properties.

The structure joins the spar with the aerodynamic nodes by using rigid bars. Then, the horizontal stabilizer is joined by using again rigid bars at the root and at the tip. The structure is showed on Figure 26.

Again, the aluminium mass is considered 0 because also this part of the tail was weighted in pieces ones built. This is the reason why the material is supposed without mass and all the structural mass is included as lumped mass.

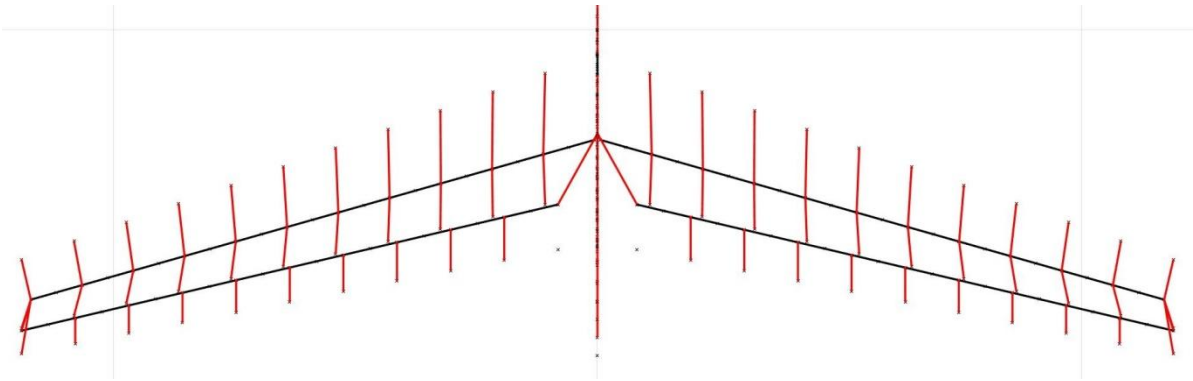

Figure 26. Horizontal tail structure.

The aerodynamic panels (see Figure 27) have been created as:

- Horizontal tail sectors: surfaces and stabilizer, both of them divided into root and center-tip.
- The surface root is divided into 2x3 aerodynamic panels while the stabilizer root into 2x4.
- The surface center-tip is divided into 10x3. The stabilizer part into 10x4.

And again, to define all this aerodynamic panels the cards **CAERO0** have been used. To link the aerodynamic forces with the structure **SET1** and **SPLINE1** cards have been applied.

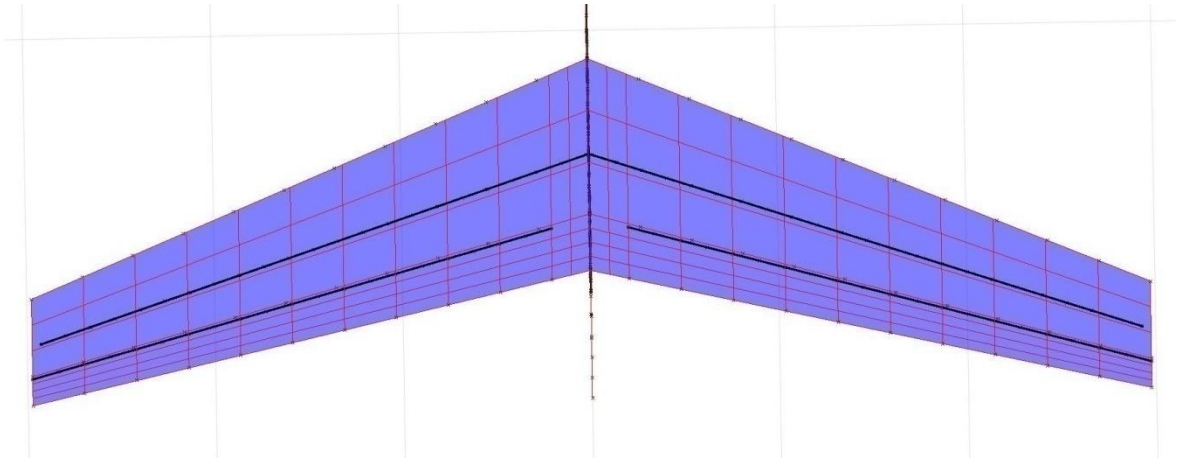

Figure 27. Horizontal tail aerodynamic panels.

4.4. JOINTS

Once defined each part of the aircraft by separate: fuselage, wing, tail cone, vertical tail and horizontal tail; it is necessary to choose the correct way to assemble them in order to:

- Simulate the real structure stiffness.
- Choose the correct nodes to connect
- Make the aircraft to respect the solid rigid vibration modes.

For the fuselage-wing union two rigid bars have been used from the closest fuselage node. This is similar to the solution adopted in Nastran.

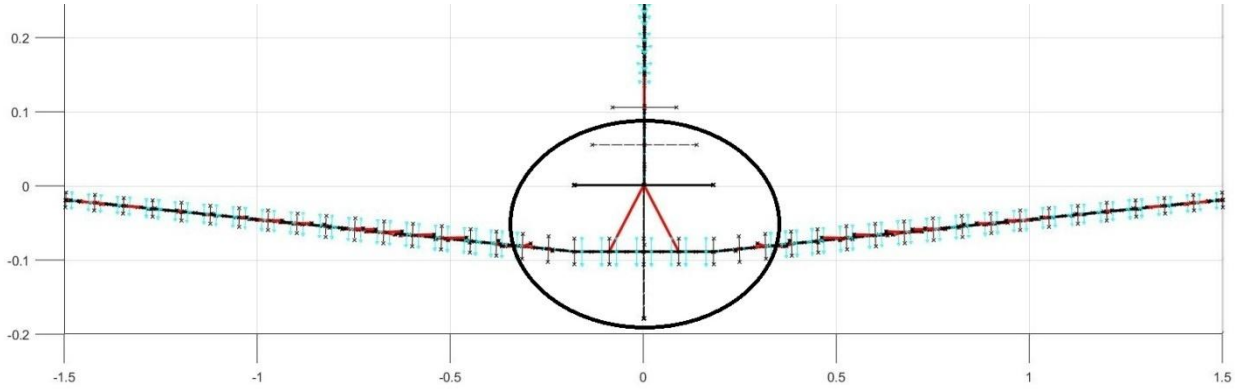

Figure 28. Wing-fuselage union.

The fuselage-cone joint has been done directly with NeoCASS as a prolongation of the fuselage as it can be seen on Figure 28. The same solution was performed in Nastran too.

The tail cone – vertical tail union has been the most difficult to create because the Nastran solution was not valid to be used in NeoCASS because of rigid bars in Nastran are less restrictive in master and slave nodes than NeoCASS, where it is necessary to obtain an absolutely linear structure without repeated nodes on rigid bars. Because of this, several solutions where tried:

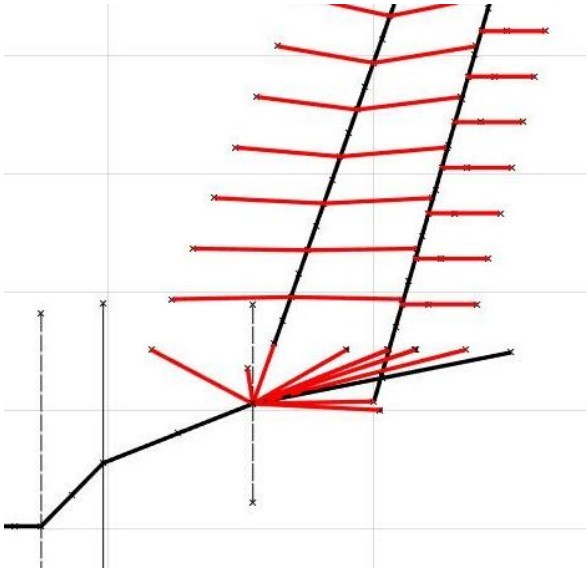

Figure 29. Tail cone - vertical tail union by using one master node.

- Rigid bars as RBE0 and RBE2: the same original problem.
- Skip some lines of the structure and join them directly to a primary master node (see Figure 29). It was not valid neither because there were too many nodes connected to the same master node and structural matrices dimensions failed.
- Create a rigid bar by defining a new material and bar properties with the objective to define a rigid bar by mean of a CBAR. For the structure it was acceptable enough, but when doing the modal analysis it was not considered rigid enough because the deformation energy was bigger than the allowed for the six solid rigid modes.

Finally, it has been necessary to scarify some aerodynamic nodes in order to simplify the union and fulfill the NeoCASS requirements to obtain a successful model. As it is shown on Figure 30, some nodes have been disengaged (crosses on the figure), and their mass repositioned to conserve as much as possible the original properties. Some aerodynamic information is lost this way, and this is the main source of mistakes of the NeoCASS model respect to the Nastran one.

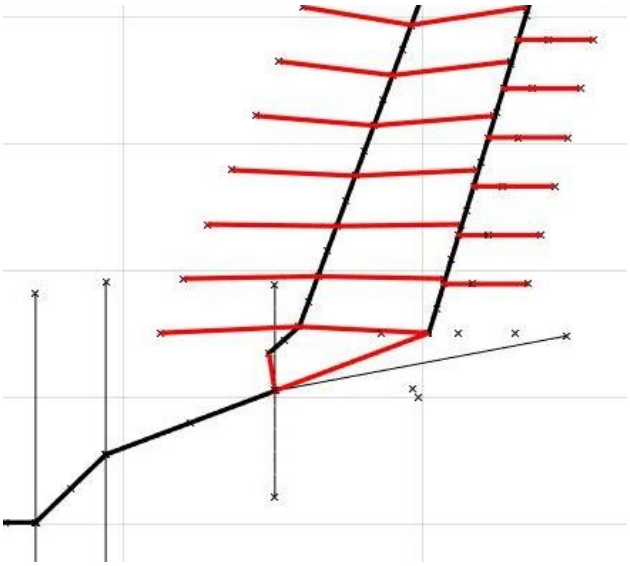

Figure 30. Final tail cone - vertical tail union.

The same problems where found when connecting the vertical with the horizontal tail. A similar solution was applied, leaving some free nodes and losing a little of aerodynamic information.

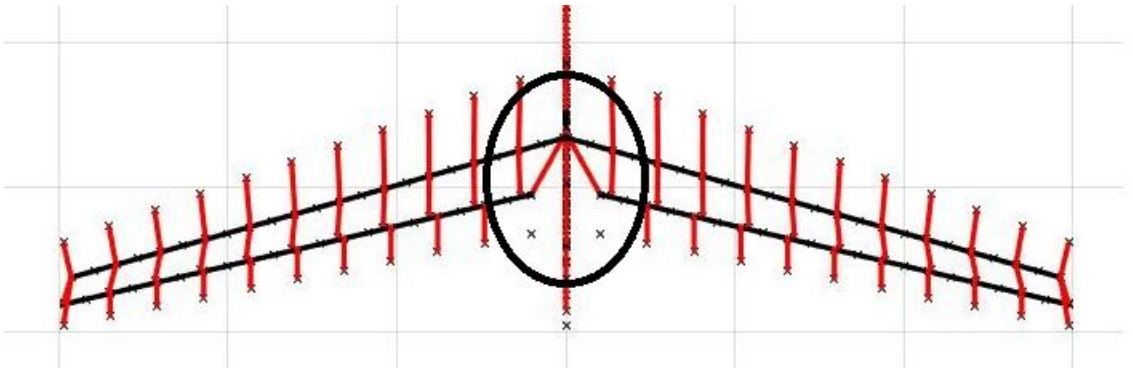

Figure 31. Vertical tail - horizontal tail union.

4.5. AIRCRAFT MODEL

Once assembled all the parts of the airplane, the complete aircraft model is shown on Figure 32.

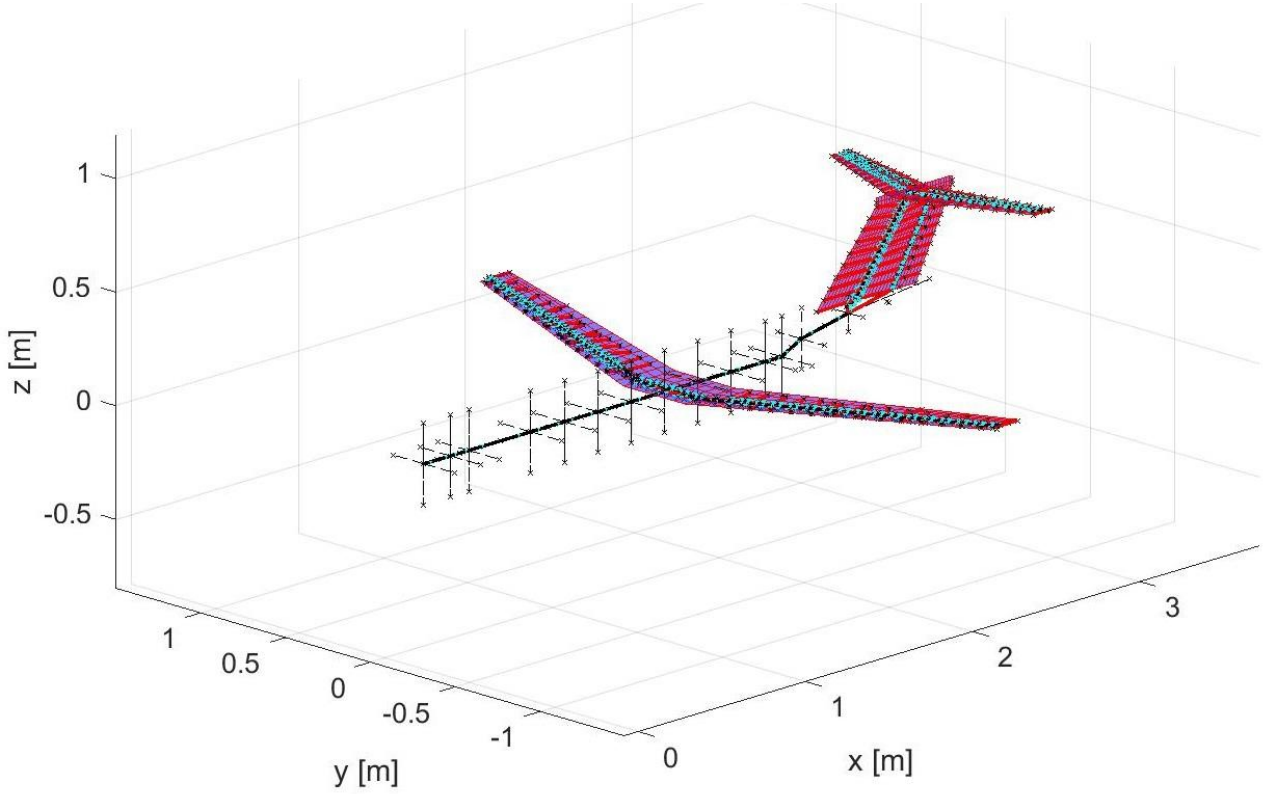

Figure 32. NeoCASS aircraft model.

Let's now compare the original one with the new model as it is shown on Figures 33 and 34. Both models have the same relative positions and dimensions.

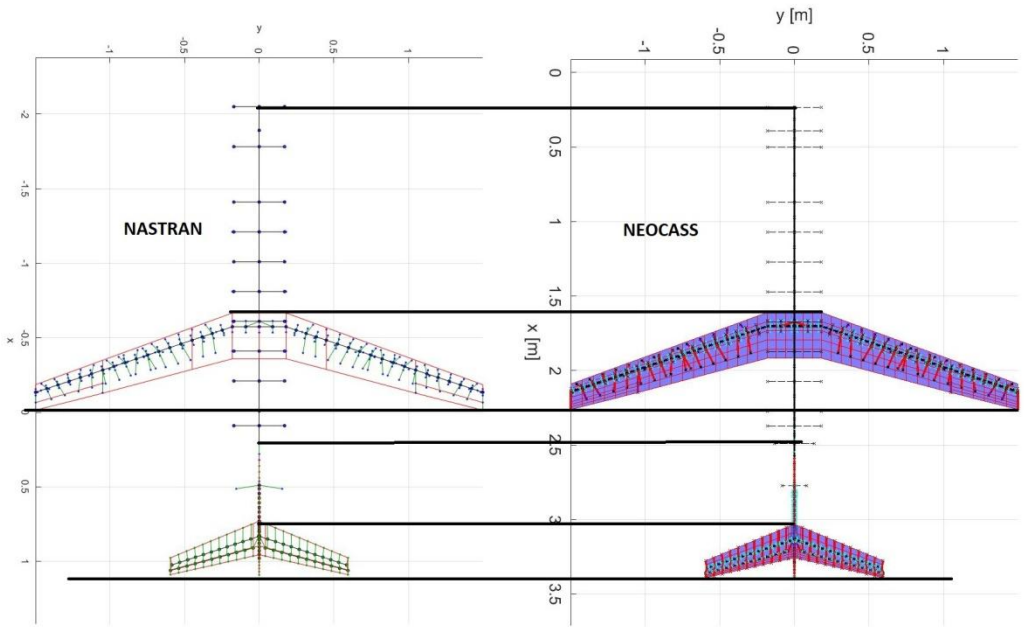

Figure 33. Top view comparison between Nastran and NeoCASS models.

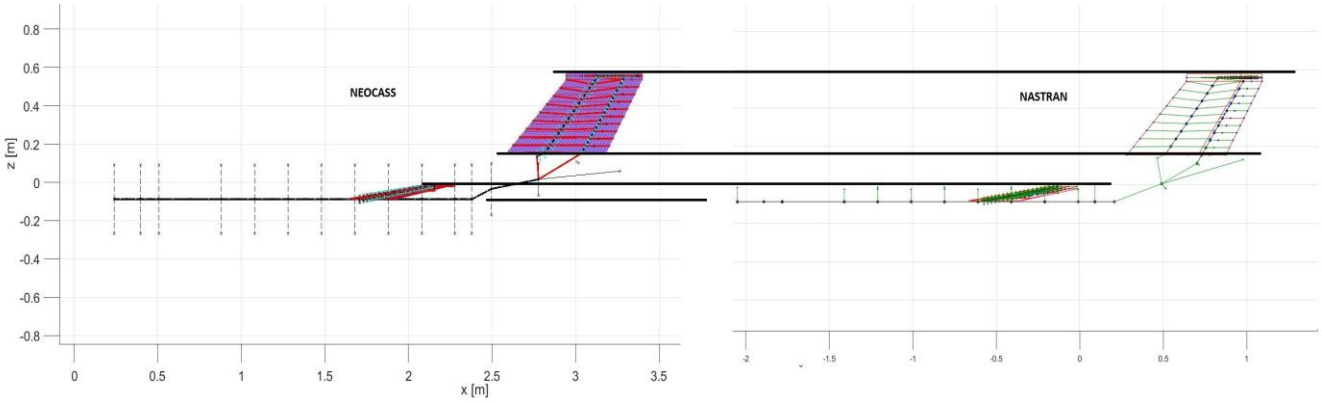

Figure 34. Profile view comparison between Nastran and NewCASS models.

To contrast the masses and center of gravity positions let's see Tables 8 and 9. The mass of the wing are the same while the fuselage and the tail have small variations (error smaller than 2%) because of the tail cone shape and the joints redefinition.

MASS	Nastran	NeoCASS
Fuselage	9.694	9.555
Wing	6.191	6.191
Tail	4.912	4.830
AIRCRAFT	20.798	20.716

Table 8. Aircraft model masses comparison in kg.

On the other hand, the X position of the center of gravity is almost correct in both fuselage and wing, while the tail suffers a bigger variation (error smaller than 2%). This is because the relocation of some masses due to the fact that the joints were redesigned and that the tail nodes are those of Acbuilder and not the original model ones.

Xcg	Nastran	NeoCASS
Fuselage	1.15	1.14
Wing	1.67	1.66
Tail	2.67	2.58
AIRCRAFT	1.66	1.63

Table 9. Aircraft model Xcg comparison in meters with reference on the front part of the fuselage with axis X oriented to the tail and coincident with the fuselage axis.

To sum up, the aircraft model has been created in the line with the original Nastran model and as it can be seen in the Figures 33 and 34, and on Tables 8 and 9, the final result is accurate enough to obtain comparable results in future flutter analysis.

5. ANALYSIS AND RESULTS

5.1. MODAL ANALYSIS

A normal mode analysis has been performed, the results for the modes with a natural frequency under 100 Hz are presented in Table 10. It can be noticed that the first six modes correspond to the solid rigid modes. Modal shapes until mode 20 can be found in Appendix C.

Mode	Frequenzy (Hz)	Mode	Frequenzy (Hz)
1	3.531E-06	**21**	49.3444
2	3.934e-05	**22**	52.6995
3	4.318E-05	**23**	55.1552
4	4.319E-05	**24**	55.9136
5	7.302E-05	**25**	63.7673
6	7.480E-05	**26**	64.8622
7	9.11712	**27**	67.5996
8	9.15187	**28**	73.5550
9	9.84641	**29**	75.8974
10	14.4680	**30**	79.4735
11	16.2920	**31**	82.3791
12	20.3703	**32**	86.3501
13	21.9743	**33**	86.3501
14	22.1016	**34**	87.9029
15	22.5038	**35**	89.3459
16	23.7356	**36**	90.534
17	25.9628	**37**	93.6007
18	31.7618	**38**	98.2789
19	43.1842	**39**	99.0113
20	44.6966	**40**	99.5639

Table 10. Modal frequencies until 100 Hz.

5.2. FLUTTER ANALYSIS

A flutter analysis has been performed with the following parameters showed on Table 11. There exist a flutter instability at v = 61.34 m/s (see Figure 35) for the mode 8 (see Figure 36), that is originated by a coupling of bending and torsional wing modes. All the flutter analysis on this thesis have been done with the 'Continuation Method' [22].

Reference chord	0.25 m
Mach number	0.1
Density	1.225 kg/m3
Reduced frequencies	0.001, 0.005, 0.01, 0.1, 0.25, 0.5, 0.6, 0.7, 0.8, 0.9, 1

Table 11. Flutter analysis parameters

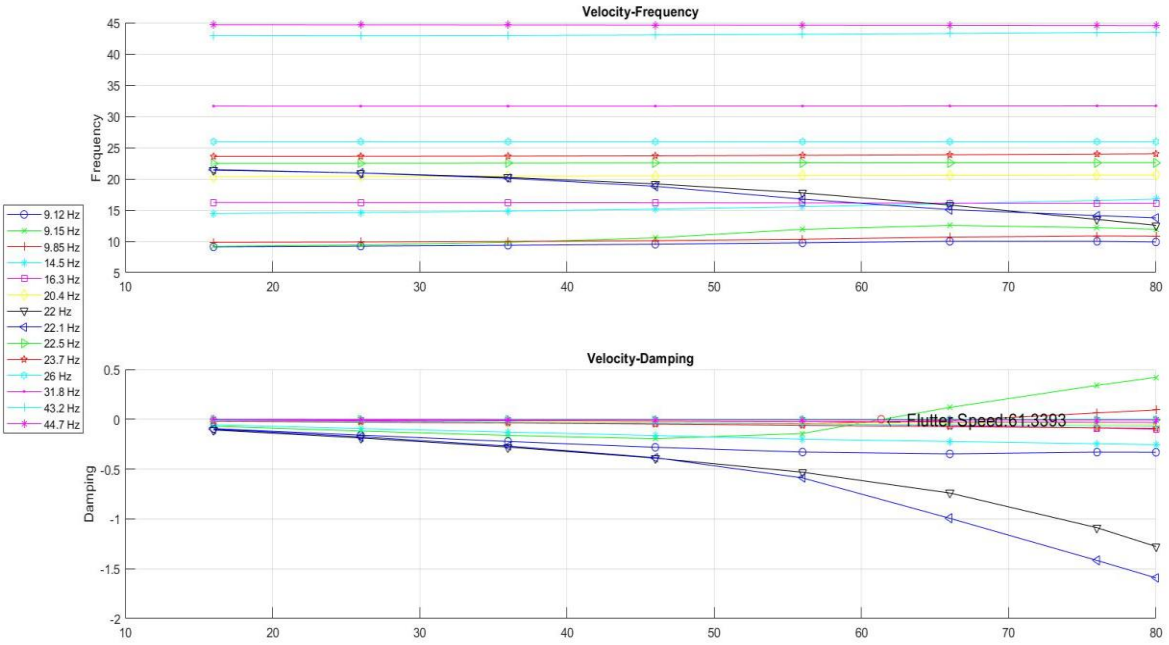

Figure 35. NeoCASS model flutter diagrams.

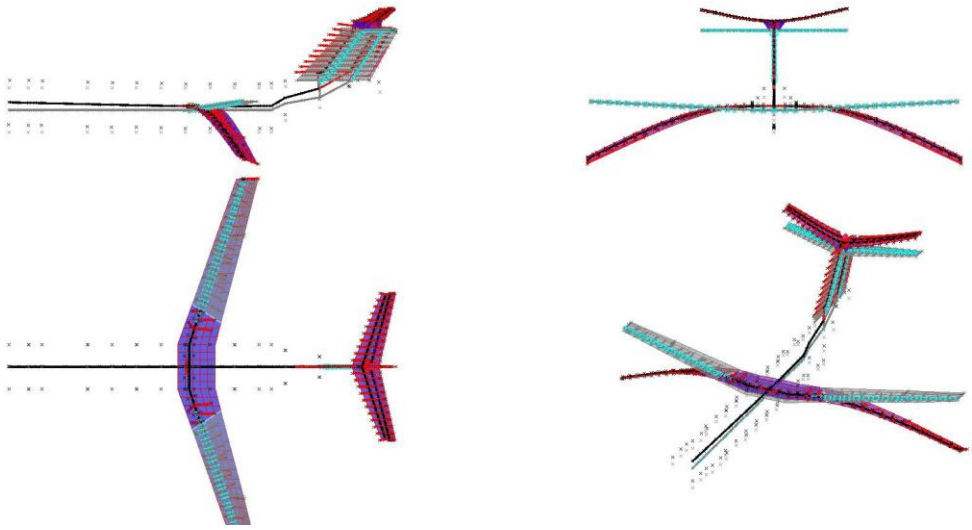

Figure 36. Flutter mode. Mode 8: f = 9.15187 Hz

Making a comparison with the Nastran flutter analysis results, one can see on Figure 37 that qualitatively the flutter solutions is are comparable even if not exactly the same, due to small differences in mode frequencies. After analyzing them, it seems to be due to the tail in the NeoCASS model is not as rigid as the Nastran one, probably because of the joints redesign and its consequences.

However, regarding again at Figure 37, the modes that are and will be affected by flutter during the tests (wing modes) are accurate enough to continue with the analysis and obtain qualitative conclusions, and also some qualitative values.

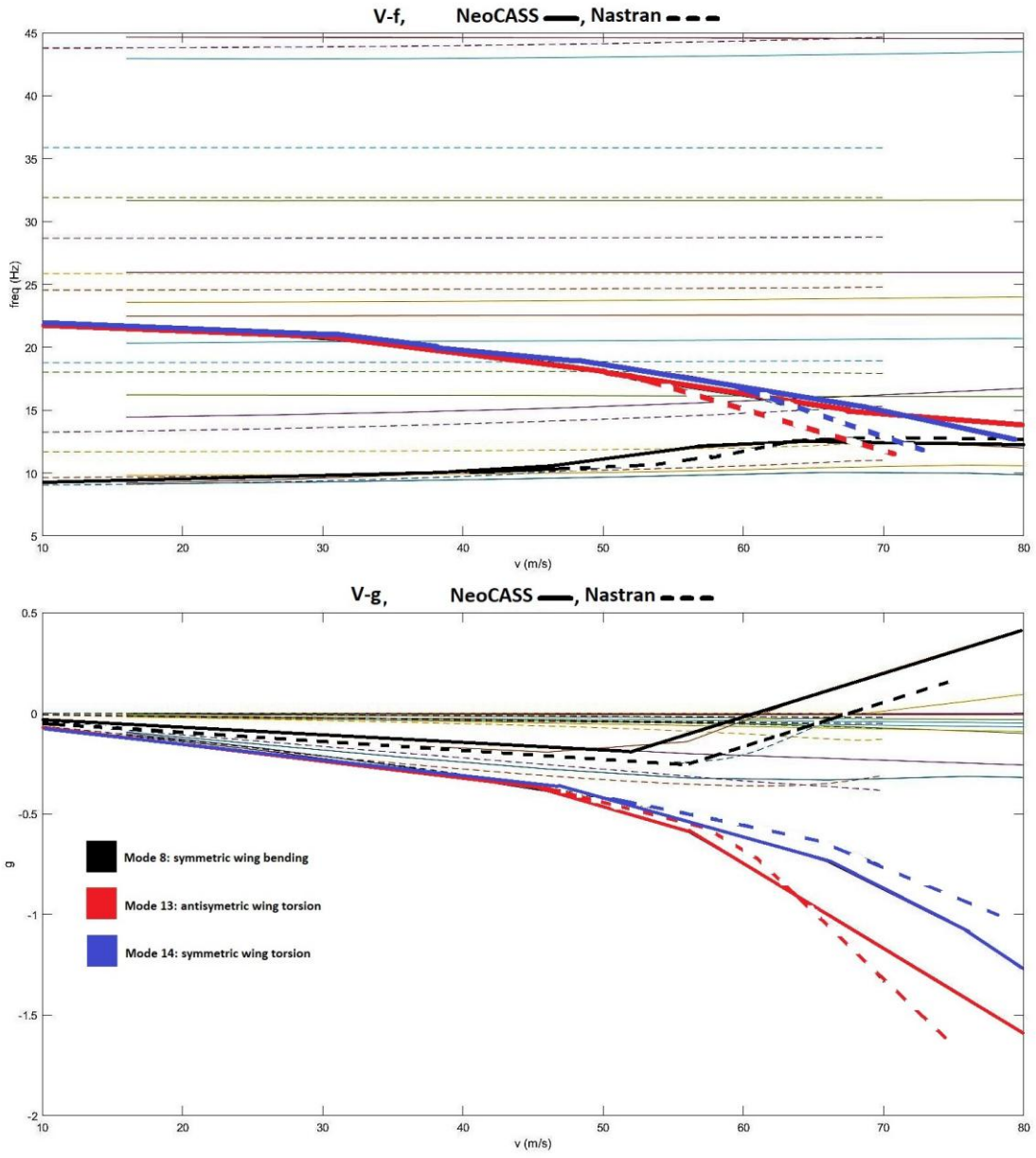

Figure 37. Nastran and NeoCASS flutter analysis comparison.

5.3. FLUTTER ANALYSIS WITH LUMPED MASS AT THE TIP

The objective of this test is to understand the flutter modes that appear and to obtain feasible flutter velocities to test the physic model in the wind tunnel. As it is shown before, flutter velocity of the model is around 60 m/s, and it is not possible to reach that velocity in wind tunnel. This is the reason why some mass should be added to the model in order to obtain a smaller velocity flutter into the wind tunnel velocity limits. The idea is to reach flutter under 45 m/s to solve the problem.

In this section it is considered a mass 'M' that varies from 0 to 250 g and is moved from back to front of the tip chordwise, considering the back the trailing edge (100% of the tip chordwise) and the front the leading edge (0% of the tip chord) by using the tip chord reference system (let's call it 'C').

The analysis consists on obtaining the flutter velocity at each point (M, C). Let's start by working on each C and just moving M and then it all together will be plotted. That graphic will be useful to decide the physic model characteristics before and during the wind tunnel tests.

5.3.1. TEST 1: MASS ADDED AT 100% OF THE TIP CHORDWISE

This test consist on studying the point (M, C) = (M, 100) by changing M value. To do this, the developed NeoCASS code has included a test section. Table 12 shows the obtained results. The flutter velocity is reduces due to the mass at C = 100 helps the excitation of the torsion modes, and so, bigger is the mass, smaller the flutter velocity is.

M(kg)	V_flutter	f (Hz) B+T	f (Hz) T
0.000	61.34	9.15	22.10
0.010	57.94	9.06	21.56
0.025	53.05	8.91	20.77
0.050	48.19	8.68	19.59
0.100	39.37	8.21	17.85
0.150	35.60	7.78	14.30
0.200	33.27	7.39	14.27

Table 12. Test 1 results: (M, C) = (M, 100%) with M variable. 'B' means bending mode while 'T' means torsion mode.

After studying the modes that gets flutter, one realizes that at the beginning there is a mode that is the composition of the 1st bending mode (major part) and the 1st torsion mode. When the mass becomes bigger, around 150 g, the flutter mode changes becoming just the 1st torsion mode. With M = 200 g, one can see that the 2nd bending mode the one that is more excited and this is the reason why the 1st bending mode disappeared. Damping is reduced when mass grows, what means that flutter will appear sooner because the structure is not damped enough to support the wind energy.

The flutter diagrams of the mode that gets flutter are shown on Figure 38.

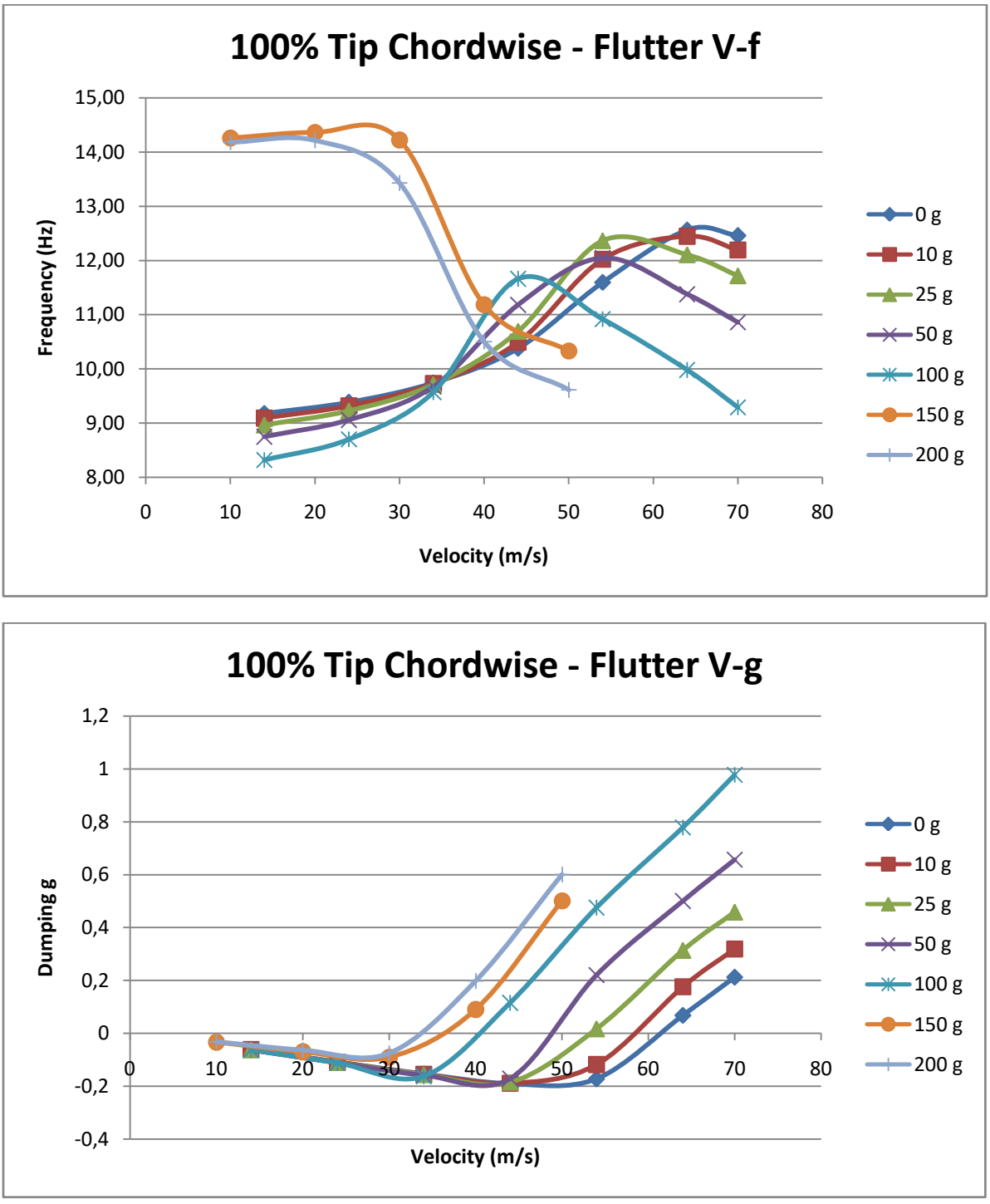

Figure 38. (M, C) = (M, 100%) flutter diagrams for the bending mode (0g to 100g) and torsion mode (150g to 200g).

This shows that is very effective to add an extra lumped mass at C = 100% if the interest is to down the flutter velocity. Nevertheless, it is important to check correctly the information in order to not get into a not desired flutter mode.

5.3.2. TEST 2: MASS ADDED AT 80% OF THE TIP CHORDWISE

Following the same steps as in test 1, the mass is now nearer to the elastic center (take into consideration that C = 100% is the limit position), and so the behavior is smoother. Table 13 and Figure 39 present the test results.

M(kg)	V_f (m/s)	f (Hz) B	f (Hz) T
0.000	61.34	9.15	22.1
0.010	58.98	9.06	21.84
0.025	56.53	8.93	21.46
0.050	51.40	8.72	50.88
0.100	47.51	8.31	19.78
0.150	45.65	7.94	19.01
0.200	40.80	7.61	18.40

Table 13. Test 2 results: (M, C) = (M, 80%) with M variable. 'B' means bending mode while 'T' means Torsion mode.

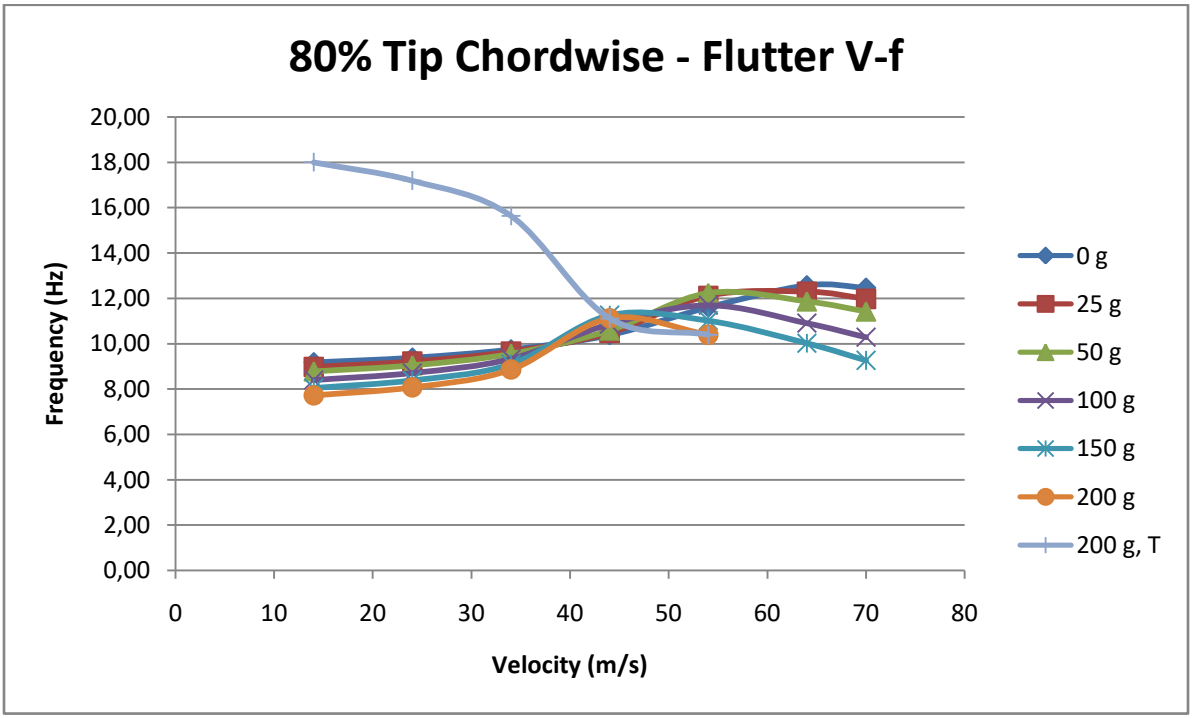

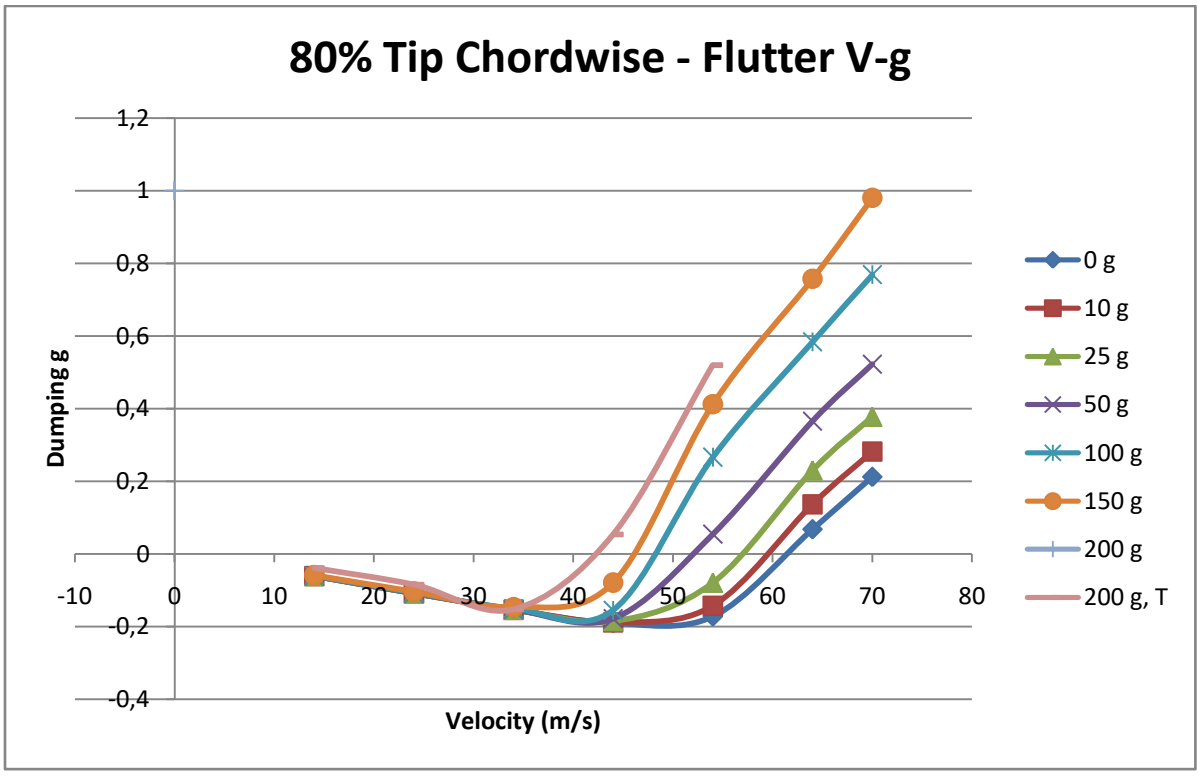

Figure 39. (M, C) = (M, 80%) flutter diagrams for the bending mode (0g to 150g) and torsion mode (200g).

As it is possible to see, the flutter velocity varies slower than during test 1 but there is still an important variation that could be useful for the physic model. Again, a torsion mode is reached with the biggest mass tried. In this case, with M = 200 g both modes gets flutter at the same time, what means that bending lose importance.

5.3.3. TESTS 3 AND 4: MASS ADDED AT 60% AND 40% OF THE TIP CHORDWISE

From this test to the last one, there only exists one flutter mode, and it is bending plus torsion. The mass now is located closer to the elastic axis, and so it is more difficult to make appear the torsion mode alone, what means also that it is more difficult to decrease the flutter velocity. Results are shown on Table 14 and Figure 40, and it can be seen that M has increased its value respect to the first tests. To obtain acceptable flutter velocities for the wind tunnel it is necessary to add between 600 g and 1 kg of lumped mass in C = 60%.

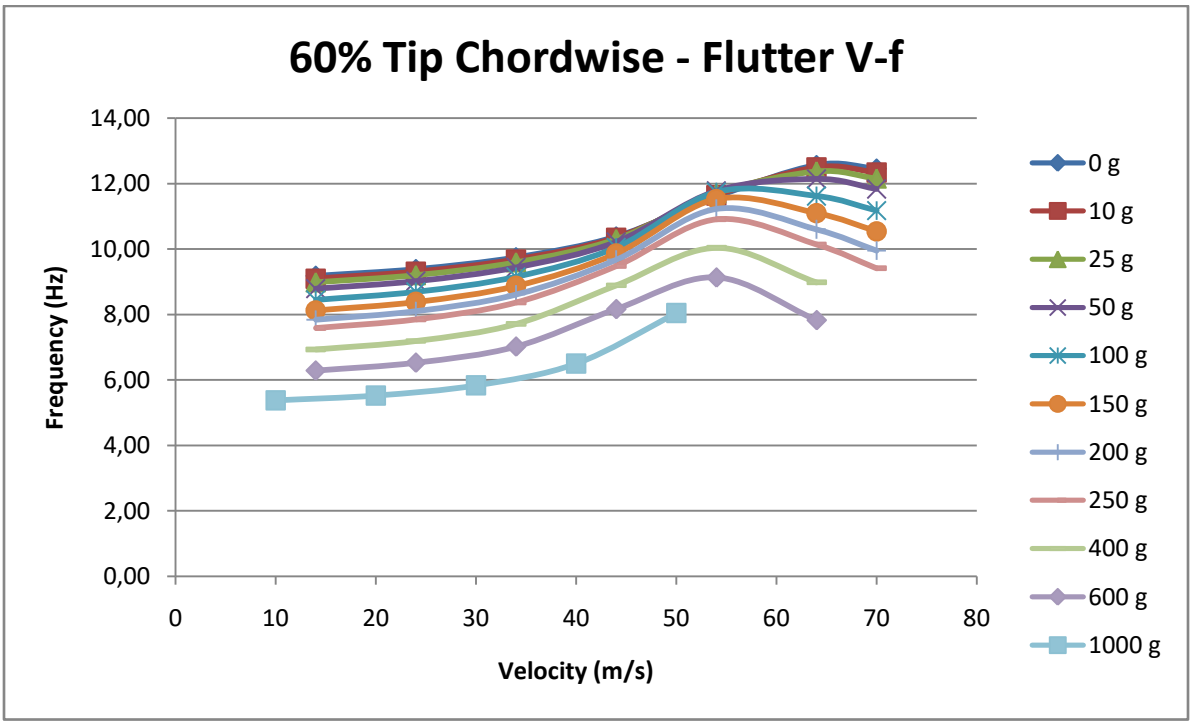

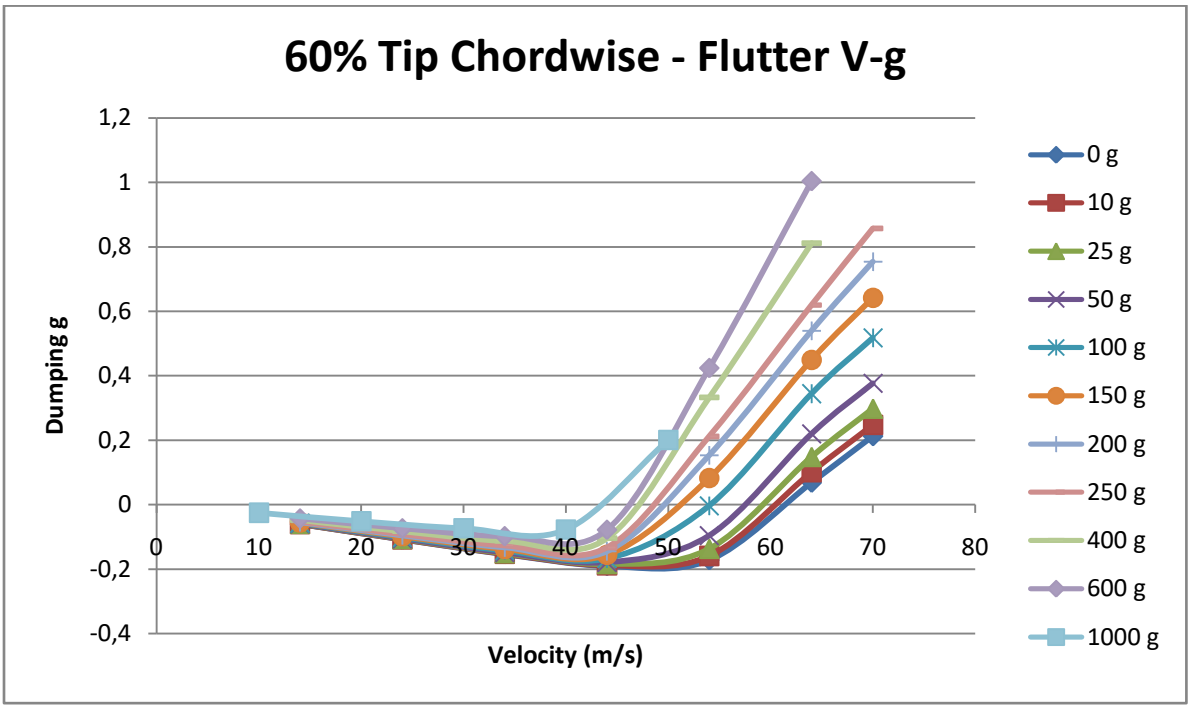

Figure 40. (M, C) = (M, 60%) flutter diagrams for the bending mode.

Moving onto test with C = 40% (Table 15 and Figure 41), it is even more extreme. The flutter velocity does not change and it is because the elastic axis is very near. In this case it is not possible with a realistic mass to obtain flutter in the wind tunnel.

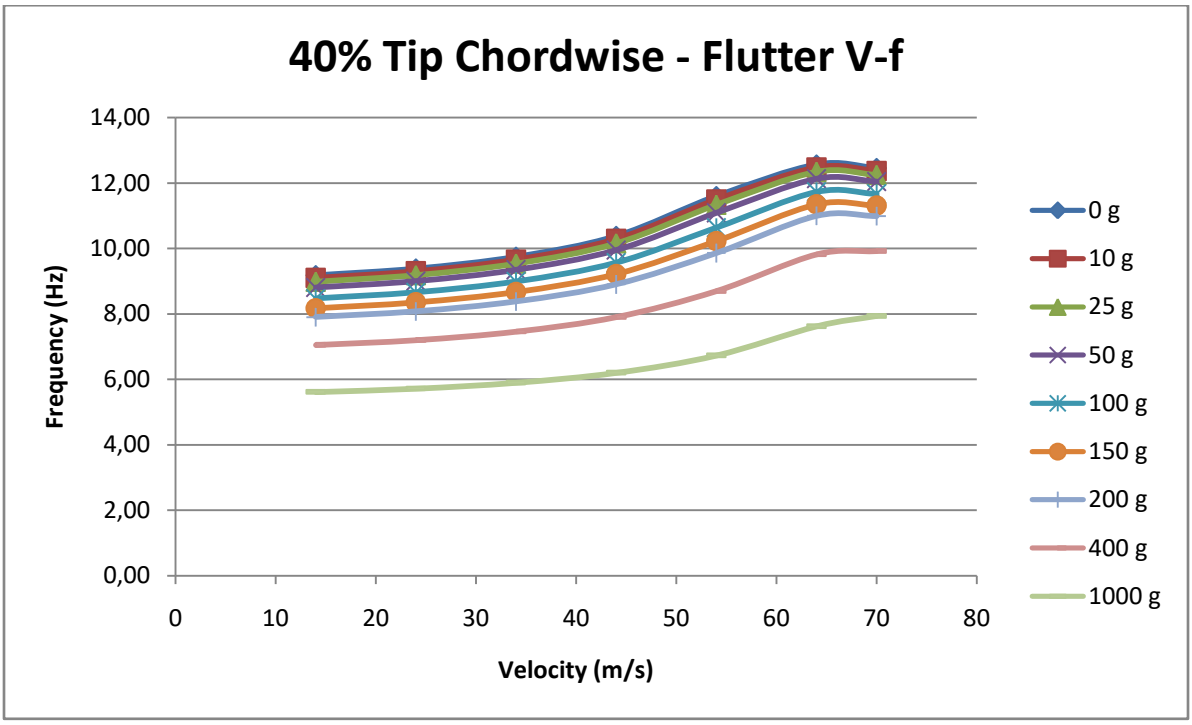

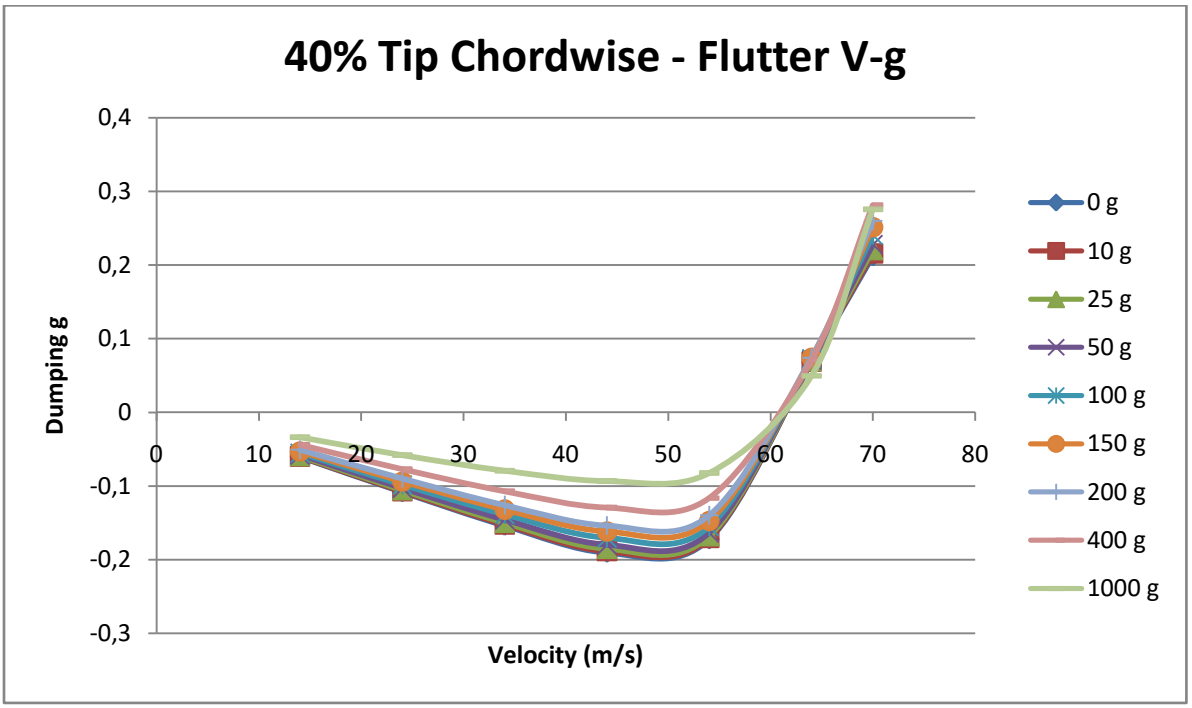

Figure 41. (M, C) = (M, 40) flutter diagrams for the bending mode.

M(kg)	V_f (m/s)	f(Hz) B
0.000	61.34	9.15
0.010	59.96	9.07
0.025	58.69	8.94
0.050	56.99	8.75
0.100	54.11	8.39
0.150	50.20	8.06
0.200	48.49	7.77
0.250	47.55	7.50
0.400	46.18	6.84
0.600	45.41	6.20
1.000	42.39	5.34

Table 14. Test 3 results: (M, C) = (M, 60%) with M variable. 'B' means bending mode.

M(kg)	V_f (m/s)	f(Hz) B
0.000	61.34	9.15
0.010	60.97	9.07
0.025	60.89	8.96
0.050	60.78	8.77
0.100	60.59	8.44
0.150	60.43	8.13
0.200	60.30	7.86
0.400	59.95	7.01
1.000	59.96	5.58

Table 15. Test 4 results: (M, C) = (M, 40%) with M variable. 'B' means bending mode.

5.3.4. TESTS 5 AND 6: MASS ADDED AT 20% AND 0% OF THE TIP CHORDWISE

Positions forward the elastic axis are reached and it means that adding extra mass is now profitable to avoid flutter. Even if a priori it is not useful for the wing tunnel test, it could be utilized to correct mistakes or calculation errors by adding extra mass in this positions. This will allow versatility and resolve some problems that may appear during the physic tests. Tables 16 and 17 and Figures 42 and 43 show the results. It is important that with C = 0% the flutter mode changes and the 2nd bending mode occurs. It can be explained because the mass in this position avoid torsion modes, and so arrives directly the mentioned one.

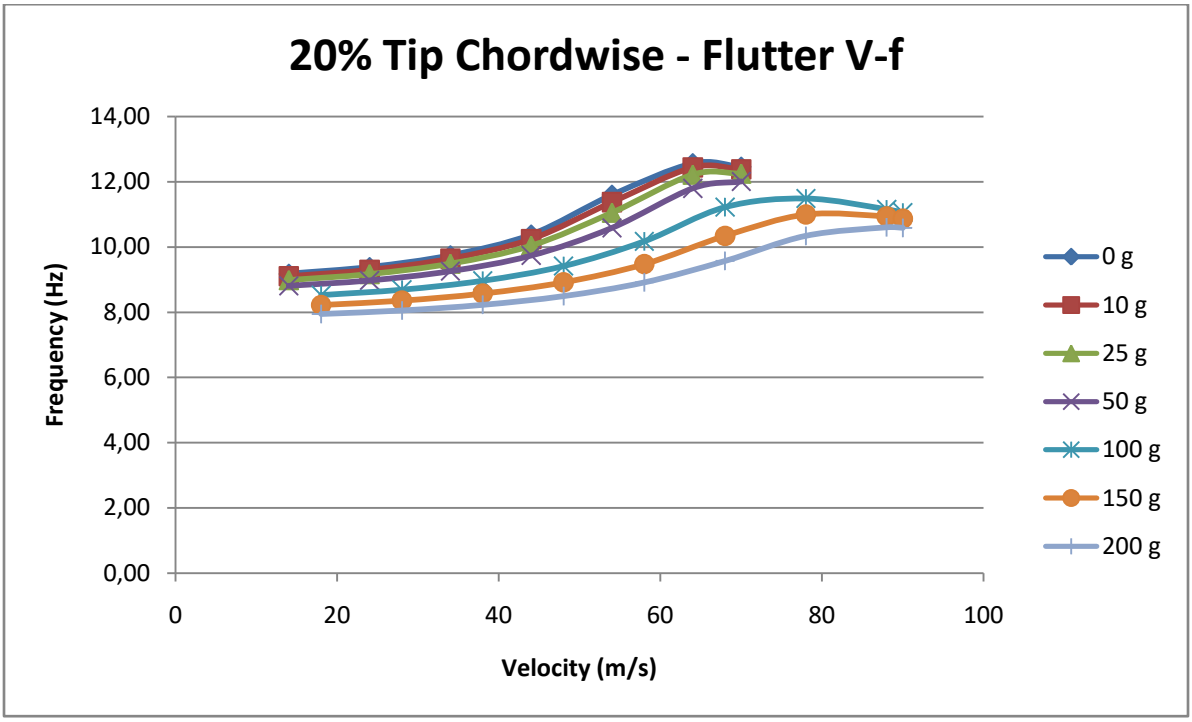

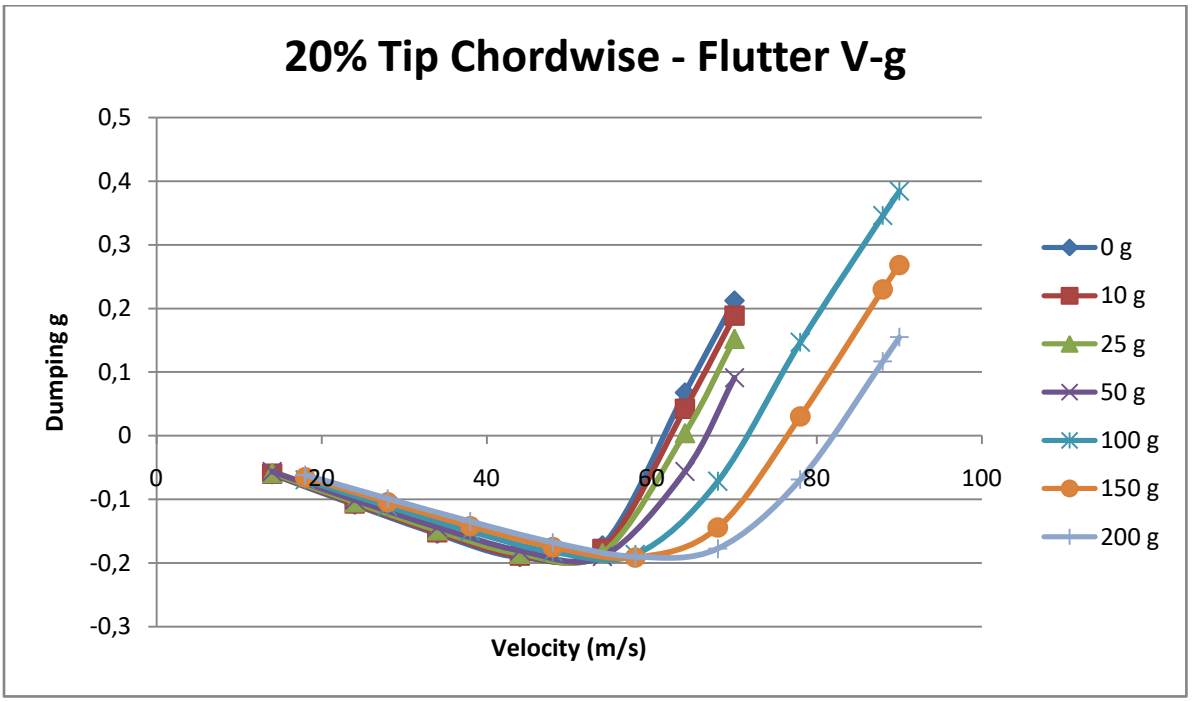

Figure 42. (M, C) = (M, 20%) flutter diagrams for the bending mode.

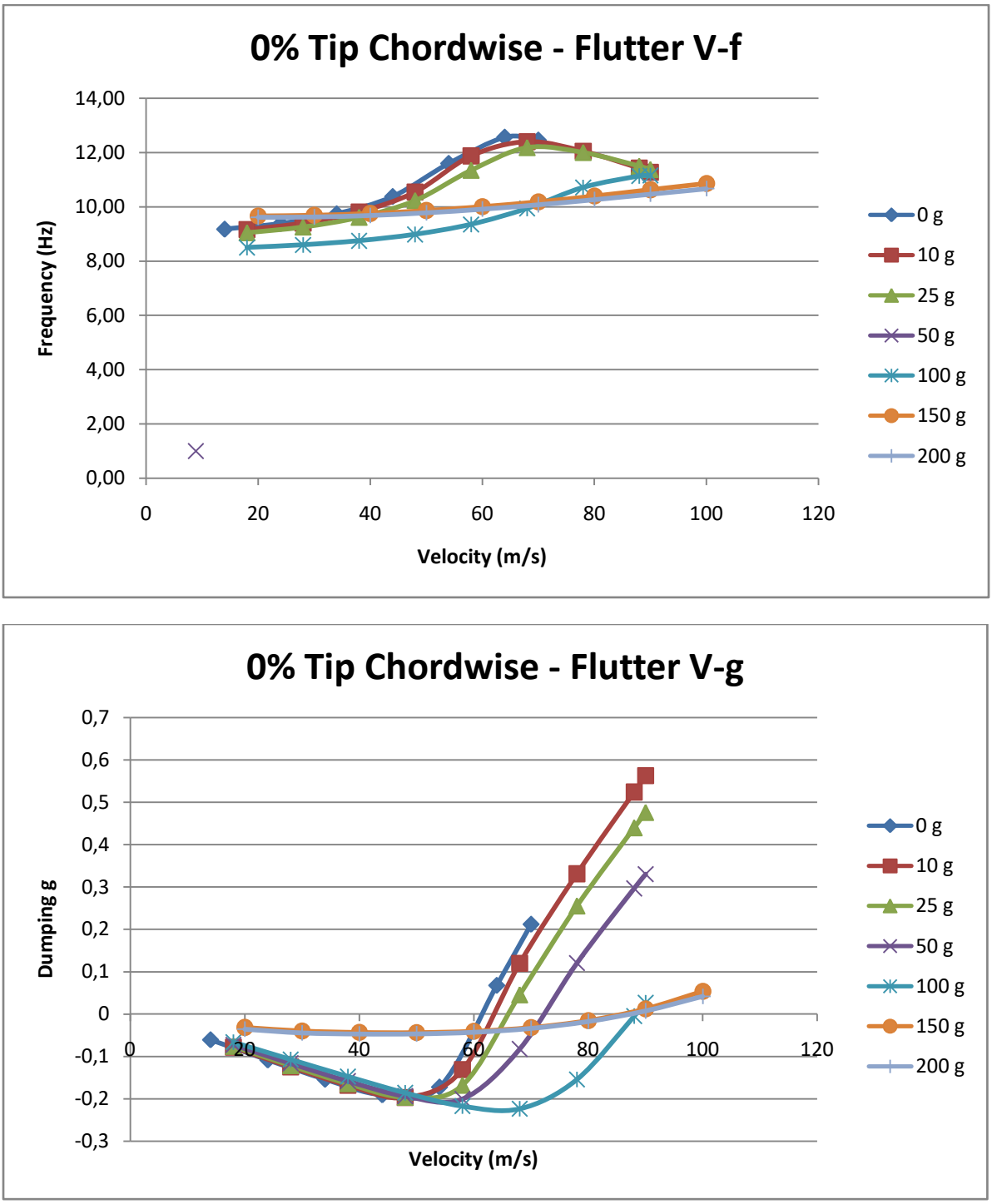

Figure 43. (M, C) = (M, 0%) flutter diagrams for the bending mode (0g to 100g) and torsion mode (150g to 200g).

M(kg)	V_f (m/s)	f(Hz) B
0.000	61.34	9.15
0.010	61.94	9.08
0.025	63.76	8.97
0.050	66.23	8.79
0.100	71.24	8.47
0.150	74.26	8.17
0.200	76.85	7.91

Table 16. Test 5 results: (M, C) = (M, 20%) with M variable. 'B' means bending mode.

M(kg)	V_f (m/s)	f(Hz) B	f(Hz) T
0.000	61.34	9.15	22.10
0.010	63.12	9.08	21.95
0.025	65.75	8.98	21.74
0.050	72.02	8.80	21.47
0.100	80.77	8.48	21.13
0.150	78.06	8.18	20.90
0.200	77.58	7.91	20.69

Table 17. Test 6 results: (M, C) = (M, 0%) with M variable. 'B' means bending mode while 'T' means torsion mode.

With an increment of mass the flutter mode is more damped and its frequency is reduced, which means that the flutter velocity rise up. However, after M = 150 g in the case of C = 0%, it is possible to see a change in this tendency, and it is because the flutter mode has changed from bending coupled with some torsion to pure torsion mode.

5.3.5. COLLECTION OF TEST RESULTS

Table 18 and Figure 44 include the main information to choose the (M, C) point depending on the desired flutter velocity desired for the wind tunnel tests.

	Mass at Tip Chord (g)					
	10	25	50	100	150	200
% Tip Chord	Flutter Velocities (m/s)					
0	63.12	65.75	72.02	80.77	78.06	77.58
20	61.94	63.76	66.23	71.24	74.26	76.85
40	60.97	60.89	60.78	60.59	60.43	60.30
60	59.96	58.69	56.99	54.11	50.20	48.49
80	58.98	56.53	51.40	47.51	45.65	40.80
100	57.94	53.05	48.19	39.37	35.60	33.27

Table 18. Flutter velocity depending on the lumped mass at the tip with chordwise variation.

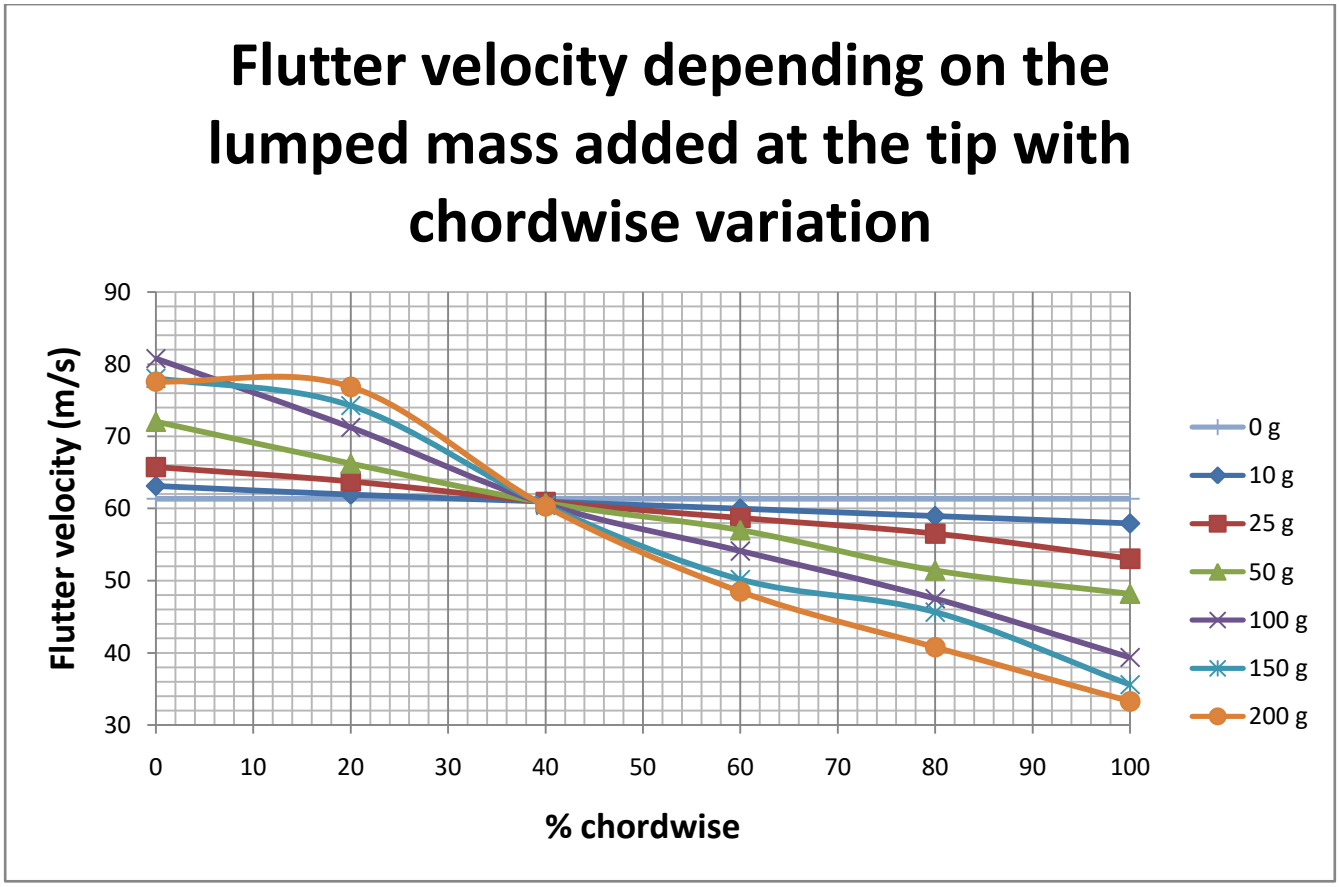

Figure 44. Flutter velocity depending on the lumped mass at the tip with chordwise variation.

It is important to remark that the flutter modes found are:

- Bending plus torsion (in the majority of the graph).
- Torsion: for (M > 150 g, C = 100%) and (M > 200 g, C = 80%). The contour of this point is an area where it is possible to find this mode.

- 2nd Bending mode for (M > 150 g, C = 0%). If position C = 0% used only to make corrections with small masses no problem should appear.

Taking into consideration these remarks and to be sure to obtain the mode formed by the coupling of bending and torsion with a flutter velocity acceptable for the wind tunnel it is recommendable the solution M = 100 g from C = 80% to 100%.

It has been registered also the information of how the bending and torsion structural modes change depending on the (M, C) conditions. This is important because the coupling of these modes makes increase or decrease the flutter velocity in the majority of cases Remembering Figure 37, one can see how both modes frequencies converge to the same causing a coupled more dangerous mode.

On Figure 45 it is shown how the torsion mode frequency is affected by these parameters. One can find the elastic axis at the point where the mode frequency does not change (between C = 30% - 40%). When the distance respect to the elastic axis or the mass are increased, the torsion mode frequency is reduced slightly next to the leading edge and significantly close to the trailing edge, what means that it will be easier to arrive to the bending-torsion frequency convergence. Nevertheless, this problem does not exist when the mass goes closer to the leading edge (even if in the graphic one can see the same effect) because it creates a wing twist angle that opposes to the aerodynamic one.

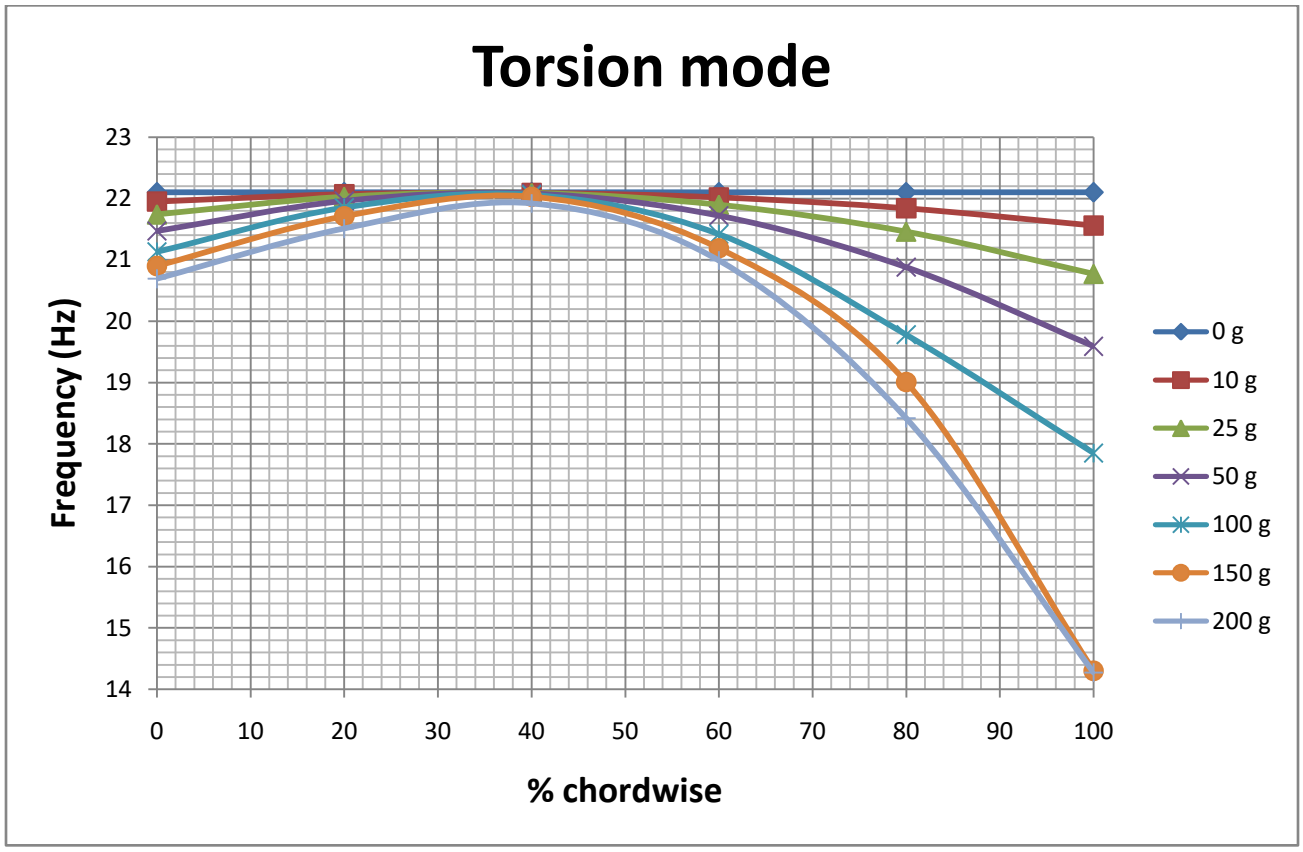

Figure 45. Torsion mode frequency depending on the lumped mass at the tip with chordwise variation.

On Figure 46 it is shown how the bending mode frequency is affected by (M, C) parameters. It is shown that the frequency is lower when getting further from the leading edge. However, this frequency decreases slower that the torsion one, and so, the torsion frequency variation is more critical for flutter. While the chordwise variation is not critical, the mass fluctuation means an important frequency change.

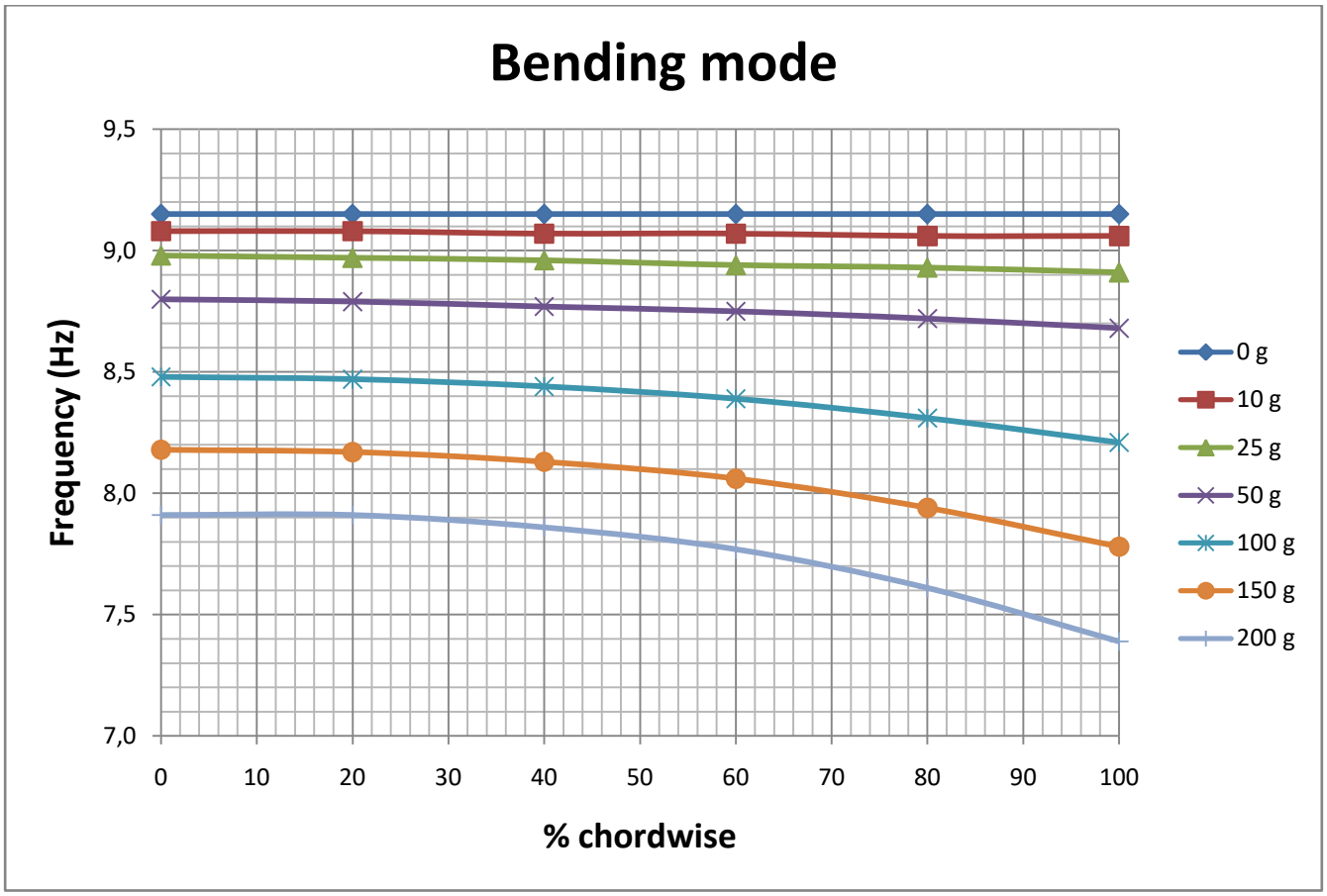

Figure 46. Bending mode frequency depending on the lumped mass at the tip with chordwise variation.

5.4. FLUTTER ANALYSIS DEPENDING ON THE ENGINES MASS AND POSITION

A parametric analysis of the engine mass and position has been performed. The mass has been changed from 0 g to 500 g and the x position of the engine (with reference system in the center of gravity of the engine and x axis parallel to the body axis, positive direction throw the tail) varies from -0.05 m to 0.10 m. A bigger range has not been studied because the engine position has a structural limit that depends on the clamping system.

Starting from the x = 0.10m position of the engine, it is possible to realize that both frequency and damping of the flutter mode (that in this case is still the bending mode) does not change significantly respect to the wing without engine. In Table 19 and Figure 47 it is shown how small that variation is.

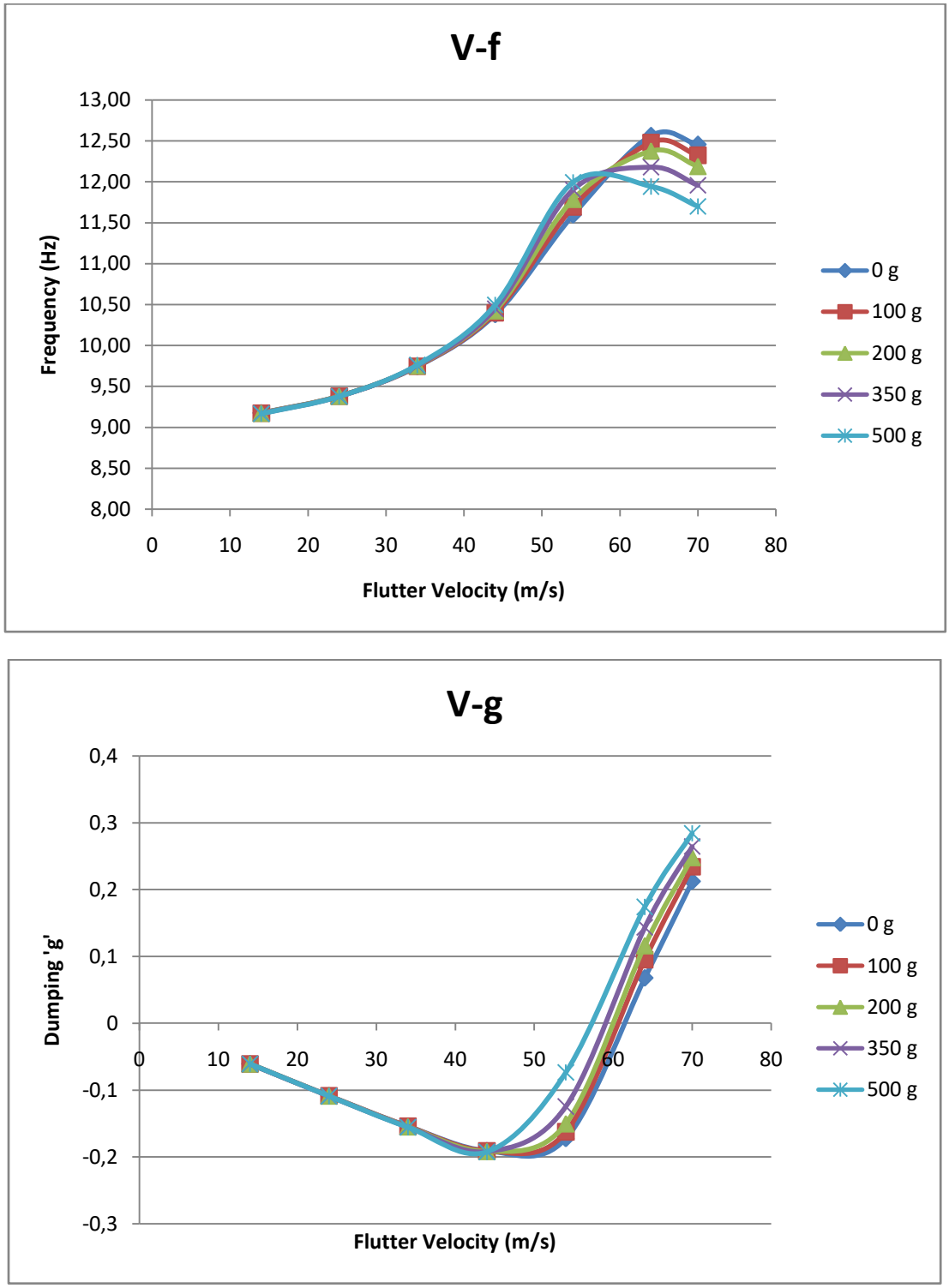

Figure 47. x = 0.10m flutter diagrams for the bending mode.

M(kg)	V_flutter	f (Hz) B	f (Hz) T
0.000	61.34	9.15	22.1
0.100	60.16	9.15	21.6
0.200	59.53	9.15	21.14
0.350	58.16	9.14	20.72
0.500	56.95	9.14	20.52

Table 19. Engine test results for x = 0.10m. 'B' means bending mode.

The flutter velocity is slightly reduced but it does not suffer a significant change. However, also a bigger mass has been tried and other problems have been found.

With 1kg of mass, the engine modes start to develop an important role in flutter analysis, meaning that it is very important to check the mass and the engine position respect to the elastic center to avoid this situation. Figure 48 shows the flutter diagrams of this configuration. In this case the engine-pylon modes participate to a flutter coupled with bending and torsion modes. This causes that the flutter speed decrease until 47.31 m/s and means that it is very important to check engine modes not to be dangerous for flutter in engineering phase of the aircraft model.

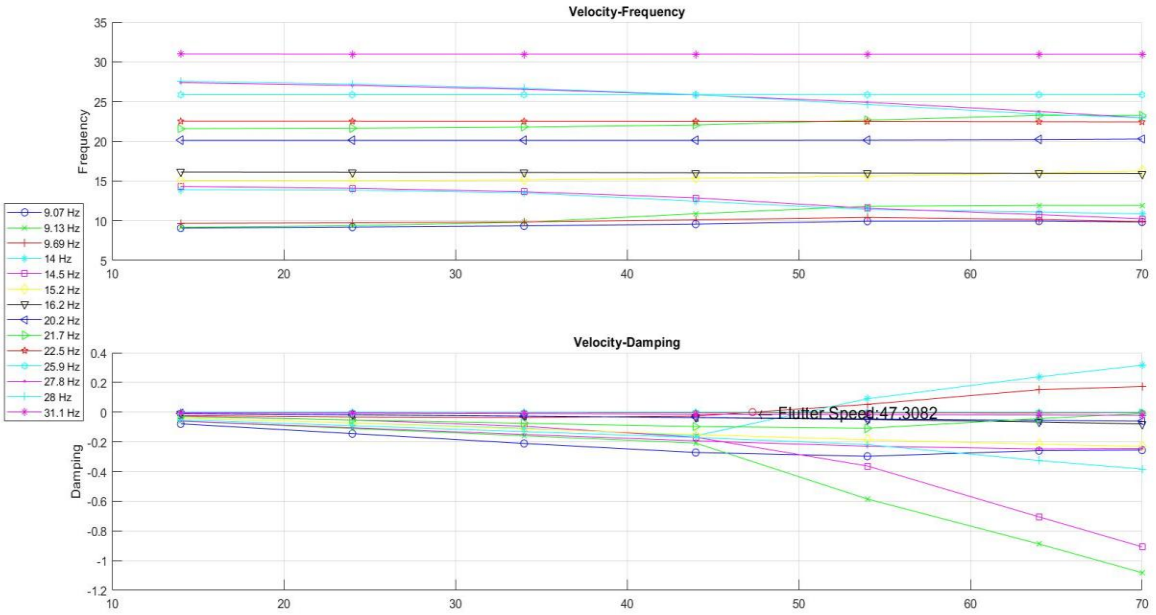

Figure 48. x=0.1m and M=1kg engine flutter test.

Tests with x = 0.05, 0.00 and -0.05 m have been performed too, causing even smaller variations than the x = 0.10m test. The final results are shown on Figures 49, 50 and 51. The flutter velocity decreases

but less than during the tip tests, what shows that the engine position (closer to the fuselage) affects just lightly to the wing without engine modes until 500 g of mass. However, as seen before, the engines danger is found in the engine modes (in example, pitch and yaw), becoming a source of flutter problems if the design is not done correctly.

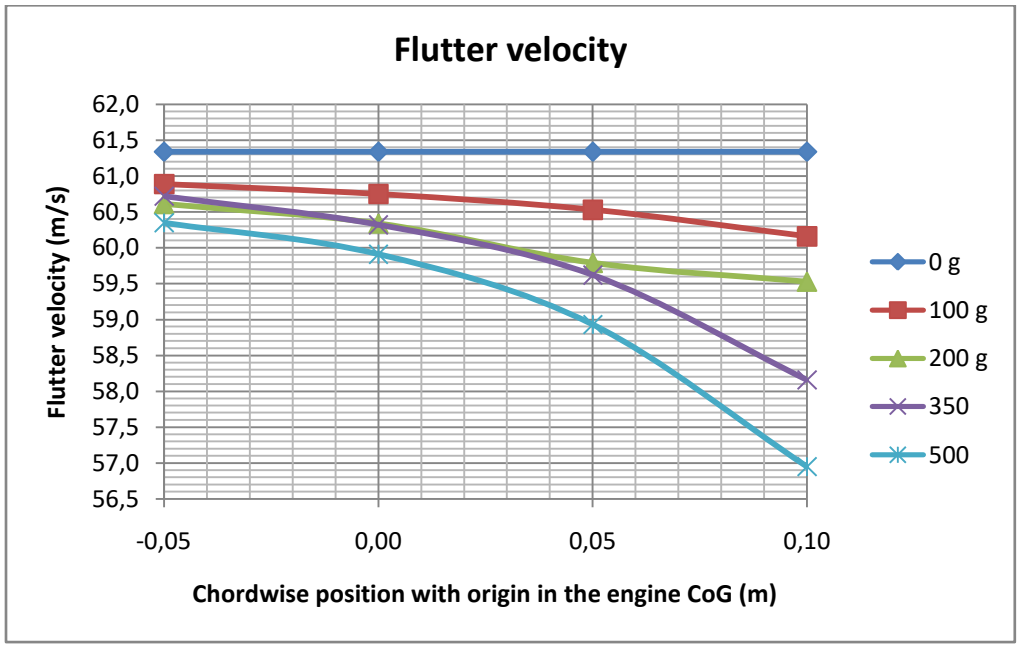

Figure 49. Flutter velocity depending on the engine chordwise position and its mass.

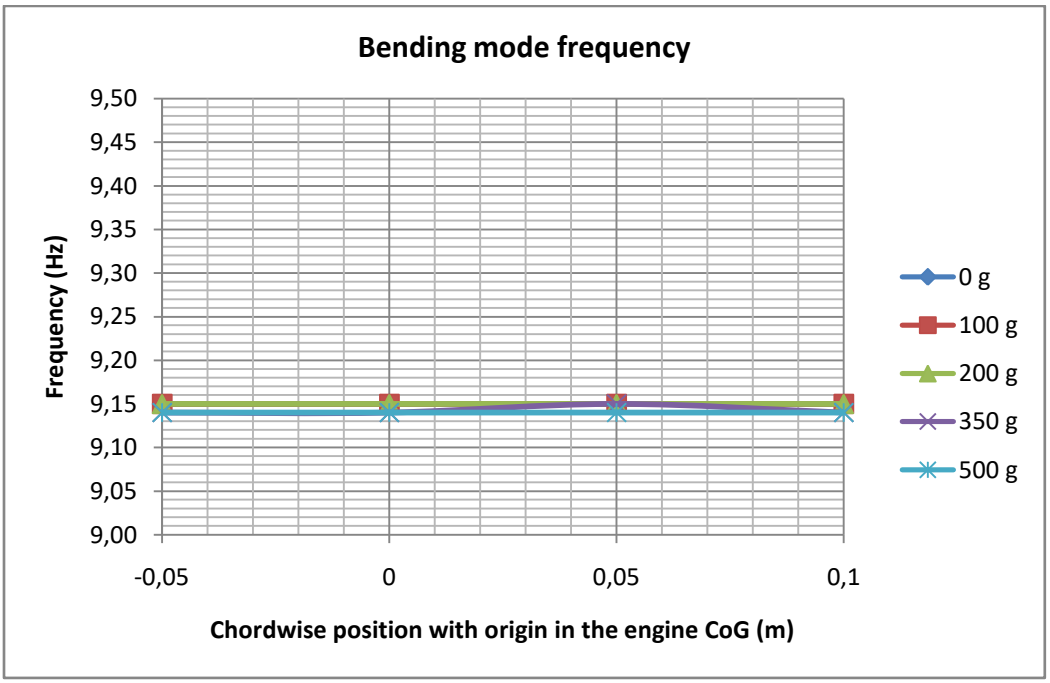

Figure 50.Torsion mode frequency depending on the engine chordwise position and its mass.

The bending mode frequency is almost unaltered due to the mass is close to the wing-fuselage union, the chordwise variation is meaningless. The torsion mode frequency decreases with the mass growth and there is also a small variation because of the chordwise position, it is not so important because the engine chordwise position does not change too much.

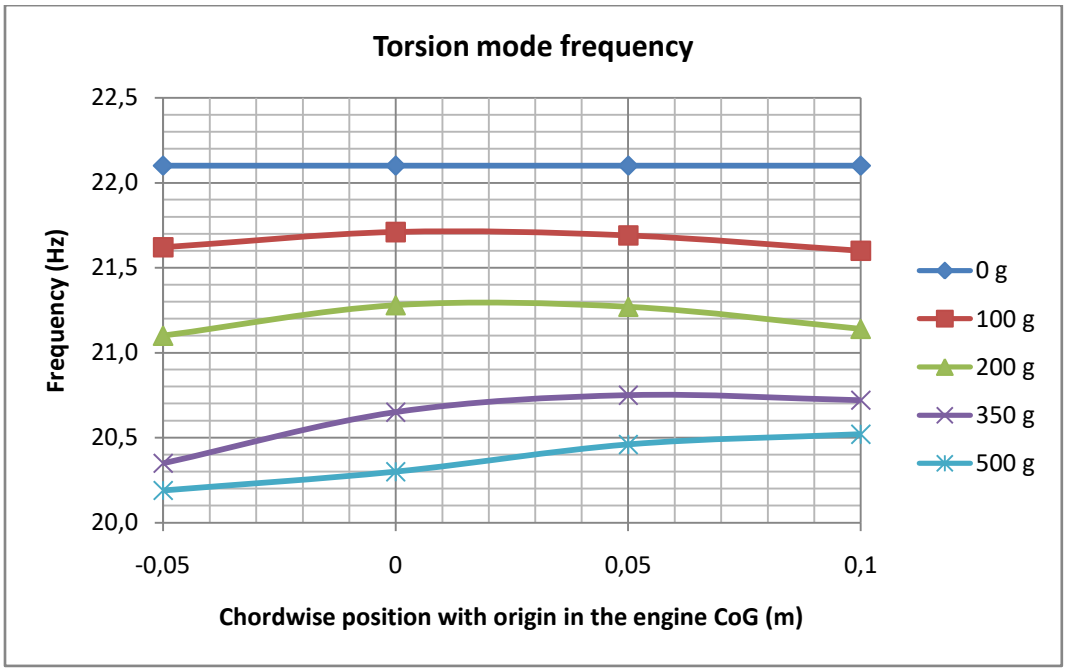

Figure 51. Bending mode frequency depending on the engine chordwise position and its mass.

Comparing the engine test to the tip test:

- Spanwise position of damping mass is critical. Closer to the tip, bending and torsion frequencies are highly altered respect to the variation suffered in the engine position, and so flutter velocity decreases.
- Chordwise position becomes more important if one wants to add a lumped mass and not for the engine problem, due to the lumped mass can be added wherever while the engine is almost fixed chordwise.
- Special attention should be taken over the engine modes. If the lumped mass were located under the wing and not into, it will show the same engine mode severe problems.

6. CONCLUSIONS AND FUTURE RESEARCH

This thesis set out to investigate the flutter by using a spanwise, chordwise and mass parametrization for a wind tunnel conventional aircraft model. In this final chapter, the research contributions highlights as well as directions for future research are discussed.

6.1. THESIS CONCLUSIONS

The certification problem has been introduced in chapter 2, the conclusions are:

1) **Certification problem:** nowadays there exist many problems that make not possible to certificate the active control for flutter suppression, mainly due to manufacturing uncertainties and possible aircraft failure condition that will work as uncertainties (in example: asymmetric fuel consumption when it is saved inside the wings, engine failure, etc.). This thesis verifies these difficulties by a parametric flutter analysis, showing how small variations can cause big frequency variations and so flutter problems.

2) **The robustness of the active control system** respect to the frequency variations must be demonstrated, but the first step is to understand the uncertainties and enclose the problem in order to make this easier and possible. This thesis includes a parametric analysis that intended to be useful as example and database for future investigation lines.

To check and cooperate with this investigation line, the introduced conventional aircraft model for the wind tunnel has been developed in NeoCASS starting from the Nastran model. The conclusions of the model and the considerations for the wind tunnel analysis are:

1) **Aircraft model:** the first step is to develop a simple conventional aircraft model and test it in both computational and wind tunnel ways, in order to slowly collect a big amount of information that will be useful to develop more complex models and understand them.

2) **Wind tunnel is limited** by the dimensions and the wind speed, what means that the model must be altered in order to achieve flutter characteristics within the limits. Parametric flutter analysis is a powerful and helpful tool. This thesis contains results that will permit to choose the mass and its correct position to alter the flutter position correctly during wind tunnel analysis.

Finally, the parametric analysis has been developed, obtaining many conclusions about the importance of adding masses to the model and the chosen position to do it. After engine and tip tests, one can conclude:

1) **Adding lumped masses to the tip** is an useful solution to control flutter modes and velocity. The model is very sensitive to this mass position because is the spanwise limit, and the bending mode suffers high variations. The torsion mode is more sensible to chordwise variations. Close to the leading edge it helps to rise up the flutter velocity because is causes a twist that is opposed to the aerodynamic one. On the other hand, next to the trailing edge it excites the torsion mode and so its frequency decreases, arriving with a lower velocity to the bending – torsion coupling that causes flutter. Bigger the mass, bigger the effect. When the mass is to heavy, there exist the possibility of flutter mode switching. Some examples have been found and they are described in Chapter 5.

2) **Engine mass and chordwise variations** do not affect significantly the bending mode because it is closer to the fuselage. However, the torsion mode suffer similar but scaled variations than suffered with the mass variation at the tip. The engine mass is bigger but the chordwise cannot be changed too much due to manufacturing limits, so it is not as important as near the tip. Nevertheless, the main problem found with engines is that they add new modes that the aircraft without them does not have (for example, engine pitch and yaw modes were found during the analysis). During the design phase it is important to check that these modes do not produce dynamic coupling able to generate flutter.

3) **Graphic solution for wind tunnel model:** Figure 44 is probably the most important conclusion of this thesis because it will let decide how to obtain the desired flutter to be analyzed during wind tunnel tests. It represents the flutter velocity depending on the chordwise at the tip and the lumped mass added.

6.2. FUTURE RESEACH

This thesis opens several future research lines, from the model to the analysis.

Using this model, perform extra analysis about the addition of lumped masses and its position:

a) Tip analysis: complete it by using more masses and more chordwise positions. Special attention to the flutter mode switching.
b) Engine analysis: make small spanwise variations.
c) Full wing analysis: perform an analysis similar to the tip one but spanwise, with the final target to define completely the wing.
d) Asymmetric analysis: to simulate possible failure and manufacturing uncertainties condition could be interesting to make small changes of symmetric masses. For example, a variation of 5% of mass in one of the engines.

Changing this model to obtain new flutter diagrams and compare them:

a) Wing span properties modification: material and beam section.
b) Wing swept angle variations.
c) New tail configuration.

Create the real dimension aircraft with Nastran/NeoCASS and compare it with the model. Try to link the results and think about the sizing problems of dimensionless parameters (Mach, Reynolds, etc).

Finally, the frozen aeroelastic model can be used to develop dedicated active flutter systems to be verified during the wing tunnel tests.

APPENDIX A: NASTRAN TO NEOCASS GUIDE

This appendix tries to provide helpful user guide for translating code from Nastran to NeoCASS by explaining the similarities and differences between cards and proposing solutions for the cards that does not exist yet in NeoCASS. This Appendix (including the cards) is based on [19] and [20].

1) **CORD2R**

The same for both Nastran and NeoCASS.

2) **GRID**

The same for both Nastran and NeoCASS.

3) **RBE2**

The same for both Nastran and NeoCASS in cards definition. However, the RBE2 NeoCASS card is much more restrictive respect to master and slaves nodes.

If next error is found: 'Setting Model dofs...done. Index exceeds matrix dimensions' one possible solution is to simplify the rigid bar structure by using a smaller quantity of them. For example, in this thesis the tail cone – vertical tail joints were redesigned in order to correct this error.

4) Nastran RBE2 to NeoCASS RBE0

RBE0 card is a simpler definition that NeoCASS uses to define rigid bars. To change from RBE2 (Nastran) card to RBE0 (NeoCASS) card one should remove the forth field of RBE2 and move forward the other fields.

1	2	3	4	5	6	7	8	9	10
RBE2	EID	GN	**CM**	GM1	GM2	GM3	GM4	GM5	
	GM6	GM7	GM8	GM9	-etc.-	A			
RBE0	EID	GN	GM1	GM2	GM3	GM4	GM5	GM6	
	GM7	GM8	GM9	-etc.-					

Table 20. RBE2 (Nastran) card to RBE0 (NeoCASS) card.

5) MAT1

The same for both Nastran and NeoCASS. However, take into consideration that Nastran accepts 0 as density value and NeoCASS gives a warning.

In this thesis, to solve this warning the solution has been to introduce a small value (1.0E-12).

6) PBAR

The same for both Nastran and NeoCASS. Nonetheless, the NeoCASS card is not complete yet. On Table 21 are shaded the fields not available in NeoCASS.

However, in NeoCASS there are not in use but they can be written, what means that it is possible to copy directly the Nastran card.

1	2	3	4	5	6	7	8	9	10
PBAR	PID	MID	A	I1	I2	J	NSM		
	C1	**C2**	**D1**	**D2**	**E1**	**E2**	**F1**	**F2**	
	K1	K2	I12	**C**	**F0**				

Table 21. PBAR card for Nastran and NeoCASS.

7) PBEAM (Nastran) to PBAR (NeoCASS)

PBEAM card does not exist yet in NeoCASS and so it is necessary to change it into a PBAR card. On Table 22 are represented the PBEAM (Nastran) card and the PBAR (NeoCASS) card. The PBEAM card includes only the parameters that one should include in the PBAR card.

To work effectively, the transformation is simply to copy and paste the parameters in the correct field.

1	2	3	4	5	6	7	8	9	10
PBEAM	PID	MID	A	I1	I2	I12	J	NSM	
	K1	K2							
PBAR	PID	MID	A	I1	I2	J	NSM		
	K1	K2	I12						

Table 22. PBEAM card (Nastran) including only useful information for PBAR card (NeoCASS).

8) PBARL (Nastran) to PBAR (NeoCASS)

See 'Appendix B: PBARL to PBAR'.

9) CBAR

The same for both Nastran and NeoCASS. Nevertheless, the NeoCASS card is not complete yet. On Table 23 are shaded the fields not available in NeoCASS.

However, in NeoCASS it is necessary to write PA = 0 and PB = 0. F0 is not active, so it can be written but it will not be read.

1	2	3	4	5	6	7	8	9	10
CBAR	EID	PID	GA	GB	X1	X2	X3		
	PA	**PB**	W1A	W2A	W3A	W1A	W2A	W3A	
			F0						

Table 23. CBAR card for Nastran and NeoCASS.

10) CBEAM (Nastran) to CBAR (NeoCASS)

CBEAM (Nastran) card offers two possibilities to define the beam orientation: G0 or (X1, X2, X3). If the first way is used it is necessary to define the vector (X1, X2, X3) by using G0. If the second form is used there is not extra work to do. This done, the CBEAM card is the same as the CBAR (Nastran) card, and one should follow number 9.

1	2	3	4	5	6	7	8	9	10
CBEAM	EID	PID	GA	GB	**G0/X1**	X2	X3		
	PA	PB	W1A	W2A	W3A	W1A	W2A	W3A	
			F0						

Table 24. CBEAM (Nastran) card.

11) CONM2

The same for both Nastran and NeoCASS.

12) CMASS1 (Nastran) to CONM2 (NeoCASS)

CMASS1 card does not exist in NeoCASS and so the masses defined this way must be rewritten as CONM2 (similar in both Nastran and NeoCASS). PID field a Property Mass card. Cards shown in Table 25.

1	2	3	4	5	6	7	8	9	10
CMASS1	EID	PID	G	C					
PMASS	PID	M							
CONM2	EID	G	CID	M	X1	X2	X3		
	I11	I21	I22	I31	I32	I33			

Table 25. Simplified CMASS1 and PMASS cards.

To transform from CMASS1 and PMASS cards to CONM2 cards one should follow the following steps:

- Copy in the correct field EID and G.
- Check if the node G includes the coordinate system X1, X2, X3. If it is included, write the field CID on CONM2. It if is not filled, write it as X1, X2 and X3.
- Depending on the value of C one can guess that PMASS M means:
  C = 1, 2, 3; M = mass

C = 4; M = I11
C = 5; M = I22
C = 6; M = I33

13) CAERO1 (Nastran) and CAERO0 (NeoCASS)

The CAERO1 (Nastran) card is included in NeoCASS with the name of CAERO0.

14) CAERO1 (NeoCASS)

This card is defined in its own way and it can be found in NeoCASS manual [20].

15) SET 1

The same for both Nastran and NeoCASS.

16) SPLINE2 (Nastran) and SPLINE1 (NeoCASS)

The SPLINE2 (Nastran) card is included in NeoCASS with the name of SPLINE1.

17) SPLINE1 (Nastran) and SPLINE1 (NeoCASS)

SPLINE1 (Nastran) card creates a surfaces spline while the NeoCASS one creates a linear spline. This means that there is not possible way to translate it. It is necessary to redefine it.

18) AESURF and AELIST

AESURF Nastran and NeoCASS cards work in the same way, the only difference is that AELIST card does not exist in NeoCASS and so the AESURF (NeoCASS) card includes directly the CAERO ID instead of the AELIST ID.

APPENDIX B: PBARL TO PBAR

PBARL is a Nastran card used to define the bar properties by including the 'TYPE' and the dimensions 'DIMi' as it is shown on Figure 52. The type is the shape of the bar section that is defined in the program code (example on Figure 53), what the user does to devise the geometry is to set the dimensional parameters.

1	2	3	4	5	6	7	8	9	10
PBARL	PID	MID		TYPE				F0	
	DIM1	DIM2	DIM3	DIM4	DIM5	DIM6	DIM7	DIM8	
	DIM9	-etc.-	NSM						

Figure 52. PBARL card for Nastran [19].

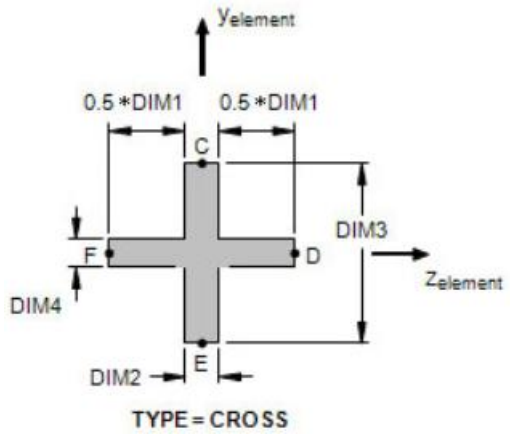

Figure 53. Example of bar section type: CROSS [20].

During the transformation from Nastran to NeoCASS code it was necessary to convert some PBARL into PBAR because NeoCASS does not include this card yet. To do it, one analyses the section to obtain the properties to write in PBAR card. This analysis has been done by using Femap. Figure 54 shows an example of how the PBARL that have been transformed and its properties.

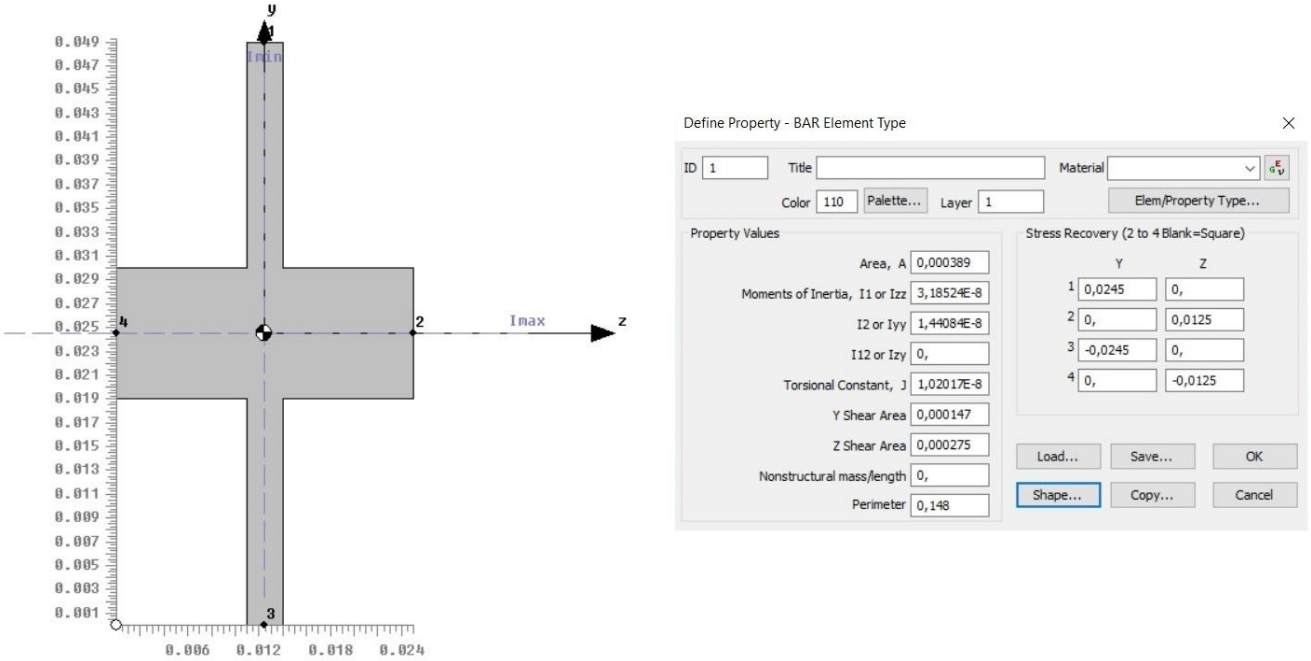

Figure 54. PBARL to PBAR

APPENDIX C: MODAL SHAPES OF NEOCASS MODEL

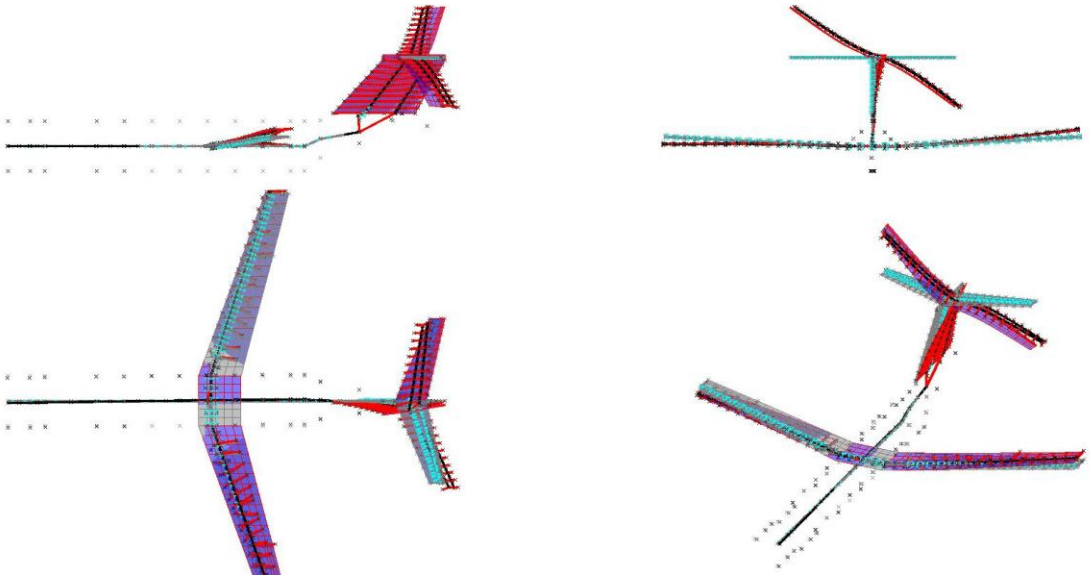

Figure 55. Mode 7, f = 9.11712 Hz

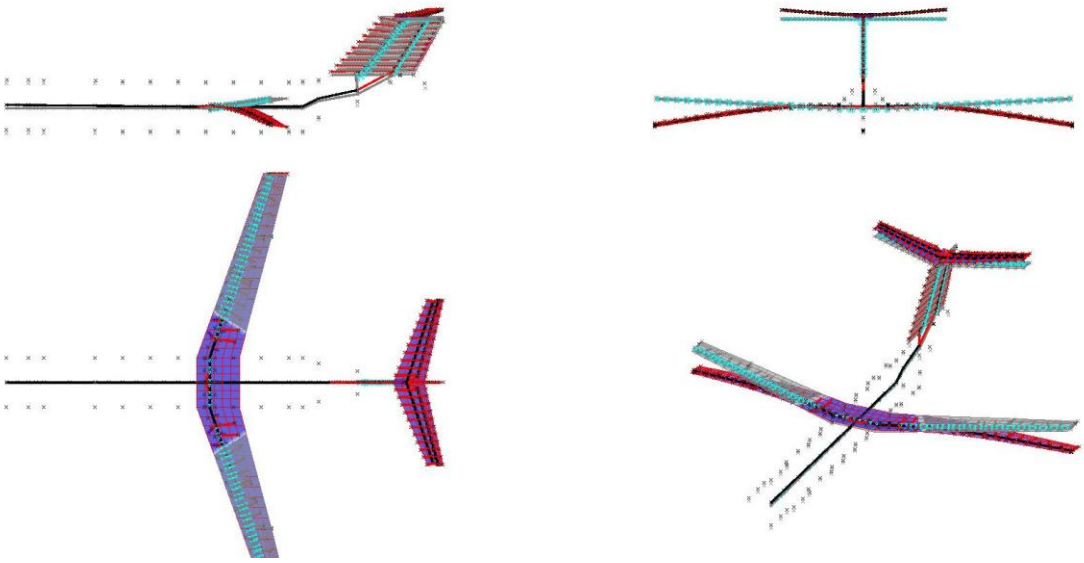

Figure 56. Mode 8, f = 9.15187 Hz

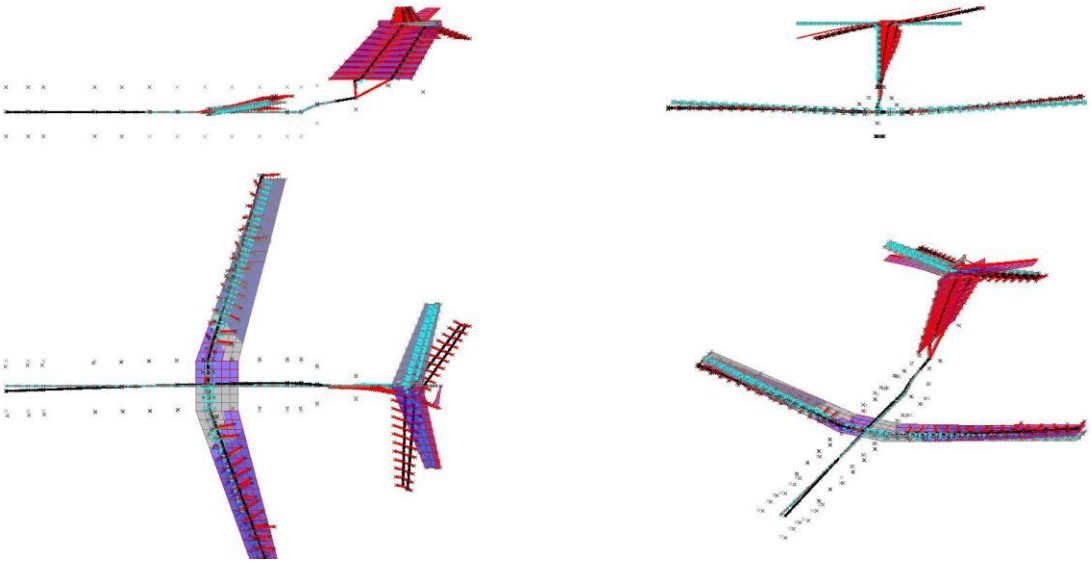

Figure 57. Mode 9, f = 9.84641 Hz

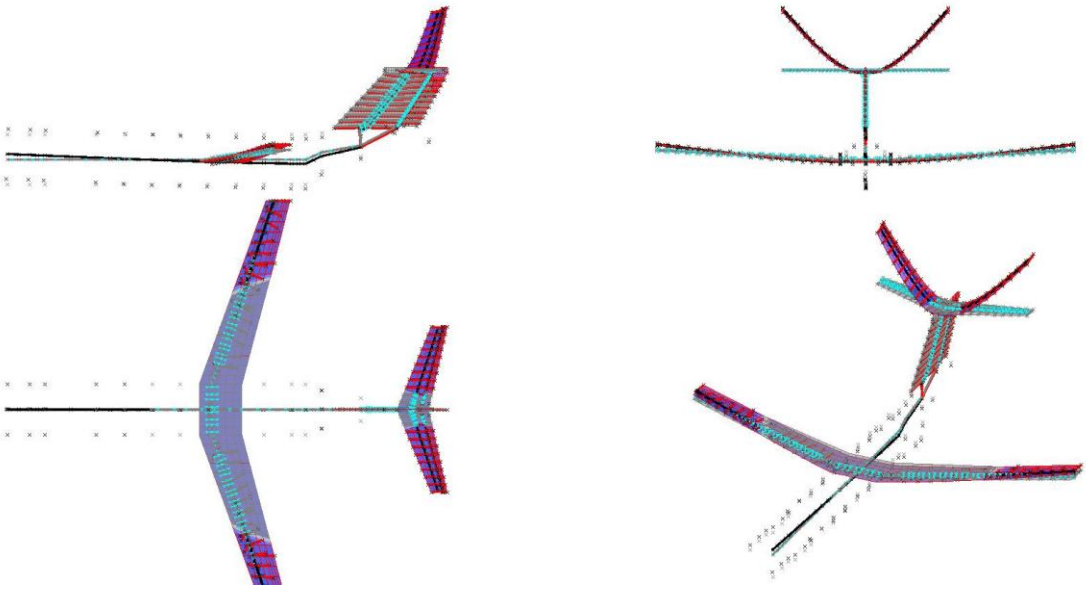

Figure 58. Mode 10. f = 14.4680 Hz

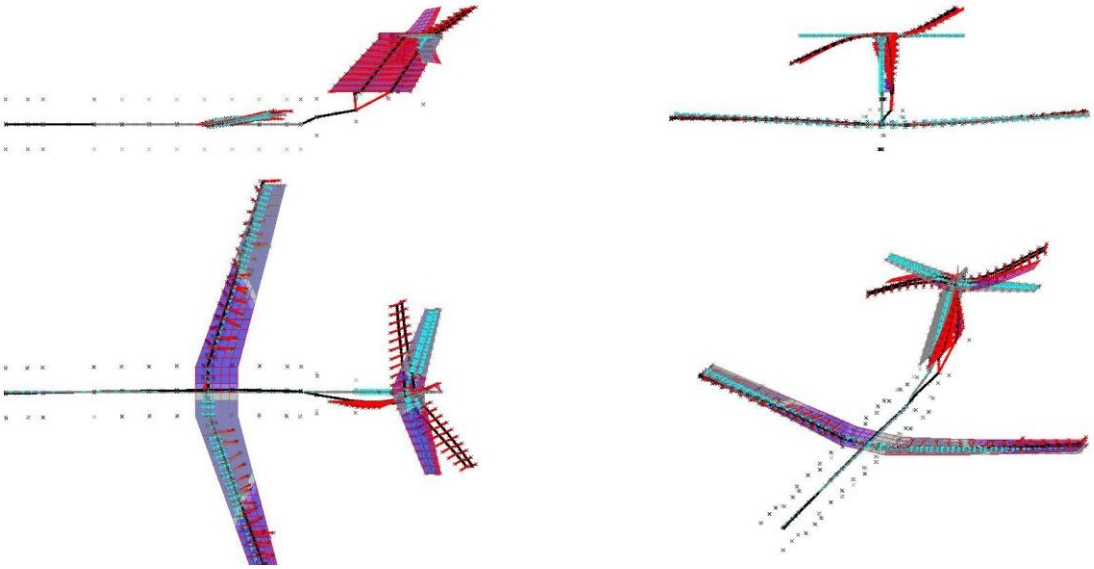

Figure 59. Mode 11, f = 16.2920 Hz

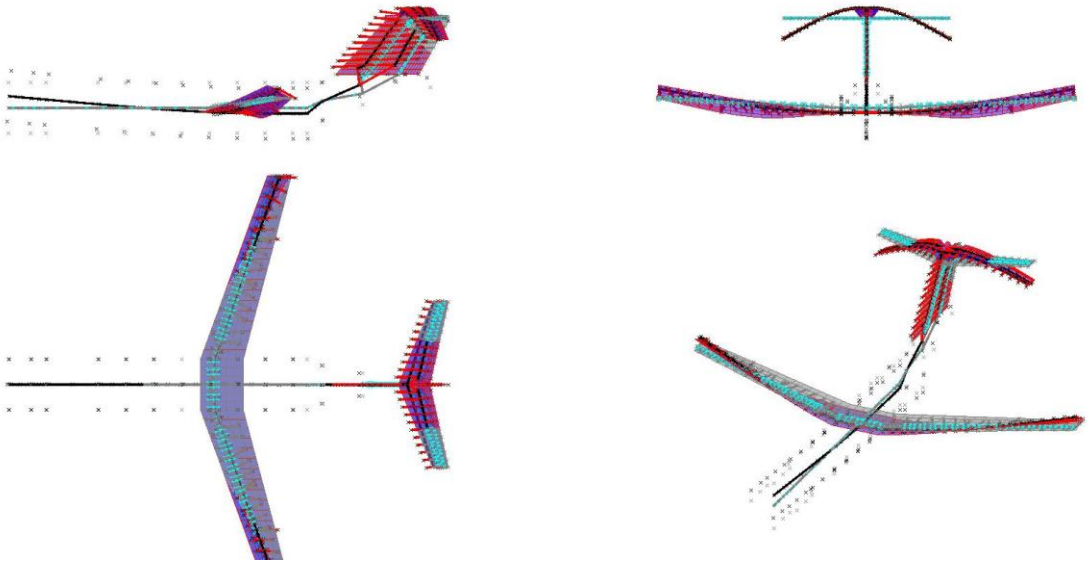

Figure 60. Mode 12, f = 20.3703 Hz

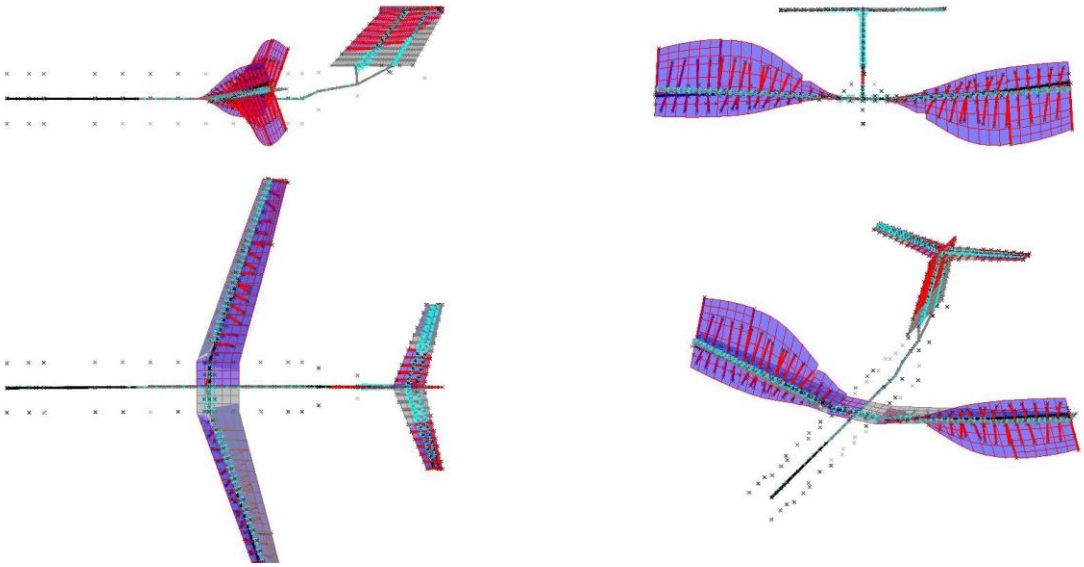

Figure 61. Mode 13, f = 21.9743 Hz

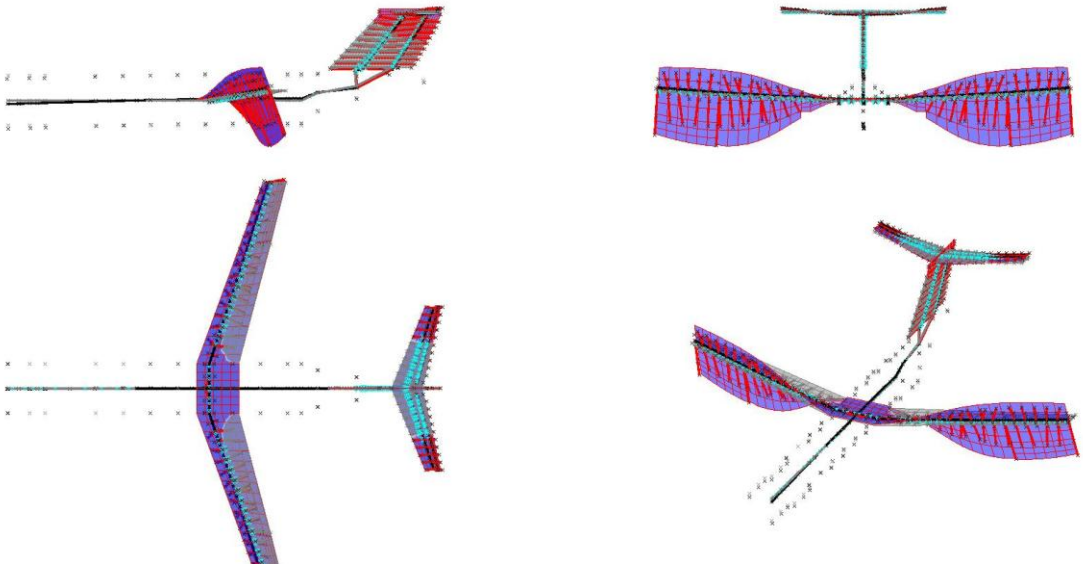

Figure 62. Mode 14, f = 22.1016 Hz

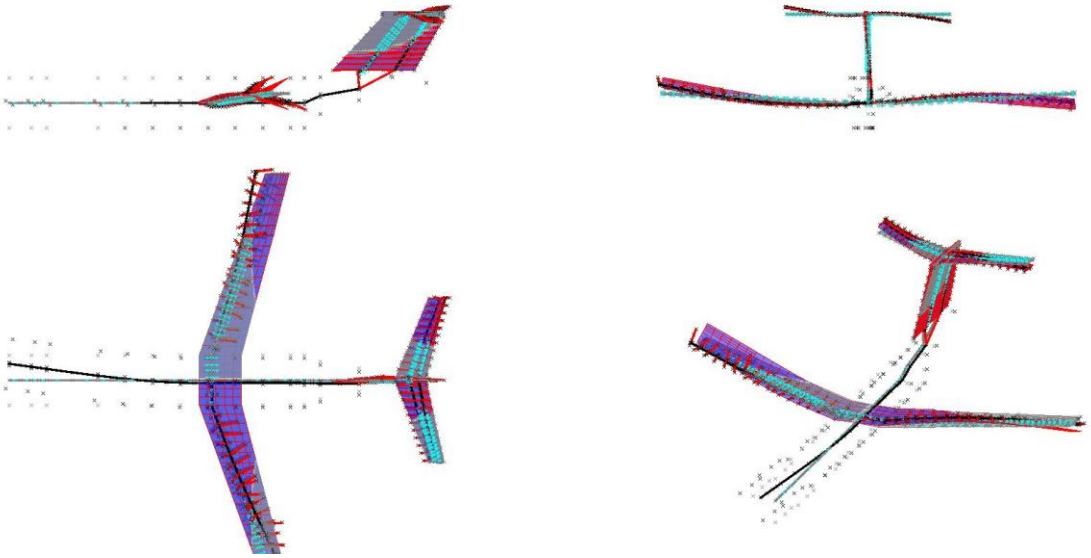

Figure 63. Mode 15, f = 22.5038 Hz

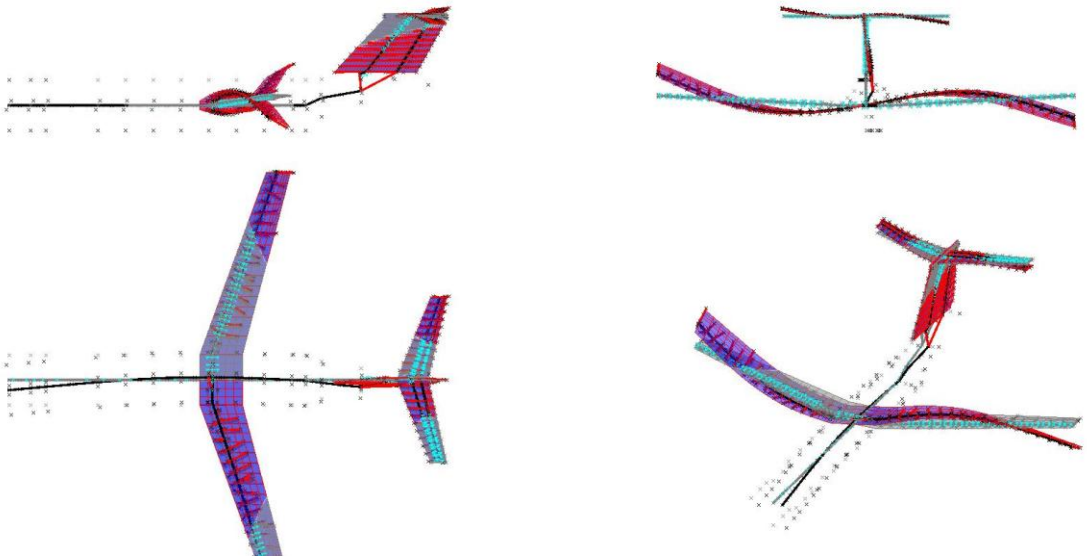

Figure 64. Mode 16, f = 23.7356 Hz

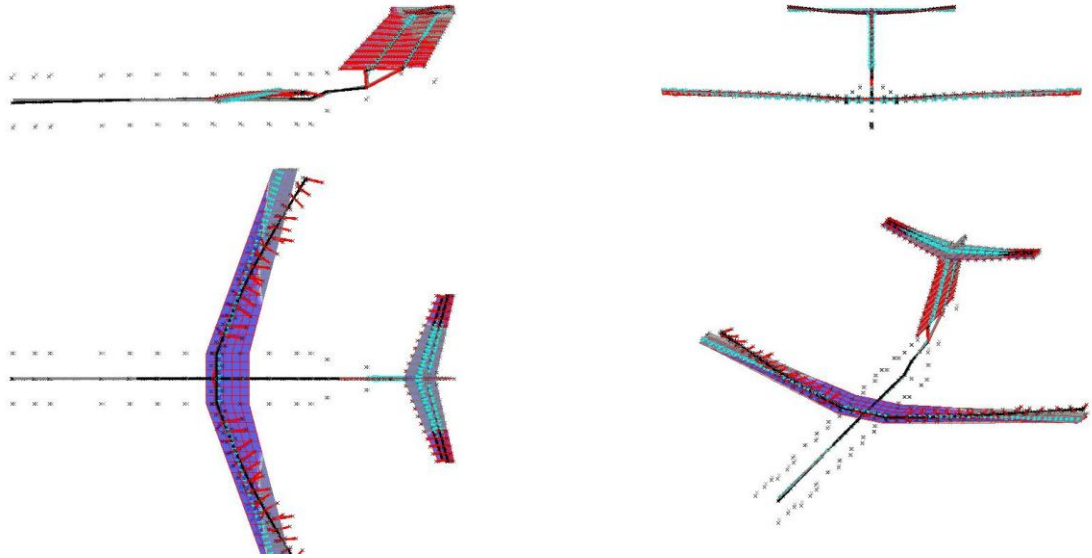

Figure 65. Mode 17, f = 25.7356 Hz

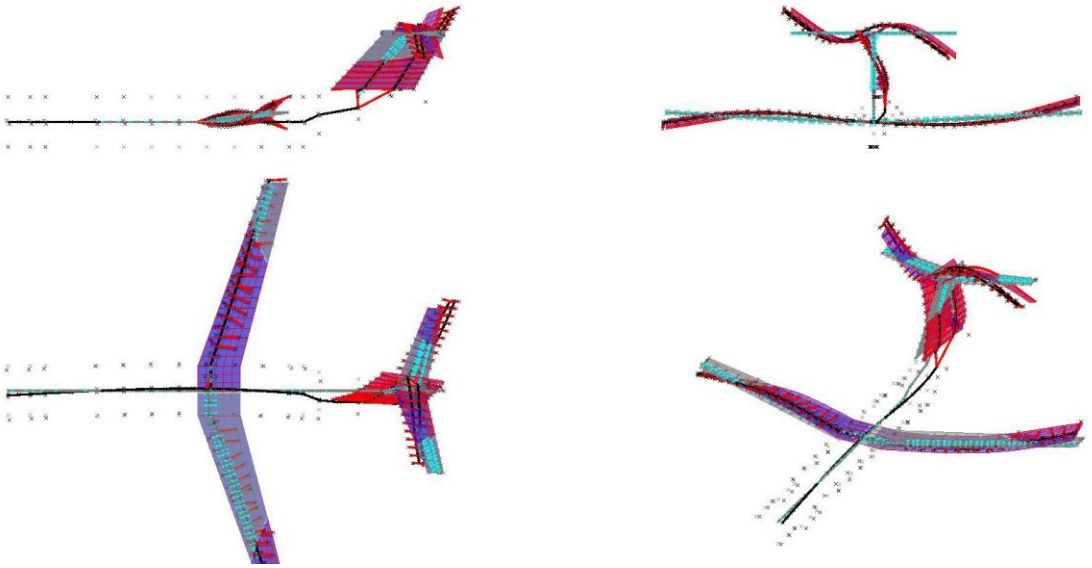

Figure 66. Mode 18, f = 31.7618 Hz

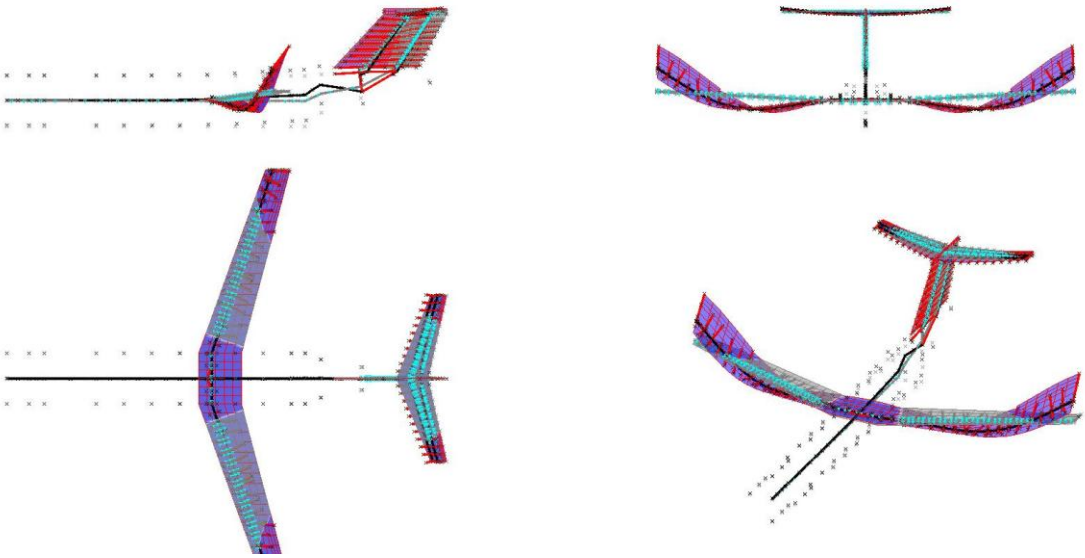

Figure 67. Mode 19, f = 43.1872 Hz

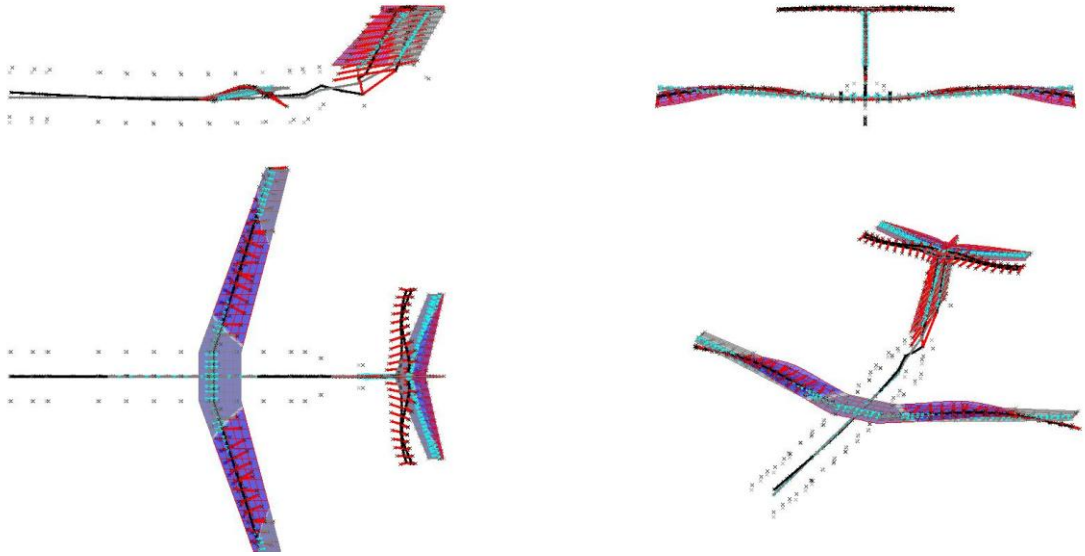

Figure 68. Mode 20, f = 44.6966 Hz

APPENDIX D: DIVE SPEEDS OF THE AIRBUS A320

The reader can obtain some reference values of dive speeds to understand better the Minimum Required Aeroelastic Stability Margin diagram. It is interesting to say that the Airbus fly by wire makes not possible to reach the dive speed. For the A320 these are the velocities:

1. Dive speed: $M_D/V_D = 0.89/381kts$
2. Maximum Operation Speed: $M_{M0}/V\_M0 = 0.82/350kts$

On the Figure 69 the consequences of exceed these velocities are shown. Reference [6] includes a video of the V_D/M_D testing of the Airbus A380 in which the reliability of this parameter can be understood. Finally, Figure 70 includes the result of testing and certification: an extract of the Airbus A320 flight crew operating manual.

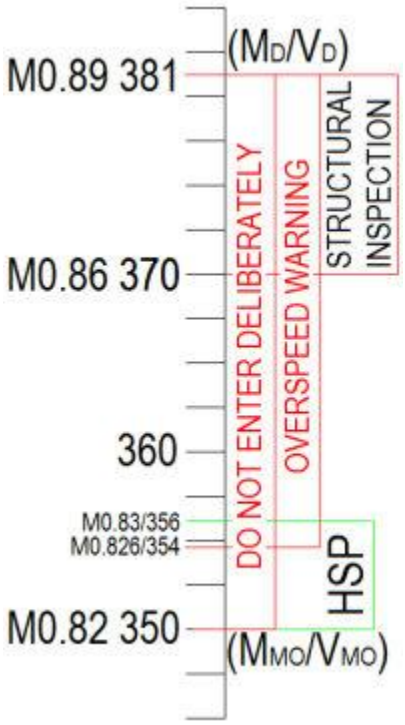

Figure 69. Dive speeds and consequences for A320 [6].

VMO/MMO DETERMINATION

Applicable to: ALL

GENERAL

VMO (the design cruising speed) is the maximum operating speed that the crew may fly within the normal flight envelope. It is not authorized to fly intentionally above this limit.
VD is the design dive speed. VMO and VD must comply with load requirements (gust loads, maneuvering loads). For example, the aircraft must be able to sustain a load factor of 2.5 up to VD. The range between VMO/VD considers normal reaction time to the crew to use standard recovery techniques for returning the aircraft to normal attitude at a speed of VMO/MMO.
The A319/A320/A321 are protected by the High Speed Protection law which automatically makes the recovery if VMO is exceeded (between VMO and VMO +6) as shown in the following table.

HIGH SPEED/MACH TABLE

MD = 0.89	VD = 381 kt	VD = VMO +31 kt
MMO +0.04	VMO +20 kt	Structural inspection required. (Refer to relevant AMM section)
MMO +0.01	VMO +6 kt	Upper limit for entry into HSP
MMO +0.006	VMO +4 kt	Overspeed warning
MMO = 0.82	VMO = 350 kt	Max operating SPEED/MACH and lower limit for entry into HSP
MMO -0.006	VMO -3 kt	Max upper speed range in DES mode.
MMO -0.02	VMO -10 kt	Managed speed target limit (ECON mode)

Depending upon the speed trend, the autopilot will disconnect at or below VMO +6 kt/MMO +0.01 and an automatic pitching up will allow VMO to be regained.
Per design, in DES mode or OP DES mode, autopilot authority is limited to 0.1 g compared to 0.15 g in EXPEDITE. This limitation was required by the launching customers for passenger's comfort.
Due to the load factor limitation, some flight paths or environment conditions depending on their magnitude, may not be counteracted by the autopilot leading to VMO/MMO overshoot.

A short exceedance of few knots above VMO has no consequences on the aircraft.

Nevertheless, an intentional exceedance is not authorized:
- By regulation
- Because above VMO/MMO the HSP (high speed protection) may be activated automatically. Any pilot input to recover the target speed may be added to the HSP order, leading to a load factor incompatible with passenger's comfort.

Figure 70. A320 Flight Crew Operating Manual extract [6].

BIBLIOGRAPHY

[1] Eli Livne, “Aircraft Active Flutter Suppression: State of the Art and Technology Maturation Needs”. University of Washington, Seattle, WA.

[2]Pablo García Fogeda, Vibrations course. Technical University of Madrid.

[3] Airworthiness Requirements of Air Commercial Regulations for Aircraft, Bulletin No. 7-A

[4] AC No: 25.629-1B, Federal Aviation Administration.

[5] AC No: 23.629-1B, Federal Aviation Administration.

[6] http://theflyingengineer.com/

[7] D. Goge, M. Boswald, U. Fullekrug, P. Lubrina, “Ground Vibration Testing of Large Aircraft – State of the art and Future Perspectives.”, Deutsches Zentrum für Luft- und Raumfahrt (DLR), Institute of Aeroelasticity, Bunsenstr. 10, D-37073 Göttingen, Germany.

[8] http://www.cfm-schiller.de

[9]M. Nejad Ensan, V. Wicjramansinghe, “Methodology for ground and flight vibration testing on light aircraft”. Can Aeronaut. Space J., Vol 60, No. 1, pp 1-8, 2014.

[10]Félix Arévalo, “Introducción a ensayos de dinámica estructural en la industria aeronáutica”. Technical University of Madrid.

[11] AC No: 25.672-1, Federal Aviation Administration.

[12] Memorandum AC 25.672-1, Federal Aviation Administration.

[13] The Active Flutter Suppression (AFS) Technology Evaluation Project, Eli Livne, Ph.D. University of Washington, Seattle, WA.

[14] Ricci, S., Scotti, A., Cecrdle, J., and Malecek, J., “Active Control of Three-Surface Aeroelastic Model,”Journal of Aircraft, Vol. 45, No. 3, 2008, pp. 1002–1013. doi:10.2514/1.33303.

[15] Mattaboni, M., Quaranta, G., and Mantegazza, P., “Active Flutter Suppression for a Three-Surface Transport Aircraft by Recurrent Neural Networks,” Journal of Guidance, Control, and Dynamics, Vol. 32, No. 4, 2009, pp. 1295–1307. doi:10.2514/1.40774.

[16] Ricci, A., and Scotti, A., “Aeroelastic Multi-Surface Roll Control of a Three Surfaces Wind Tunnel Model,” AIAA Paper 2009-2511, 2009. doi:10.2514/6.2009-2511.

[17] Ricci, S., and Scotti, A., “Gust Response Alleviation on Flexible Aircraft Using Multi-Surface Control,” AIAA Paper 2010-3117, 2010. doi:10.2514/6.2010-3117.

[18] Sergio Ricci, X-DIA Nastran model v0.0.1. Politecnico di Milano.

[19] “MSC.Nastran 2001. Quick Reference Guide”. MSC.Software Corporation.

[20] L. Cavagna, S. Ricci, “NeoCASS Next generation Conceptual Aero Structural Sizing”, 2013.

[21] User’s Guide Reference manual TORNADO 1.0 RELEASE 2.3 2001-01-31.

[22] P. Mantegazza and C. Cardani. “Continuation and direct solution of the flutter equation”. Computers & Structures, 8(2):185–192, 1978.